2018

Nano Enhanced Surface Modification of Titanium Dental Implants for Improving Osseointegration and Biocompatibility

Salaie, Ranj

Copyright Statement

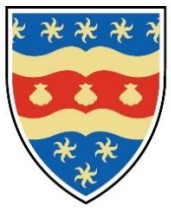

UNIVERSITY OF
PLYMOUTH

Nano Enhanced Surface Modification of Titanium Dental Implants for Improving Osseointegration and Biocompatibility

by

Ranj Nadhim Jalal Salaie

A thesis submitted to University of Plymouth
in partial fulfilment for the degree of

DOCTOR OF PHILOSOPHY

School of Biological and Marine Sciences

December 2018

Dedication

I would like to dedicate this thesis to my grandparents, my parents **(Professor Dr. Nadhim Jalal Salaie** and **Dr. Drakht Arshad Hawezy**), my parents in law (**Dr. Dara Meran** and **Dr. Zhean Anwar**), my wife **Zhala** and my sibilings **Amanj** and **Rawa.**

Acknowledgements

I would like to express my gratitude to Professor Richard Handy for supervising this project, giving valuable advices and also financially support part of my project on behalf of Plymouth University. My gratitude also goes to Professor Waleed Al-Murrani, Professor Christopher Tredwin (Dean of dental school), Dr Huirong Le and Dr Alexandros Besinis. I would like to specially thank the technicians; Lynne Cooper, Andrew Atfield, William Veevers, Andrew Fisher, Andrew Arnold, Zoltan Gombos, Michel Kiernan, Terry Richards and Rob Clough for their help. Special thanks to my parents, wife and siblings for their continuous support and encouragement. I also want to take an opportunity to thank my friends in our research group who helped me throughout my project.

Author's Declaration

At no time during the registration for the degree of Doctor of Philosophy has the author been registered for any other University award without prior agreement of the Doctoral College Quality Sub-Committee.

Work submitted for this research degree at the University of Plymouth has not formed part of any other degree either at the University of Plymouth or at another establishment.

This study was partly supported by HCDP programme of Kurdistan Regional Government (KRG), Kurdistan, Iraq. This project was also funded by Professor Richard Handy (on behalf of University of Plymouth) and my father Professor Nadhim Jalal Salaie.

A programme of advanced study was undertaken, which included

1-Postgraduate research skills and methods module.

2-Contemporary applications of cell biology, covering the recent issues and technologies about cell culture (module).

I have also participated in one-day courses about critical thinking, the use of end note and excel data management.

Presentation at conferences:

Ranj N. Salaie, Alexandros Besinis, Huirong Le, Christopher Tredwin, Richard D. Handy. Biocompatibility of Surface-modified Titanium Dental Implants with Silver and Hydroxyapatite Nanoparticles. British Society of Dental Research Conference, September 2015, Cardiff, **Poster** number 66.

Ranj N. Salaie, Alexandros Besinis, Huirong Le, Christopher Tredwin, Richard D. Handy. Biocompatibility of Surface-modified Titanium Dental Implants with Silver and Hydroxyapatite Nanoparticles. Postgraduate Society Conference of

Plymouth University, December 2015, Plymouth, **Oral presentation** 7, Abstract book p7.

Ranj N. Salaie, Alexandros Besinis, Huirong Le, Christopher Tredwin, Richard D. Handy. Biocompatibility and adhesion of silver nano-coating on titanium dental implants. British society of dental research conference, September 2017, Plymouth, **Oral presentation** 091, Abstract book p132.

-Gave a presentation in Three minutes thesis presentation competition in University of Plymouth, 16th June 2017.

-Participated in postgraduate society conferences in Plymouth University on 12/November/2014, 24/March/2015, 16/March/2016 and postgraduate society research showcase on 5/December/2016.

Awards

Best presentation award in postgraduate society conference in Plymouth University, December 2015.

Word count of main body of the thesis is 43,746

Signed ……..

Date …….

Nano Enhanced Surface Modification of Titanium Dental Implants for Improving Osseointegration and Biocompatibility

Ranj Nadhim Jalal Salaie

Abstract

Dental implants are prone to bacterial colonisation and infection which subsequently cause dental implant failure. Coating the dental implant with an antibacterial agent and a biocompatible agent can inhibit the bacterial colonisation and infection without disturbing the biocompatibility of the implant. This study aimed to coat medical grade titanium alloy implants with silver and hydroxyapatite (HA) nanoparticles. The reason for using silver was to introduce antibacterial activity to the coated dental implants; and then using HA to preserve biocompatibility and manage the silver exposure of the primary human osteoblast cells. Medical grade titanium alloy discs measuring 15 mm in diameter were polished and silver plated to produce a uniform layer of silver nanoparticles on the surface. The electroplating method was followed by nano or micro HA deposition and curing at 500 °C to produce an HA coating and thereby achieving nano silver plus nano HA (Ag+nHA), or nano silver plus micro HA (Ag+mHA), coatings on titanium alloy. The coating quality was assessed by electron microscopy. The bonding strength of the coating was investigated by the pull-off test and chemical stability in the cell culture media was studied by conducting dialysis and dissolution experiments. A series of experiments were conducted to investigate the biocompatibility of the coatings with primary human osteoblast cells over 7 days, cell health was assessed using biochemistry and microscopy. A differentiation experiment was conducted for 21 days to investigate the osteoblast cell mineralisation on the coatings and gene expression profile of the cells. Results showed that the specimens were successfully coated with nano silver and HA particles. The pull-off test showed

that the coatings had reasonable bonding strength to the substrate. Dialysis and dissolution experiments showed that the coatings were stable in the cell culture media despite some silver release from the coatings. The biocompatibility experiments showed that there was a consistent amount of silver release (1-2 mg L^{-1}) from the silver containing specimens. The human primary osteoblast cells were healthier on Ag+nHA compared to Ag and Ag+mHA over 7 days. The differentiation experiment showed that there was a constant silver supply over 21 days from all silver containing coatings. Cell viability over 21 days was significantly higher in Ag+nHA compared to Ag and Ag+mHA ($p < 0.05$). Moreover, the cells were mineralised and produced Ca^{2+} and P in all the treatments. In conclusion, Ag+nHA was more biocompatible compared to Ag and Ag+mHA and can have a potential for clinical use.

List of contents

List of tables

List of figures

Chapter 1

Literature review

1.1 Introduction

Dental implants are devices that are surgically inserted into the jawbone to enable the attachment of supragingival prosthesis such as single crowns, implant supported bridges, implant supported dentures (over dentures); and also maxillofacial reconstructions (Misch 2007). Dental implants are used as a replacement for missing teeth that have been lost due to dental caries, trauma, periodontal disease and developmental anomalies (Sykaras *et al*., 2000). The phenomenon of integration between the dental implant and the surrounding jaw bone is called osseointegration, which is defined as a direct structural and functional connection between ordered living bone and the surface of a load-carrying implant (Branemark *et al*., 2001).

When the implant is installed, it must be stable inside the jawbone (primary stability); this consequently results in the formation of new bone around the implant (osseointegration). On the other hand, failure of the implant to obtain primary stability during insertion leads to the formation of fibrous encapsulation (fibrointegration) which results in dental implant failure (Lioubavina-Hack *et al.*, 2006). Primary stability is achieved by the means of friction between the implant surface and the surrounding jawbone. However, the stability of the implant in the tissue may decrease in the first weeks as a result of compression necrosis in the neighbouring bone. The primary stability decreases with time at the benefit of secondary stability, which is attributed to the physiological bonding at the bone-implant interface. This period between primary and secondary stability can be the most vulnerable to the dental implant failure (Lavenus *et al*., 2010).

1.2 Biocompatibility of dental implant materials

Titanium exhibits good biocompatibility, corrosion resistance and tensile strength, making it the most commonly used biomaterial for constructing dental implants (Albrektsson *et al*., 1981; McCracken, 1999; Ehrenfest *et al.,* 2010; Özcan and Hämmerle, 2012). There are four grades of commercially pure titanium and two titanium alloys (Ti-6Al4V, Ti-6Al4VELI) that are used for biomedical applications. As a result of the excellent combination of biocompatibility, corrosion resistance and mechanical properties, Ti06Al4V which is medical grade titanium alloy, is the most commonly used for dental implant construction (Kuroda *et al*., 1998). Adding aluminium and vanadium in small quantities to Ti metal results in increased strength compared to the commercially pure titanium alone (Van Noort, 1987). Additionally, another advantage of titanium is the formation of oxide layer which spontaneously forms in the air and/or body fluids. Titanium comes in contact with the body via cells which interact with this oxide film (TiO_2); it will also make the surface suitable for cell adhesion and makes the titanium highly corrosive resistant and less toxic (Elias, 2011).

When a biomaterial is placed in the body, from the perspective of clinical safety, it should not cause any adverse effects on the surrounding tissues. A precise definition of biocompatibility is debated, but from the view point of immunity, biocompatibility is the ability of the material to stay in the same situation without influencing the host response (Williams, 2008). However, broadly there are three types of biomaterials: biotolerant materials such as gold and stainless steel, they are not rejected by the body and the tissue responds by the formation of fibrous capsule around them; bioinert materials such as titanium and titanium alloys that promote bone apposition from their surface resulting in contact osseointegration; and bioactive materials like hydroxyapatite (HA) and tricalcium phosphate which induce ion exchange with the

surrounding tissue causing the formation of a chemical bond along the interface (Sykaras *et al.*, 2000).

1.3 Complications associated with dental implants

Despite their wide use for replacing missing teeth, dental implants still face problems that limit their success in the long term for a patient. Dental implants have advantages over traditional dentures including durability, comfort and convenience for the patient. However, occasionally implants fail, and while the failure rates are modest (7%) (Chee and Jivraj, 2007), the prospect of further surgery is a concern for patients. Thus achieving success at the first attempt of implantation is preferable. The problems associated with dental implants generally arise from three main causes: Infection (Peri-implantitis); mechanical overload; and impaired healing (Hadi *et al*., 2011; Sakka and Coulthard, 2011). Peri-implantitis can be defined as an inflammatory process affecting the soft and hard tissues surrounding an osseointegrated implant resulting in rapid loss of supporting bone and associated with bleeding and suppuration (Lindhe and Meyle, 2008), while, peri-implant mucositis can be defined as a reversible inflammatory change of the peri-implant soft tissue without bone loss (Renvert *et al*., 2008). Dental implant surfaces are highly susceptible to infection because of biofilm formation on the dental implant surface and an impaired host immune response due to the surgical trauma that damages nearby blood vessels (Zhao *et al*., 2009). The metabolic acid produced by the microbes in the somewhat anaerobic conditions of the wound, and the inflammatory response of the patient, can also prevent osseointegration (Zhao et al., 2009). Subsequently, the implant becomes loose, and/or for infection control, needs to be removed.

Bacteria adhere to the tooth and implant surfaces by the formation of a complex biofilm. The biofilm is a microbial-derived sessile community characterised by microbes that are irreversibly attached to a substratum and/or interface to each other, embedded in a matrix of extracellular polymeric substances produced by microbes (Subramani *et al*., 2009). The first stage of biofilm formation is the formation of a portentous layer on the surface of the implant (Gibbons & Houte, 1973).The portentous layer can act as a suitable base for subsequent biofilm formation. Bacterial cells embedded in the biofilm become more resistant to the host defence mechanisms as well as to antibiotics, compared to free-floating cells (Prosser *et al*., 1987; Costerton *et al.,* 1999). Consequently, in combination with poor blood supply to the tissues around the implant after surgery, peri-implantitis cannot be easily treated or prevented using systemic antibiotics. Alternative approaches include coating the dental implant surface with an antibacterial agent to prevent biofilm formation and subsequent bacterial infection (Zhao *et al*., 2009). However, biofilm formation is an essential step in osseointegration, and any anti-microbial coating should ideally be selective for pathogenic microbes.

Bacteria are widespread in oral cavity; saliva contains 108 bacteria /ml along with proteins and glycoproteins that selectively bind to the surfaces of teeth, dental implant, restorations and prosthetic appliances (Subramani *et al*., 2009). Bacteria can adhere to the supra gingival part of the dental implant (i.e., the abutment and crown) to cause inflammation which consequently becomes peri-implantitis, and can ultimately lead to bone loss (Quirynen *et al.*, 2002). There are microorganisms which are harmless and normally found in the oral flora. These include some lactobacillus species that help in digestion (Walter *et al*., 2008). However, others that are most commonly associated with peri-implantitis are the same as those that cause chronic

periodontitis some of them include *Prevotella intermedia, Porphyromonas gingivalis, Actinobacillus actinomycetemcomitans, Bacterioides forsythus, Treponema denticola, Prevotella nigrescens, Peptostreptococcus micros, Fusobacterium nucleatum Staphylococcus spp. streptococcus spp.* and *Candida spp.,* early colonisers include *Staphylococcus spp*. and *Streptococcus spp*. (Leonhardt *et al*., 1999; Norowski and Bumgardner, 2009; Mahesh *et al*., 2011, Besinis *et al.,* 2017).

1.4 Dental implant surface modifications for improving osseointegration

As the implant surface is the first component to interact with the bone, several modifications have been done on the implant surface attempting to improve biocompatibility and osteoconductivity in order to enhance bone formation and subsequent biological fixation in the jaw bone (Coelho *et al*., 2009; Smeets *et al*., 2016). Surface treatments play a vital role in the success of dental implants. Modifying the dental implant surface enables the surface to enhance adhesion and differentiation of osteoblasts during the initial phase of osseointegration (Junker *et a.,l* 2009; Tomsia *et al*., 2011; Rupp *et al*., 2018). Dental implant surface topography can be classified into macro-, micro- and nanoscale topographies. The macro topography of an implant is based on its visible geometry (e.g; threads and tapered design). Combination of appropriate implant surface topography and adequate surgical technique while implant hole preparation can be considered as fundamental bases of clinical success of dental implants (Coelho *et al*., 2015). Recently, researchers have focused on micro- and nano- topographies (Besinis *et al.,* 2015; Smeets *et al*., 2016).

Albrektsson was the first to claim that the surface topography is important for osseointegration (Albrektsson *et al.*, 1981). This idea attracted the attention of many

researchers (Le Guehennec *et al*., 2007; Tomsia *et al*., 2011). It is now accepted that osseointegration and the primary stability of the implant can be enhanced by changing the surface topography (Albrektsson and Wennerberg, 2004). In dentistry, surface roughness has been classified into several categories: smooth surfaces have a value of less than 0.5 µm (height of the peaks), a minimally rough surface is 0.5 – 1 µm, moderately rough surface is 1-2 µm and rough surface is higher than 2 µm *(*Albrektsson and Wennerber*g,* 2004; Parekh *et al*., 2012). Moderately roughened surfaces are most commonly used in dental implants (Albrektsson & Wennerberg, 2004). Studies have shown that the bone to implant contact can be increased by increasing implant surface roughness (Fischer *et al*., 2012). Researchers have demonstrated that obtaining topographic surface modification of dental implant surface (roughness value of 0.5 to 2 µm) can increase the bone to implant contact and also biomechanical interaction of the interface between them (Coelho *et al.*, 2009). The response of cells to surface topography depends both on the cell type and the composition of the substrate. For example, fibroblast and epithelial cells adhere strongly to smooth surfaces. In contrast, osteoblasts proliferate better and collagen formation is greater on moderately rough surfaces (Wennerberg, 1998;Bachle and Kohal, 2004). Furthermore, increased surface roughness also induces fibrin clot stabilisation, which promotes direct growth of bone forming cells (Mendonca *et al*., 2008). However, bacterial adhesion and biofilm formation is also easier to establish on rough surfaces compared to smooth ones (Subramani *et al.*, 2009). Additionally, excessive roughness can be detrimental to the implant strength and also complicates implant removal when necessary (Tomsia *et al.*, 2011).

Dental implants had machined surfaces until early nineties; involving turning, milling, and/or polishing during the manufacturing process (Buser *et al*., 2012;

Esposito et al., 2014). Machining procedures which were considered as the gold standard for implant surface design, results in minimally rough surfaces of 0.4 – 0.8 µm, which requires several months for osseointegration (Coelho *et al.*, 2009). Machined surfaces allow bone cells to grow and mineralise to produce new bone; with typical healing times of 3 to 6 months depending on local factors such as bone quantity and quality (Abraham, 2014). Researchers have tried various methods for surface modification; including acid etching, sandblasting, grit-blasting, anodizing, nanoparticles deposition, etc. Some of these methods can enhance osseointegration by producing a rough surface that increases the surface area for bone contact and firm mechanical interlock, consequently improved implant stability (Romanos *et al.*, 2002; Ehrenfest *et al*., 2010). Besides increasing surface roughness, surface treatment also results in a higher friction coefficient and insertion torque than untreated implants, thus improving primary stability (Dos Santos *et al.*, 2011).

Common methods that are used for modifying the dental implant surface are: machining, acid etching, plasma spraying, grid blasting and anodization (Le Guehennec *et al*., 2007). Acid etching can be used for creating a clean and uniform surface finish which is free of contaminations (Liu *et al*., 2004). Acid etching treatment produces a surface with micro cavities with having defined edges. Usually a strong acid such as: hydrofluoric (HF), nitric (HNO_3), and sulphuric (H_2SO_4), or a combination of these acids is commonly used to acid etch dental implant surfaces (Jemat *et al*., 2015). Acid etching increases the metal surface roughness resulting in homogenous roughness (Guo *et al*., 2012). Moreover, etching the dental implant surface with various concentrations of H_2SO_4 significantly increased the surface roughness (Iwaya *et al.,* 2008). This type of surface induces osteogenic cell retention and migration toward the implant surface (Cho and Park, 2003; Braceras *et al*., 2009; Al-Radha *et*

al., 2012). However, acid etching procedure can cause hydrogen embrittlement of the titanium leading to the creation of micro cracks on the surface of implant that may lead to enhanced corrosion or fatigue of the metal. It also makes the titanium brittle and more susceptible to fracture (Yokoyama *et al*., 2002).

Titanium Plasma Spraying (TPS) is another method that is used for roughening dental implant surfaces. In this method titanium powders are injected into a plasma torch at high temperature forming a film about 30 µm thick (Le Guéhennec *et al*., 2007). Surface roughness value obtained by TPS is around 1.82 µm (Sykaras *et al*., 2000). The surface area of dental implants after TPS is approximately six times the initial surface area (Schroeder *et al*., 1981); depending on implant geometry, initial powder size, plasma temperature, and distance between the nozzle output and target (Coelho *et al*., 2009). Another frequently used method is grit- blasting in which hard ceramic particles are used to roughen the surface, and the degree of roughness is dependent on the size of particles used (Le Guehennec *et al*., 2007). Various particles are used for blasting the titanium surface such as aluminum dioxide, titanium dioxide and calcium phosphate (Sykaras *et al*., 2000). The grit-blasting technique significantly increases the surface roughness. Bacchelli and co-workers found that the surface roughness value after grit-blasting the surface of titanium with Al_2O_3 grit (250–500 µm) was 1.74 ± 0.12 µm (Bacchelli *et al*., 2009). Moreover, blasting dental implant surfaces with titanium oxide having 25 µm as an average particle size produces, 1-2 µm implant surface roughness (Le Guehennec *et al*., 2007). The disadvantage of this technique is the possibility of particles' release or dislodgment into the surrounding tissue after implant insertion that can have a detrimental effect on osseointegration. Besides improving and enhancing the osseointegration process, grit-blasting can also accelerate bacterial adhesion on the implant surface. Al-Radha *et al*. (2012) found that

bacterial adhesion on implant surfaces blasted with ZrO_2 particles is better compared to the control. A combination of grit-blasting followed by acid etching is also beneficial since it results in increasing total surface area of the implant, compared to machined surfaces. Additionally, any remnant particles that have been left after blasting procedure which are toxic to the cells can be removed by acid etching. Roughness values of 0.5 to 2 µm can be obtained with this dual surface treatment (Coelho *et al*., 2009). Sandblast, Large-Grit, and Acid Etching (SLA) uses a strong acid to induce an erosion on surfaces that have been blasted with large-grit sand particles resulting in a formation of pits and cavities which increases the surface roughness hence improving tissue integration and cell proliferation (Zinger *et al*., 2004; Kim *et al*., 2008; Hung *et al*., 2013).

Anodisation is another method that thickens the oxide layer to 1000 nm on titanium. Mechanical interlocking with the bone and biochemical bonding are improved due to the oxide layer on anodised titanium surfaces as well as higher clinical success as compared to machined implant surface of similar shapes (Parekh *et al*., 2012). However, this superior clinical performance is due to the change in chemical composition not the surface roughness, since, minimal rough surface is created after anodization, so comparisons are often made with minimally rough surface implants rather than moderately roughened implants. It can also change surface topography and physical properties (Wennerberg & Albrektsson, 2009).

All of the surface treatments (modifications) above have several advantages but also possible drawbacks. The surface roughness is not biologically active in attracting bone cells, also, the treatments may not provide any antimicrobial properties to the surface, beyond the inherent chemistry of the material.

Coating the dental implant surface with osteoconductive and/or antibacterial agents might therefore be desirable. A wide range of biomaterials have been used as dental implant coatings, such as bioactive ceramics like HA. HAs have been used as bioactive ceramics that can adsorb more proteins, integrins as well as osteoblast precursor cells than commercially pure titanium (Woodard *et al*., 2007; Hasegawa *et al*., 2016; smeets *et al*., 2016). HA itself has no inherent antibacterial properties (Kilpadi *et al*., 2001). Antimicrobials include inorganic agents like silver as a coating over the HA, as well as antibiotic incorporated HA. For the latter, HA has been loaded with antibiotics (amoxicillin or vancomycin), (Alt *et al*., 2006; Harris *et al*., 2006). But there are still technical limitations to this approach, antibiotic agents can be damaged by the high temperatures needed for the HA coating formation. Alternatively, significant amounts of antibiotic agent can be absorbed onto the surface of calcium phosphate, which then causes burst release of antibiotics (80-90% release) within the first 60 minutes of implant placement (Radin *et al*., 1997). Coatings loaded with organic disinfectants such as chlorhexidine have also been tried; and shows antibacterial activity especially with *Staphylococcus aureus* (Campbell *et al.*, 2000). However, chlorhexidine can be toxic to the osteoblast cells through the same toxicity mechanism to the bacterial cells (Harris *et al.*, 2006; Zhao *et al*., 2009), and the disinfectant effect is very transient.

1.5 Nano-enhanced surface modifications of the dental implant

Recently, nanotechnology has opened a new scope of research in enhanced biomaterials. Nanotechnology can be defined as ‘using materials and structures with nanoscale dimensions, usually in the range of 1-100 nm’ (Handy and Shaw, 2007).

Nanoparticles are now playing a vital role in the field of biology and medicine as a result of their small size and targeted effects, as well as interacting with biomolecules (Navalakhe and Nandedkar, 2007). Products containing nanotechnology can be broadly classified into three major groups: either the material is made mainly of nanoparticles, or a commercial product is give a nano coating on the surface, or during manufacture nanoparticles may be incorporated into a traditional material such as a polymer (Handy and Shaw, 2007). The most common type of nanomaterials that are used in dental implants and other biomaterials are in the form of coatings (Tomsia *et al*., 2012).

Positive results have been achieved with nanophase materials (ceramics and metals) regarding osteoblast cell adhesion, proliferation and calcium deposition as well as improved bioactivity and biocompatibility as compared to micro-meter scale grains. In addition, they possess better antibacterial activity than micro-meter sized grains (Engel *et al.*, 2008; Hajipour *et al.*, 2012). Combination of osteoconductive and antibacterial nanoparticle coating on the titanium dental implant might be an effective solution for the current problems of dental implants. For the antibacterial aspect, several nanomaterials have been used (Besinis *et al*., 2015). Samuel and Guggenbichler. (2004) incorporated silver nanoparticles in polymers like polyurethane and silicone used for catheters and found that a silver nano-impregnated catheter can exhibit excellent antimicrobial activity. Moreover, it has been found that nano Ag-Cu doping can potentially increase the corrosion resistance of dental amalgams (Chung *et al.,* 2008). Another application of nanoparticles (HA) is to repair enamel mineral loss, since the building block of enamel is similar to 20 nm HA, and so the artificial material (nano HA) can adsorb to the tooth structure thereby suppressing secondary caries formation and preserving the hardness of the enamel (Li *et al.*, 2008). Dental

composite incorporated quaternary ammonium polyethylenimine (PEI) nanoparticles have improved antibacterial activity on account of preventing biofilm formation (Beyth *et al*., 2006). Nanoparticles have superior antibacterial effects as compared to classic organic antibacterial agents (Hajipour *et al.*, 2012). This is due the ability of nanoparticles to coat the surface giving a persistent antibacterial property.

1.6 Antibacterial activity and biocompatibiltiy of silver nanoparticles

Silver nanoparticles are known to have a strong antibacterial activity against a wide range of microorganisms (Morones *et al*., 2005; Besinis *et al*., 2015). However, the possible cytotoxic effects of silver nanoparticles can limit their use in biomedical fields (Ahamed *et al.*, 2010). The exact mechanism of cellular and bacterial toxicity of silver nanoparticles is still being investigated, possibilities include the release of free metal ions from the surface of the particle (dissolution), or oxidative stress by generation of reactive oxygen species (ROS) from the surface of particles (Besinis, *et a*l., 2014; Reidy *et a*l., 2013; Greulich *et al*., 2012). However, it is still unclear whether the toxic effect of silver nanoparticles is exerted by the particles themselves or by dissolution of silver ions (Albers *et al*., 2013). The mechanisms of free metal ion toxicity are well known for silver. Silver ions increase cellular permeability that can cause leakage of cellular contents, including the subsequent disruption of DNA replication. It also inhibits the Na^+K^+-ATPase to cause osmotic disturbances that lead to this leak (Marambio-Jones and Hoek, 2010). Theoretically, eukaryote cells might take up intact silver nanoparticles (e.g., by endocytosis) into sub-cellular locations where there could be a localised release of a high concentration of silver ions which can bind to biomolecules and interacting with membrane-bound receptors (Reidy *et al*., 2013). Silver ions have a high affinity for thiol (-SH) groups that are available in proteins,

amino acids, etc., and conformational change due to silver binding can inactivate proteins. The latter may also be involved in bacterial inactivation (Liau *et al*., 1997). Indeed, the presence of some biomolecules can enhance silver dissolution in the biological medium *(*Gondikas *et al., 2012;* Loza *et al*., 2014). This subsequently results in increasing total silver concentration in the cell culture medium that might have toxic effects to the cell monolayer, depending on whether or not the ligand bound silver becomes bioavailable to the cells. Bioavailability is the proportion of a drug or other substance (metal) which enters the circulation (or cells) when introduced into the body and so is able to have an active effect. Silver ions can precipitate as an insoluble salt (silver chloride) in the presence of chloride in the culture media hence decreasing the toxicity (Greulich *et al*., 2011).

Researchers have tried to solve the problem of infection by coating the dental implant surface with silver nanoparticles. Metal nanoparticles are frequently used in dentistry as an attempt to tackle bacterial infection (Melo *et al*., 2013). The interest is to replace the traditional micron-sized antimicrobial metal powders with their nanoscale counterparts (Besinis *et al*., 2015). This approach attempts to prevent bacterial biofilm formation and subsequent colonisation. For example, Juan and co-workers found that a silver nanoparticle modified titanium surface had remarkable antibacterial and anti-adhesive activities against *Staphylococcus aureus* and *Escherichia coli*. (Juan *et al*., 2010). Moreover, Besinis *et al. (2014)* found that silver nanoparticles were more antibacterial to *S. mutans* than the traditional chlorhexidine disinfectant used in dentistry.

Despite having positive antibacterial activity, the possibility of adverse effects of silver nanoparticles on human and other mammalian cells due to prolonged exposure at various concentration levels are still being elucidated (Asharani *et al*.,

2008). Table 1.1 shows examples of the toxicity of silver nanoparticles on different mammalian cells.

Table 1.1 Examples of the toxic effect of silver nanoparticle on different mammalian cells

Target cells	Particle type and size	Exposure concentration/time	Key aspects	Study
Human osteoblast cells	Silver nanoparticles used were in the form of a nanosilver colloidal dispersion with a nominal silver content of 10 wt.% in a stabilizing matrix.	24h, 7days and 21 days / 10 mg g^{-1}	No silver nanoparticle-induced cytotoxicity against OB was detected after 24 h and 7 days. While, after 21 days a significant impairment of cell viability was observed	(Pauksch *et al.*, 2014)
Primary osteoblast cells	Average size of silver nanoparticles was 50 nm. Information about the type of particles are not given	194.3, 146.1 mg L^{-1} for 72 hours	Mean half maximal inhibitory concentration of silver nanoparticles was 194.3 mg L^{-1} for cell viability and 146.1 mg L^{-1} for cell differentiation. The molar concentration (mmol) of free Ag+ within the culture medium was 0.063 for osteoblast viability and 0.059 for osteoblast differentiation.	(Albers *et al.*, 2013)

Human fibroblast cells	Starch-coated silver nanoparticles were used. Average size of the particles were not given.	25 and 50 mg L^{-1} for 24, 48 and 72 hours	For 25 mg L^{-1}, the concentration of intracellular adenosine triphosphate (ATP) content of the cells was not different statistically within the control after day 1 and day 2. However, statistically significant difference was observed after 3 days. While for 50mg L^{-1}, ATP content started to decrease significantly from the second day.	(Asharani *et al.*, 2009)
Human hepatoma cells	Size of silver nanoparticles were 7-10 nm. They were stabilized with polyethylenimine.	Higher than 1 mg L^{-1} For 24 hours	Up to 0.5 mg L^{-1} of silver nanoparticles causes increased cell viability for 120% as well as cell proliferation in relative to the unexposed control. however, exposure of more than 1.0 mg L^{-1} of silver nanoaparticles exhibited significant cytotoxicity	(Kawata *et al*., 2009)

Primary liver cells (mouse)	Spherical silver nanoparticles were used and the size range was 7-20 nm.	225 mg l^{-1} , 900 mg L^{-1} respectively for 24 hours	Quantification of AO/EB stained primary fibroblasts of unexposed cells was 98±1% while the number of cells which were exposure to 225 mg L^{-1} SNP, was 71± 3% and 32 ± 2% cells were survived after exposure to 900 mg L^{-1}.	(Arora *et al.*, 2009)
Human hepatoma cells	Citrate capped silver nanoparticles (size not defined)	1 and 10 mg L^{-1} for 24 hours	MTT assay showed that the cell viability after exposure to 1 mg L^{-1} silver nanoparticles was 80% of unexposed control, while it was 70% for 10 mg L^{-1}.	(Vrcek *et al.,* 2016)

The results in the previous table indicate that silver nanoparticles can be toxic to different cells at different concentrations. It is been shown that silver nanoparticles can be toxic to osteoblast cells at a certain dose and the toxic dose for inhibiting cell differentiation is smaller than that for cell viability. Additionally, with the increase of silver concentration and exposure time, fibroblast cell damage increases. The results also conclude that the toxic effects of silver nanoparticles increase with exposure time.

The challenge when using silver nanoparticles in medicine and dentistry is to use silver nanoparticles at a condition which can kill the bacteria without having toxic effects to the cells. However, several experiments have been conducted proving that the minimum lethal dose of silver nanoparticles to bacterial and human cells is the same. For example, Greulich *et al*. (2012) argued that the lethal dose of silver nanoparticles to *Staphylococcus aureus* and human mesenchymal cells are at the same concentration (50 mg L^{-1}). However, Shrivastava *et al*. (2007) demonstrated that 25 mg L^{-1} was enough to kill gram negative bacteria.

It could be challenging to define the cytotoxic concentration of silver nanoparticles (or silver ion). Since the toxic effect of silver nanoparticles can be different in different cell lines, for example, Hela cells (epithelial adenocarcinoma cell line of the cervix) were more sensitive than HacaT Cells (immortal; non-cancerous human keratinocyte cell line) when exposed to silver nanoparticles for 72 hours at the same condition (Mukherjee *et al*., 2012).

Moreover, the size of nanoparticles potentially affects their toxicity. For example, smaller particle sizes of silver are sometimes more toxic to the bacteria and cells due to the large number of atoms present on the surface that can interact with bacteria or induce higher amount of silver ion release (Marambio-Jones & Hoek, 2010). In cells, exposure to a 10 nm primary diameter size of silver nanoparticles for 24, 48 and 72

hours had greater apoptotic effect than 50 and 100 nm sizes (Kim *et al.*, 2012). This is also the case for bacterial cells, as it was found that the 10 nm silver nanoparticles were the most effective against bacteria compared to larger sizes (Varren *et al*., 2007). Another factor is particle shape; the strongest antibacterial activities have been achieved with particles containing more facets such as triangular particles. This could be due to the larger atom densities on the facet that lead to the availability of more atoms for interaction (Morones *et al*., 2005; Pal *et al*., 2007; Marambio-Jones & Hoek, 2010).

Besides achieving promising antibacterial activity, coating nanoparticles on the surface of the titanium dental implant can potentially increase bone to implant integration since tissue responses and extracellular matrix formation are occurring at nanoscale level. Thereby, coating implants with nanoparticles of bioactive ceramics such as HA can promote cell adhesion and integration with the surrounding bone tissue (Tomsia *et al*., 2011). In dental implants, the non-physiological surface (TIO_2) is exposed to a physiological environment. So a physiological transition can be established through generating a coating that mimics the composition of the living bone (Jonge *et al*., 2008). The chemical composition of HA is biocompatible and safe to the surrounding tissues, it is mainly composed of calcium phosphate which is bioactive material and resembles the mineral constituents of human bone. So by virtue of its chemical composition, traditional HA coated titanium can more rapidly incorporate with the living bone as compared to the uncoated titanium (Piattelli *et al*., 1993). HA coating also acts as a barrier to reduce the release of metallic ions that can be toxic to the surrounding tissue, so HA coated Ti6Al4V is more resistant to corrosion than uncoated Ti6Al4V (Kwok *et al.*, 2009). It could be argued so far that HA nanoparticles coating on silver nanoparticles can potentially reduce Ag induced toxicity,

as it was found that coating silver nanoparticles with other materials (e.g., carbon) that prevent direct contact between Ag and the cells, can reduce their cytotoxic effects (Samberg *et al*., 2010). Moreover, since HA is bioactive, ion-exchange between HA coated titanium and the surrounding body fluid leads to the formation of a carbonate apatite layer on the implant that is chemically equivalent to the mineral phase in bone. This inevitably results in enhanced healing process (De Jonge *et al*., 2008). Better long term clinical successes have been achieved using HA coated titanium dental implant as compared to uncoated titanium dental implant which is the result of superior initial rate of osseointegration (Le Guehennec *et al*., 2007). HA has more ability to absorb cell attachment proteins, purified integrins and the whole osteoblast precursor cells than titanium. Thus, HA coated implants can have improved protein and cell adhesion as well as enhanced binding capacity as compared to uncoated titanium (Kilpadi *et al*., 2001). Shi and co-workers investigated the size-dependent effect of nanoparticles of HA and they found that nanoparticles with diameter of 20 nm was most effective in promoting osteoblast cell growth and preventing apoptosis (Shi *et al*., 2009).

There are two fundamental approaches to the synthesis of Ag-HA composites on medical grade Ti alloy. The first involves growing a layer of biocompatible material on the surface of the alloy, for example micron-scale HA (Hung *et al*., 2013), or a material with topography that promotes osteoblast adhesion such as TiO_2 nanotubes (Lee *et al*., 2015). Then, this biocompatible layer is covered with silver nanoparticles (e.g., by reduction of a silver solution, Gunputh *et al*., 2018). Having the silver as the uppermost layer, in theory, offers a biocidal advantage. Any dissolved silver released from the coating will be directly toxic to microbes. In the case of silver nanoparticles, both metal dissolution from the particles and direct contact of the particles with

microbes can be toxic (Reidy *et al*., 2013; Besinis *et al*., 2014a; b). However, there remains a problem in that the osteoblast cells have limited access to their preferred substrate (i.e., the HA) underneath the silver layer.

The alternative approach is to coat the Ti alloy with silver, and then add a layer of biocompatible HA. The silver coating is typically achieved by electroplating and depending on the silver solutions, voltage and temperature used; silver nanoparticles may be grown on the surface (Besinis *et al*., 2017). Then either a micron- or nano-HA can be added as a final coating. Crucially, provided the HA coating has some porosity (i.e., spaces in between the HA particles), then the antibacterial properties of the silver layer is retained. For example, Besinis *et al*. (2017) found that nano silver and nano HA coating on titanium dental implants had a significantly better antibacterial activity against *Streptococcus sanguis* than uncoated titanium.

1.7 Hypothesis

The failure of dental implants arising from bacterial infection remains a concern. Nanotechnology offers the potential to improve implant success. Silver is a profound antibacterial agent that can provide antibacterial activity of the implant surface, HA is a biocompatible agent that can mask silver toxicity to the human primary osteoblast cells and preserve the biocompatibility of the coated dental implant. The hypothesis of this study is that coating the dental implant surface with nano silver and nano HA would provide antibacterial activity whilst maintaining the biocompatibility of the implant surface with human primary osteoblast cells, and that these properties may be enhanced at the nanoscale.

1.8 Aim and objectives

The aim of this study was to investigate the biocompatibility of silver and HA nanoparticle coating on medical grade titanium dental implants. The specific objectives were:

1- To successfully coat the medical grade titanium discs with silver and HA coatings.
2- To investigate the stability of nano-coatings in cell culture medium by conducting the dialysis experiment to measure the release of dissolved silver.
3- To investigate the bonding strength of the coatings by conducting mechanical pull-off test.
4- To demonstrate the biocompatibility of silver nanoparticle coating on medical grade titanium to osteoblast cells. This was determined in cultured osteoblasts

with a range of toxicological endpoints including LDH release and the Alamar blue assay for cell viability.

5- To investigate the effect of silver nanoparticle coating on medical grade titanium on osteoblast cell activity and functioning. This was performed by measuring alkaline phosphatase (ALP) enzyme activity in the external media and the cell homogenate.

6- To investigate the effect of silver nanoparticles on cell electrolyte concentrations and Na^+ K^+-ATPase activity (osmotic health of the cells), as it is known that silver interferes with Na^+ and K^+ pump.

7- To measure the long-term silver release to the external media. This is to ensure continous supply of antibacterial silver.

8- To study the differentiation and mineralisation of human primary osteoblast cells on the coatings. This was achived by measuing Ca^{2+} and P in the cell homogenate after 21 days, also conducting the mRNA expression study on osteoblast differentiation and mineralisation genes (e.g; ALP, osteocalcin and RUNX-2) using quantitative real time PCR (qPCR).

Chapter 2

Sample preparation, characterisation and method development

2.1 Introduction

Several methods have been tried to produce an osteoconductive and antibacterial coatings on the surface of titanium dental implants. In particular, silver has been introduced to the surface of implant made of titanium and its alloys to enhance their antibacterial activity. Several techniques have been used to produce a silver layer on titanium dental implants. For example, (Ewald *et al*., 2006) used physical vapour deposition (PVD) to produce a silver coating of approximately 2 μm in thickness on a titanium substrate. Moreover, silver has been ion implanted into the titanium and Ti-Al-Nb alloy to improve antibacterial characteristics, wear performance and corrosion resistance (Wan *et al*., 2007). Moreover, TiO_2 nanotubes have been grown on the surface of titanium implants and then the layer is covered by silver nanoparticles using chemical reduction of a silver solution (Gunputh *et al*., 2018).

Several different methods have been used to produce silver and HA coatings. However, trying a new coating method could be effective in producing a novel nano-sized coating on the surface of titanium. Silver nanoparticles can be coated on titanium dental implants by an electroplating method. According to this method sliver ions dissolve from the anode and reduces on the titanium substrate which has been connected to the cathode. The silver coating produced can have effective antibacterial characteristics. In addition to silver particles and silver nitrate, Spadaro *et al*. (1974) found that silver generated from the anode electrode can inhibit bacterial growth. On the other hand, HA nanoparticles can be coated on a silver layer using sintering method at a temperature which is below the melting point of silver. The former can improve biocompatibility and promote osseointegration process.

The bioavailability of silver nanoparticles in different biological media can vary as a result of the ionic strength of silver, high affinity of silver and -SH groups and

ability to form poorly soluble silver chloride salt. This can occur typically in complex biological media as they contain oxidising species, glucose, chloride and proteins which affects the release of silver ions from silver nanoparticles (Zook *et al*., 2011; Loza *et al*., 2014).

It has been found in literature that complexation of silver ions can occur as a result of presence of organic molecules which thereby accelerate the dissolution. However, selenide-containing compounds (eg; cysteine) can cover the particle surface and prevent the dissolution. For example, Loza *et al*. (2014) found that silver ion release from silver nanoparticles was blocked in the presence 1 g L^{-1} cysteine. Dissolution of silver nanoparticles in cell culture media (DMEM) is higher as compared to the inorganic salt solutions (Zook *et al*., 2011). This might be due to the complexation of silver nanoparticles with the proteins and other components in the cell culture media. Silver ions tend to bind to chloride and produce a silver chloride which is a poorly soluble salt (Greulich *et al*., 2011). In the present thesis, the effect of different cell culture medium on silver dissolution from coated titanium discs was investigated. The results of this study demonstrated the amount of dissolved silver in each cell culture medium. Therefore, the most suitable cell culture medium which induced minimum silver dissolution was identified and used for the biocompatibility and mineralisation experiments.

One of the limitations of using biochemical assays in the presence of nanoparticles is the possible interference that might occur between components of the assay and the nanoparticles. Nanoparticles in general have been found to interfere with lactate dehydrogenase (LDH) assay components (Han *et al*., 2011). Silver nanoparticles in particular have also been found to interfere with LDH assay. Oh *et al*. (2014) found that silver nanoparticles can adsorb the LDH enzyme which in turn leads

to under estimation of the actual LDH level. Reactive oxygen species that are produced by silver nanoparticles inside the cell are also able to inactivate LDH. Silver nanoparticles can attract proteins to form a layer on the surface of the particle known as a protein corona (Hellstrand *et al*., 2009). In any biochemical assays that incorporate silver nanoparticles with proteins, silver interference with the assay components should be tested prior to the experiment.

The aim of this chapter was to successfully coat the titanium discs with silver and HA particles and investigate the bonding strength of the coatings to the titanium alloy surface as well as the stability of these coatings in different cell culture media. A secondary aim was to investigate the interference of silver nanoparticles with biochemical assays used in the biocompatibility and mineralization experiments.

2.2 Materials and methods

2.2.1 Preparation of titanium discs

Grade five titanium alloy Ti6Al4V (ASTM Grade 5) measuring 15 mm in diameter and 1 to 1.5 mm thickness were prepared by laser cutting; method for preparing the discs is based on Besinis et al. (2017). All discs were polished with (800-1200 grade) sand papers using a rotary instrument (Grinder-Polisher, Buehler, UK Ltd, Coventry, England). Six and one µm diamond solutions (Diamond solution, Kemet International Ltd, Parkwood Trading Estate, Maidstone, Kent ME15 9NJ UK) were used for the final polish. Discs were subsequently cleaned with alkaline solution (20 g L^{-1} of NaOH and Na_2CO_3 solution) in an ultrasonic bath of distilled water (Metason 129T, Struers). Further cleaning with 5% HCl solution was carried out for 3-5mins.

2.2.2 Silver electroplating

Electroplating is a process that uses electrical current to reduce dissolved metal cations so that they form a coherent metal coating on an electrode. Electroplating is used for coating a metal with a thin layer of another metal. The metal to be coated is connected to cathode (positive side) and the coating metal to the anode (negative side) of the DC power. Both metals are put in a chemical solution (electrolyte) which allows an electric current to flow. The electroplating method was derived from Besinis *et al*., 2017. Briefly, the clean titanium discs were hung on silver or platinum wires connected to the cathode of a voltage supply, while the silver plating source consisting of a fine silver sheet (1 mm thickness, 50 mm x 100 mm, Cooksongold Ltd, UK) comprised the anode. The disc and silver sheet were immersed in an electrolyte containing (0.2 M $AgNO_3$, 4 M succinimide and 0.5 M KOH, Sigma Aldrich, UK) at 40 ^{O}C and the voltage was adjusted to 1 V and left for 3 minutes. The resulting silver plated discs were washed with distilled water to remove the electrolyte.

2.2.3 Hydroxyapatite coating using a sintering technique

The HA nanoparticles solution was purchased from (Fluidinova, Rua Eng. Frederico Ulrich 2650, 4470-605 Maia, Portugal); while a 15 % wt/v dispersion of HA microparticles was prepared by adding 15 g of HA powder (Fluidinova, Rua Eng. Frederico Ulrich 2650, 4470-605 Maia, Portugal) to 100 ml of Milli-Q water (18.2 MΩ), the solution was then vortexed for 10 minutes. The silver plated discs were individually placed in the wells of 24 well microplates (flat-bottom, sterile, polystyrene microplates, Greiner 662160, Bio-One Ltd., UK) and then 20 µl of the appropriate HA dispersion

(nano- or micro- particles) were deposited to the top of surface of the discs and distributed evenly with a pipette. The discs were left in an incubator at 37 ºC to dry for 48 hours. Finally, the specimens were transferred to porcelain dishes and placed in a programmable furnace for sintering (Carbolite, ELF 11/14, UK). The rate of temperature increase in the furnace was 10 ºC/min until 500 ºC was achieved. This final temperature was maintained for 10 minutes. These heating rates and temperatures were selected following the method describes by Besinis *et al*., 2017. Subsequently, the now HA and Ag coated discs were left in the furnace to cool down to room temperature.

2.2.4 Surface roughness measurements of the specimens

The surface roughness values were measured using the method previously descibed by Besinis *et al*. (2017). In brief, measurements were taken using an Olympus LEXT Confocal Microscope OLS 3000, with a total magnification of 50× and an optical zoom of 1×. Gaussian filters were applied to the profiles with a cut-off wavelength value of 85.2 μm. Surface roughness was measured at three different locations in each of 3 replicates from each treatment. Following the surface roughness values, the topographical investigations were performed by taking 3D images using an Olympus LEXT Confocal Microscope OLS 3000.

2.2.5 Investigating surface morphology by scanning electron microscopy (SEM) and energy dispersive spectroscopy (EDS) analysis

The silver plated, as well as the nano- and micro- HA- coated discs were examined under SEM mode (JEOL / JSM-7001F, with an Oxford Instruments INCA X-ray analysis system attached) to confirm the presence, quality, and composition of the coatings. At least one disc of each type from each batch of discs prepared were examined (n = 3 discs/treatment). Detective energy was 15 KeV at a working distance of 10 mm. A thin layer of Chromium was sputter coated on the specimens to increase conductivity and therefore the resolution for imaging. Moreover, qualitative and quantitative metal analysis were carried out on at least one disc of each type from each batch of discs prepared (n = 3 discs/treatment) using Energy Dispersive Spectroscopy (EDS, spot size, 10 μm; accelerating voltage, 15 kV; working distance, 10 mm). The, data and spectra analysis were performed using the Aztec 2.2 software supplied with the instrument.

2.2.6 Investigating the particle size of nHA and mHA by transmission electron microscopy (TEM)

The HA primary particle size in nHA and mHA solutions which were used to coat the specimens was investigated using transmission electron microscopy (TEM, JEOL-1200EX II). The solutions were prepared as described earlier in section 2.2.3, they were diluted with Milli-Q water by factor 2000 (nHA) and 1000 (mHA) to decrease the concentration of the dispersion to approximately 100 mg L^{-1} (Besinis *et al*., 2014). This enables better visualisation of particles and facilitates measuring dimensions to

accurately work out the primary particle size. Image J software (version 1.49) was used to determine primary particle sizes manually.

2.2.7 Investigating the stability of the coatings in cell culture medium by dialysis experiment

The stability of silver nanoparticles coating may be affected by the cell culture medium since organic molecules are able to enhance silver dissolution in the ionic form. The dialysis method was based on Handy *et al*. (1989). A dialysis experiment was performed to investigate the effect of standard cell culture medium which is Dulbeco's modified eagle medium (DMEM) supplemented with 10% foetal bovine serum (FBS) (Fisher scientific UK) and 1% of penicillin-streptomycin (Life Technology), on the dissolution of silver nanoparticles coating on titanium. The cumulative amount of silver ion was measured from the dialysis tubing and from the external media in the beaker. All the beakers were acid washed in a 5% nitric acid bath for 24 hours before the experiment in order to remove any particles or ions that may have been stuck on the walls of the beaker from previous use. The final stock solution was DMEM supplemented with 10% FBS and 1% antibiotic and antimicotic. The control to cell culture medium in this experiment was Milli-Q deionised ultrapure water. In this experiment, there were four experimental groups: blank, silver plated discs, silver plated+nHA discs and silver plated+mHA discs, x3 beakers (250 ml) for each group (triplicate) all were put in Milli-Q water (control) and cell culture medium. The discs were put in cellulose dialysis bags (product code: D9777, cellulose membrane with molecular weight cut off at 12,000 Da, pore size < 2 nm, Sigma-Aldrich Ltd, Dorset, UK). The pore size allows ions to permeate the dialysis membrane but not particles. The bags were closed tightly from the bottom by making knots that did not allow the

solution to leak from the bag. then the discs were put in the bags and finally 4 ml of solution added to the bag and then the open end was secured with a mediclip (to prevent leakage) in a position which is just 1 cm above the level of solution so as not to compress the solution. Finally, another knot was made at the top above the mediclip. The bags were hung from stands using a nylon thread which were knotted to the stand tightly, and then the bags were put into the 250 ml beakers containing 246 ml stock solution, magnetic stirrers were put in all beakers and the experiment was run under stirring (RO 15P power, Ika-Werke GmbH & Co. KG, Staufen, Germany). Once the bags were placed in the beakers, 5 ml sample from the media were taken, 4 ml as a zero time point sample and 1 ml for measuring the pH. This was followed by series of 5 ml samples from the beakers at 30 min, 1, 2, 3, 4, 6, 8 and 24 hours. The pH was measured at each time point and one extra beaker with a stock solution was used just to monitor the temperature of the media.

2.2.8 Dissolution of silver nanoparticles in different cell culture medium

The results showed that there were some silver dissolution in the standard cell culture medium (DMEM+10%FBS+1%antimicrobial), to better investigate the cause of dissolution, this experiment used Ag+nHA discs in cell culture medium with different concentration of FBS to study the effect of the FBS in culture medium on dissolution of silver ions. And also the Physiological saline (modified Kerb's ringer) was compared with DMEM to see its effect on silver dissolution. Another medium which is human osteoblast cell culture medium (HOB) was used as an experimental group. The control of this experiment was (DMEM+10%FBS and 1% antimicrobial) with the disc. While (DMEM+10%FBS and 1%antimicrobial) without the disc and (Physiological

saline+10%FBS+1% antimicrobial) as well as (HOB+1%antimicrobial) without discs were used as blanks. The experimental groups were DMEM+ 5%FBS and 1% antibiotic, DMEM+ 1%antibiotic, (75% DMEM + 25% Physiological saline) + 10%FBS + 1%antimicrobial, (50% DMEM + 50% Physiological saline) + 10%FBS + 1%antimicrobial, Physiological saline + 10%FBS + 1% antimicrobial and HOB + 1%antimicrobial. Composition of physiological saline is shown in Table 2.1. All the experimental groups were in triplicates. The experiment was run under sterile condition, samples (discs) were sterilised by gamma radiation (radiation dose 36.42-40.72 kGy for 10 hours) and were placed in 24 well-microplates. Subsequently, 0.6 ml of cell culture medium was added to each well and the plates were incubated for 72 hours in 5% CO_2 / 95% air incubator (HETO-HOLTEN Cell House 170) maintained at 37°C. The media were replaced every day with a fresh media and the concentration of silver ions was measured in the stock media with ICP-MS (ICP-MS, X Series 2, Thermo Scientific, Hemel Hempstead, UK) after acidification with 20 µl of 100% nitric acid. After 3 days, the samples were washed with Milli-Q water and coated with a thin layer of chromium then visualised under SEM to investigate the effect of FBS on physical stability of the coatings.

Table 2.1. Components of modified kerbs ringer solution (physiological saline)

Chemicals	**Concentration (mmol)**
Sodium chloride (NaCl)	118
Potassium chloride (KCl)	3
Magnesium sulfate pentahydrate ($MgSO_4.5H_2O$)	1
Calcium chloride ($CaCl_2$)	2
Bicarbonate buffer ($NaHCO_3$)	25
Potassium dihydrogen phosphate (KH_2PO_4)	1.2
Glucose	10

2.2.9 Pull-off test

Pull off test is a quantitative method of characterising the adhesion between a coating and a specific substrate. In this study, the adhesion between the coatings and the titanium was tested. Square titanium alloy specimens (31 x 31 mm) were used. The control in this experiment was uncoated titanium disc, treatments were silver plated titanium (Ag), silver plated plus HA nanoparticles (Ag+nHA) and silver plated plus HA micropartilces (Ag+mHA), 6 replicates were used in the test. The protocol was derived from Gombos and Summerscales, (2016) according to ISO standard (EN ISO 4624:2016). Six specimens were tested on each occasion, to ensure proper alignment while fixing the specimens during the test, an alignment tool was used which prevents misalignment and can hold 6 specimens together (Figure 2.1).

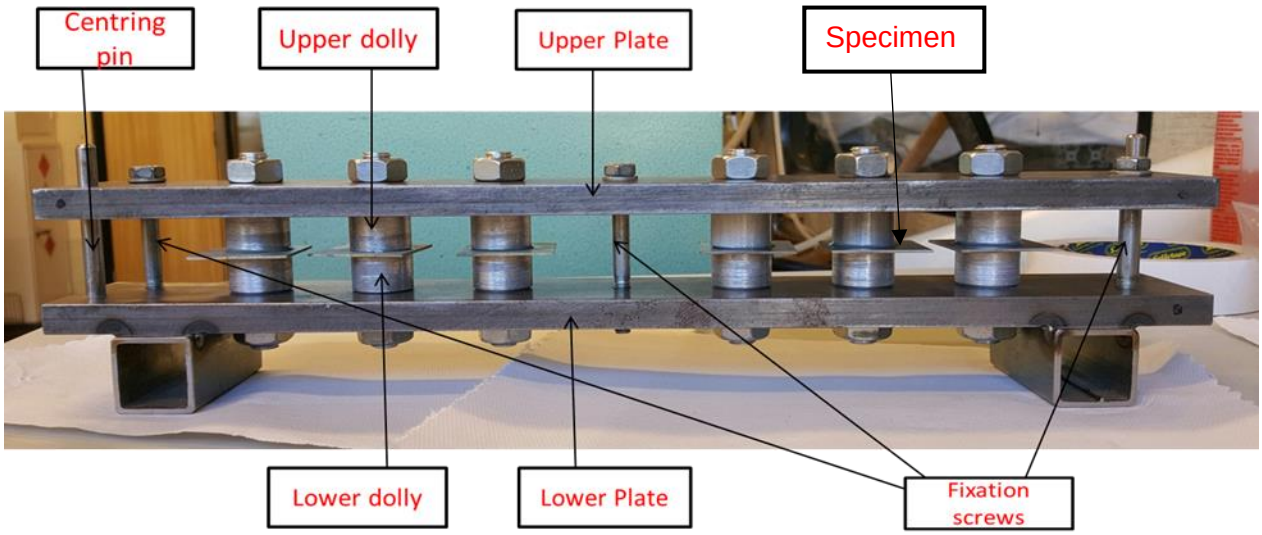

Figure 2.1. Composition of the alignment tool, note the specimen between two counter dollies.

The procedure started by roughening the uncoated side of the specimen using sand paper (D-56-746, grit size 120, 116 µm particle size, Wolfcraft GmbH, Kempenich, Germany) to increase the mechanical keying of the adhesive. Aluminium faced cylindrical test “dollies`” were prepared, each dolly was prepared to have a round 20 mm diameter surface on one side, 12 mm thickness, and M10 thread on the other side (bottom). The dolly’s face was machined perpendicular to its axis and their surface sandblasted in a Guyson Super 6 Blast cleaner Cabinet (serial no. 68668, Guyson International Ltd. Otley, Yorkshire, England) with brown alumina blast abrasive media (Guyson NFK 100 Brown Saftigrit CSS12 issue 8) for 5 seconds. Thereafter, the dollies were sonicated with acetone in ultrasonic bath (Struers, Metason 120T) for 5 min to remove any debris from the dollies that can affect the adhesive bonding. The dollies were then positioned in the alignment tool to check the assembly, sufficient amount of an adhesive (DEVCON home, 2 Ton epoxy resin) was prepared by mixing the two components (Resin and Hardener) together at a 1:1 ratio. A thin film of the

adhesive was applied to the lower dollies, then the specimen was placed on the surface of lower dolly and a thin film of adhesive was applied to the surface of upper dollies and then the counter dollies were assembled by securing the upper plate of the alignment tool to the lower plate. At this step, the upper dolly was glued to the coating surface and the lower dolly was glued to the other side of the titanium alloy substrate (Figure 2.1). The test apparatus was left over night to allow the adhesive to set. After 24 hours, the cured adhesive around the circumference of the dollies was removed using a cutter (DeFelsko PosiTest Pull-Off Adhesion Tester cutting tool with 20 mm inner diameter), this step prevented increased bonding surface area which will introduce an error to the tensile strength measurements. The dollies were extended using a 60 mm long and 16 mm diameter steel adapter with M10 metric internal thread on both sides which could then be easily installed in Instron type 500.625 M2 16 grips for the pull-off test permitting a longer gripping surface. An Instron 5582 (system ID: 5582J7466, S1-16754) universal test frame with a ±100 kN load cell (cat.no. 2525-801, ser.no. UK195) was used for the test setting a 1 N preload and a test speed of 0.5 mm min^{-1}.

The test ends in “failure”; during the test, the tensile strength at which the coating fails was measured. The force required pulling the dolly off or the force the dolly withstands yields the tensile strength in Newton per square millimetre or mega Pascals (MPa). Breaking strength is the maximum load the specimen (coating) sustains during the test. Failure will occur along the weakest plane within the system comprised of the dolly, adhesive, coating system, and substrate, and will be exposed by the fracture surface. The software used for the test is Bluehill version 2.33. Stress/strain curves are shown in Appendix 2, Figure 1. After the test, the specimens

were kept clean and ready for S.E.M. and EDS analysis to examine the surface of the coating to check the surface topography after coating failure.

2.2.10 Silver interference with lactate dehydrogenase assay

LDH is an enzyme which is normally found in the cytoplasm of animal cells and is implicated as a biomarker of cell injury. The basis of this assay in the current experiment is that osteoblast cells contain LDH, while cell culture media normally does not. The presence of LDH in the culture media is therefore interpreted as a leakage of LDH enzyme from the cells through a compromised cell membrane. LDH activity was measured every day in the external media, and after 7 days in the cell homogenate. The method followed Campbell *et al*. (1999) who used 100 µl of sample added to the reacting mixture (2800 µl of 6 mmol L^{-1} sodium pyruvate in 50 mmol L^{-1} phosphate buffer at PH 7.4, plus 100 µl of 6 mmol L^{-1} NADH solution), mixed directly in a 3 ml cuvette and the change in absorbance is measured over 2 minutes at 340 nm (Jenway 7315 spectrophotometer).

Silver nanoparticles can interfer with components of biochemical assays, so it is mandatory to test the possible interference of the nanoparticles used in the experiments and the assays used. An interference test was conducted by soaking a silver coated titanium disc (Ag+nHA) in cell culture media (DMEM + 10%FBS + 1%antibiotics) for 24 hours. Then the media was removed and used for the interference test. In the actual test, the positive control was the LDH enzyme in phosphate buffer and the negative control was the buffer without LDH enzyme, the treatment group was the LDH enzyme and phosphate buffer with 25% cell culture medium (containing silver ions). The effect of silver ions on LDH activity was then investigated.

2.2.11 Silver interference with protein assay

The Bicinchoninic assay (BCA) is one of the colorimetric kits that offer speed and convenience for routine protein measurements. The method works by reducing copper ions by peptide bonds in the protein in alkaline conditions. The produced Cu ion binds to the dye, bicinchoninic acid, and this will result in a colour change of the dye from green to purple. The procedure used 10 µl of each sample (cell homogenate or bovine serum albumin BSA) into a 96-well microplate with 200 µl of fresh colour reagent, the plate was then mixed thoroughly on a shaker for few seconds then covered and incubated in 37℃ for 30 minutes. Absorbances of the samples were read at 592 nm (VersaMax, molecular devices, Berkshire, UK). To plot a calibration curve, the protein assay standards (bovine serum albumin) were diluted with phosphate buffer saline (Phosphate buffer tablet from Sigma Aldrich) dissolved in 100 ml of ultrapure deionized water, pH 7.4) to give the final protein concentrations of 2, 1.6, 1.2, 0.8, 0.2, 0.1 and 0 (no added BSA) mg L^{-1}).

Silver and BCA kit interference was tested. In this experiment, silver nanoparticles (5mg L^{-1} and 50 mg L^{-1}) in Milli-Q water were prepared. The control was the protein assay standard without silver nanoparticles and the treatments were the protein assay standard with 5 mg L^{-1} silver nanoparticles and 50 mg L^{-1} silver nanoparticles, simply, the final test solution was 0.5 ml BSA and 0.5 ml of silver solution (5 or 50 mg L^{-1}). The absorbance was read at 592 nm and the effect of silver nanoparticles on the standard curve was determined. BCA standard curve is shown in Appendix 2, Figure 2.

2.2.12 Trace metal analysis

The concentration of released silver from the coatings was measured by ICP-MS (X Series 2, Thermo Scientific, Hemel Hempstead, UK). Sample prepration for ICP-MS was started by acidifing the stock samples with 70% nitric acid so as to prevent nanoparticle agglomeration and sticking to the glass/tube walls. For the dialysis experiment, 0.1 ml of 70% nitric acid was added to the samples and for the dissolution experiment 0.02 ml of 70% nitric acid was added to the samples. A series of standards were prepared containing 0, 20, 50 and 100 µg L^{-1} silver, the test samples were diluted until the concentration of silver ranged from 0-100 µg L^{-1} so as to closely match the standards.

2.2.13 Statistical analysis

Data are presented as mean ± S.E.M and most of the data were analysed using Statgraphics software version 16, the difference between the treatment and the control as well as between treatments were analysed using (one way ANOVA, Tukey test). While two way ANOVA was used to investigate if there was a time effect. The curves obtained from the dialysis experiment were fitted using (SigmaPlot 12.0 Systat Software, Inc). All statistical analysis used a 95% confidence limit, so that p values < 0.05 were considered statistically significant.

2.3 Results

2.3.1 Investigating the primary particle sizes of nHA and mHA by transmission electron microscopy TEM

The primary particle sizes of Ag and HA particles were investigated, to ensure that the particles were in the expected size range. The results of TEM confirmed that the primary particle size of nHA and mHA was 23.90±1.49 nm and 4.72±0.38 µm, respectively. SEM images of silver nanoparticles showed that their average size was 111.58±14.99 nm (Figure 2.2).

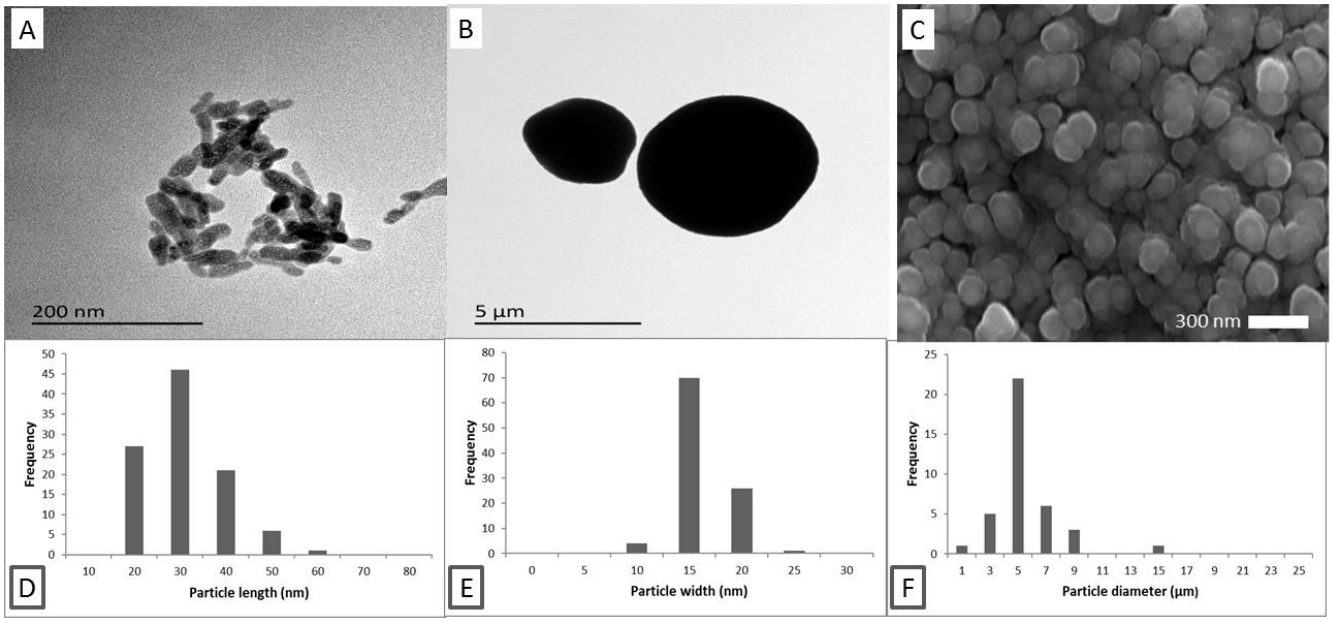

Figure 2.2. TEM images of HA nanoparticles (A) and microparticles (B) showing their primary particle size which is (25.95 nm in length and 13.59 nm in width) and 4 µm respectively. (C) SEM image of electroplated silver nanoparticles showing the primary particle size which is 111 nm. (D and E) are the primary particle size distribution of nHA stock solution (particle length and width respectively), (F) is the primary particle size distribution of mHA stock solution.

2.3.2 Surface roughness measurements of the specimens

The surface roughness values are shown in Table 2.2. No significant difference was observed between uncoated polished titanium and silver plated titanium (Ag). Applying HA nanoparticles caused increased surface roughness by almost 0.7 µm as compared to unpolished titanium and silver plated titanium. While HA micro particles caused even more increase in the roughness value which was measured as 2.17 ± 0.18 µm.

Table 2.2. Surface roughness values of the titanium discs.

Specimens	Roughness value (µm)
Uncoated polished titanium	0.23 ± 0.01 [a]
Ag plated titanium	0.32 ± 0.01 [a]
Ag+nHA coated titanium	0.94 ± 0.19 [b]
Ag+mHA coated titanium	2.17 ± 0.18 [c]

Data are mean ± S.E.M (n = 3), different letters mean statistically significant difference within each other, one way ANOVA ($p < 0.05$).

2.3.3 Investigating quality of the coatings using SEM and EDS

Scanning electron microscopy images showed that coatings were successfully applied onto the discs (Figure 2.3). The silver coated titanium disc showed a uniform layer of silver at the nano scale (Figure 2.3 A). The Ag+nHA samples were also coated uniformly with densely packed layer of HA nanoparticles (Figure 2.3 C), although some cracks occurred which probably arose from the sintering process. The micron scale

HA particles were successfully coated onto the silver coated titanium discs without cracking (Figure 2.3 E).

EDS analysis (Figure 2.4) confirmed the expected surface composition of the discs. The surface composition of silver coated samples was mainly silver (78%), followed by oxygen (16%), and titanium (3%). Moreover, the surface of Ag+nHA samples were mostly composed of calcium (31.2%) followed by phosphorous (13.8%) and silver (8.9%); confirming that most of the silver was covered by the layer of nano HA. In contrast, in the Ag+mHA discs the surface had more silver (28.6%), and slightly less calcium (22.6%) and phosphorous (9.8%). For the micron scale HA the large particles enabled gaps between the particles where the silver coating could be observed.

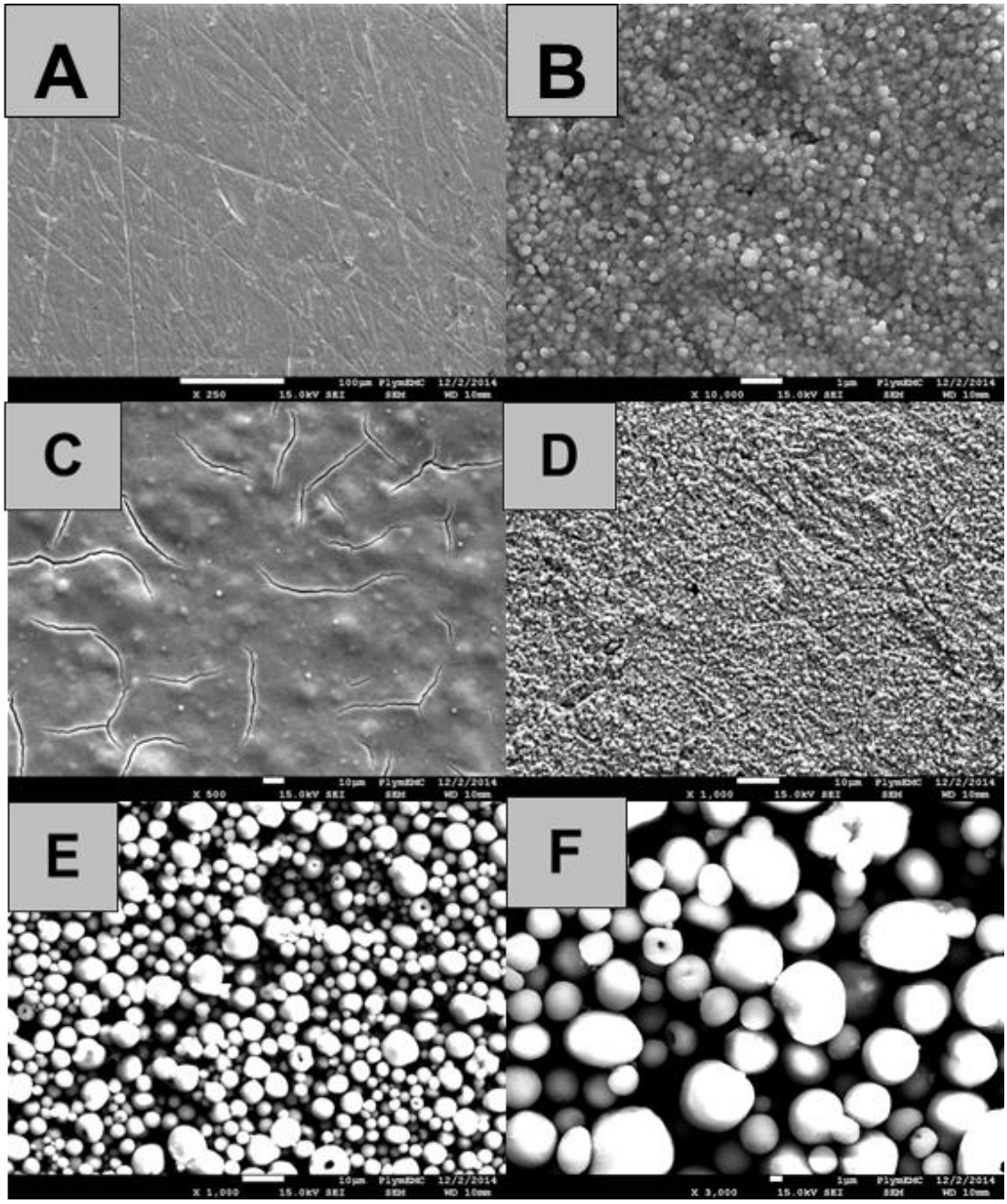

Figure 2.3. SEM images of coated titanium discs; (A) x 250 (100 µm) and (B) x 10 K (1 µm) of the silver plated titanium alloy. Note the particles are at nano scale and fully covering the titanium surface. (C) x 500 (10 µm) and (D) x 1.0 K (10 µm) are Ag+nHA surfaces. Note the nHA particles have successfully produced an even coating on the silver plated titanium. (E) (x 1.0 K (10 µm) and (F) x 3.0 K (1 µm) of the Ag+mHA discs. The mHA particles have successfully been coated on the substrate.

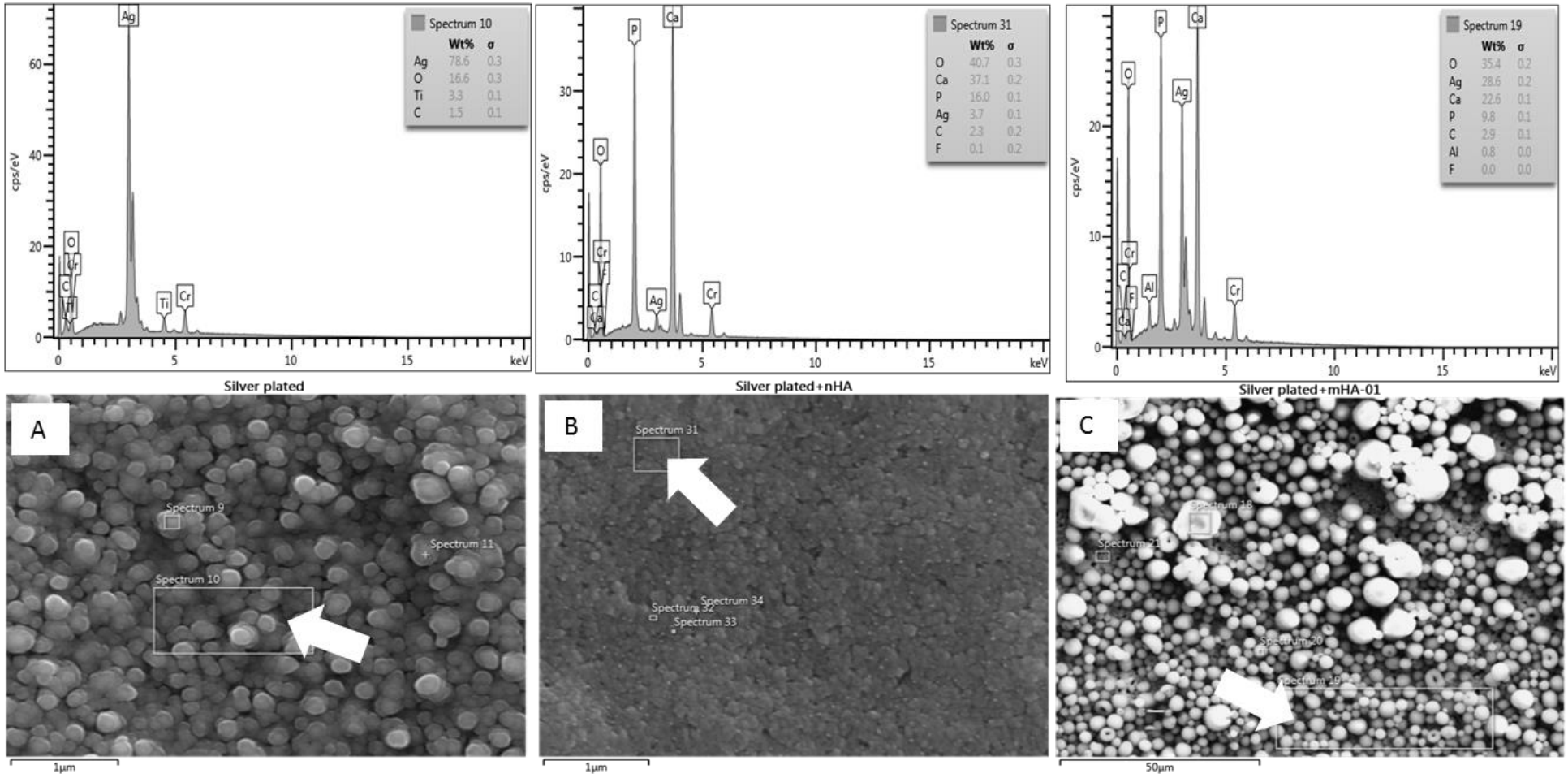

Figure 2.4. EDS spectra of coated titanium discs: (A) silver plated titanium, (B) Ag+nHA, (C) Ag+mHA showing the percentage of the elements composing the surface structure of the coated titanium discs. Arrows are showing the area on which the analysis was made.

2.3.4 Investigating the stability of the coatings in cell culture medium (DMEM + 10%FBS + 1%animicrobial) by dialysis

Dialysis was conducted to investigate the stability of the coatings in DMEM cell culture medium. The results showed that silver concentration in beakers was higher in Milli-Q than cell culture medium (Figure 2.5 and 2.6). It was found that the highest silver concentration in beakers over 24 hours was from Ag+mHA samples in Milli-Q water which was around 18 ppb (Figure 2.6), whereas the highest value measured from cell culture medium was from Ag+mHA samples that released around 2.5 ppm silver over the same time period. Silver concentration released from all specimens to the beakers was increasing gradually over 24 hours. Although silver release from Ag+mHA in Milli-Q was decreased in the first 4 hours then started to increase again. Ag+mHA samples released significantly higher silver as compared to Ag+nHA and Ag coated samples in both cell culture medium and Milli-Q water ($p < 0.05$). Specimens in the cell culture medium released significantly more silver as compared to the ones in Milli-Q in the dialysis bag (Figure 2.7). Silver concentration in dialysis bags released from Ag+mHA in cell culture medium was 11 ppm, while it was only 4 ppm in Ag+nHA samples and 1 ppm for Ag coated samples. However, silver concentration released from all specimens was lower in Milli-Q water in comparison to the cell culture medium. Ag coated samples released significantly less silver than Ag+mHA and Ag+nHA both in dialysis bags and inside the beakers in both test groups. Futhermore, pH values of the media during the experiment is shown in Appendix 1, Table 1.

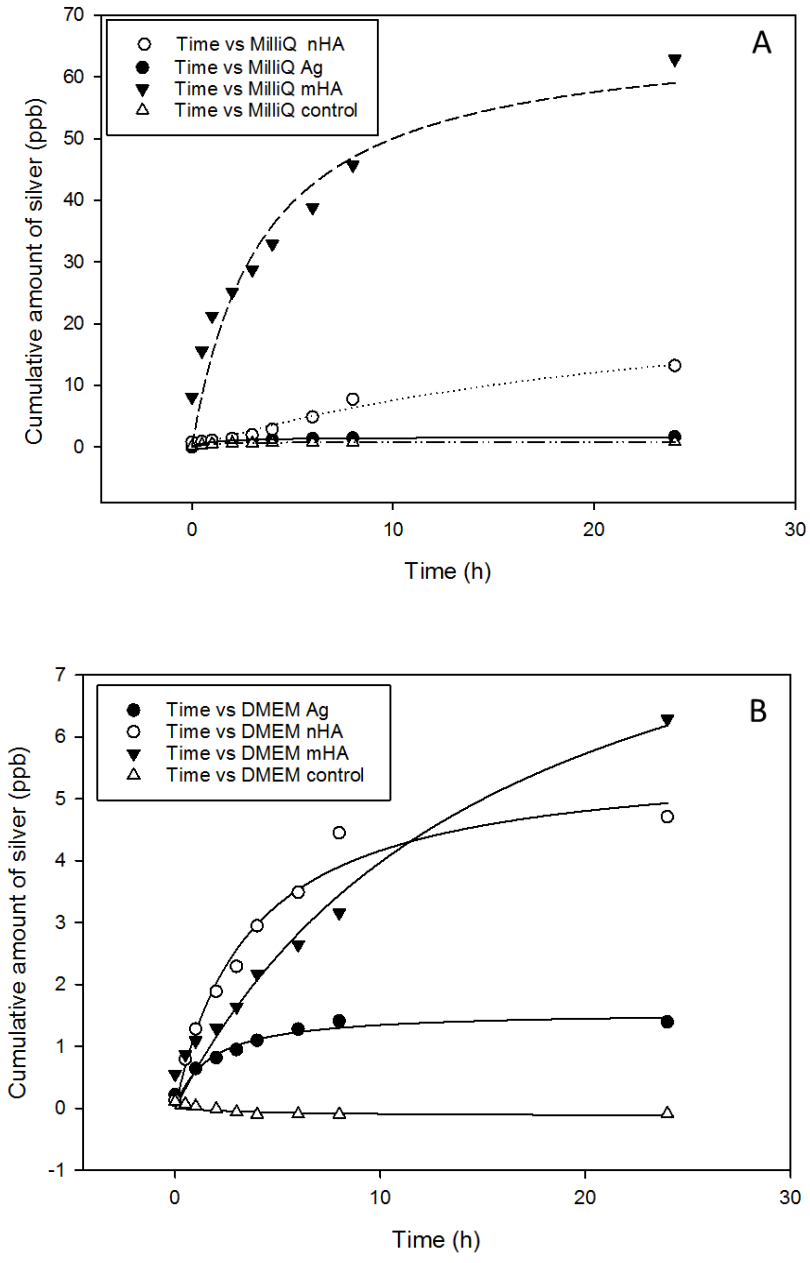

Figure 2.5. Cumulative amount of silver ion release (ppb) from discs to the external media in the beakers (n = 3). External media was either ultrapure water (Milli-Q) (A) or cell culture medium (DMEM) (B).Curves were fitted using SigmaPlot 13 (Systat Software, Inc.) applying the legal binding one site saturation (rectangular hyperbole function). Abbreviations refer to the type of sample in a specific media.

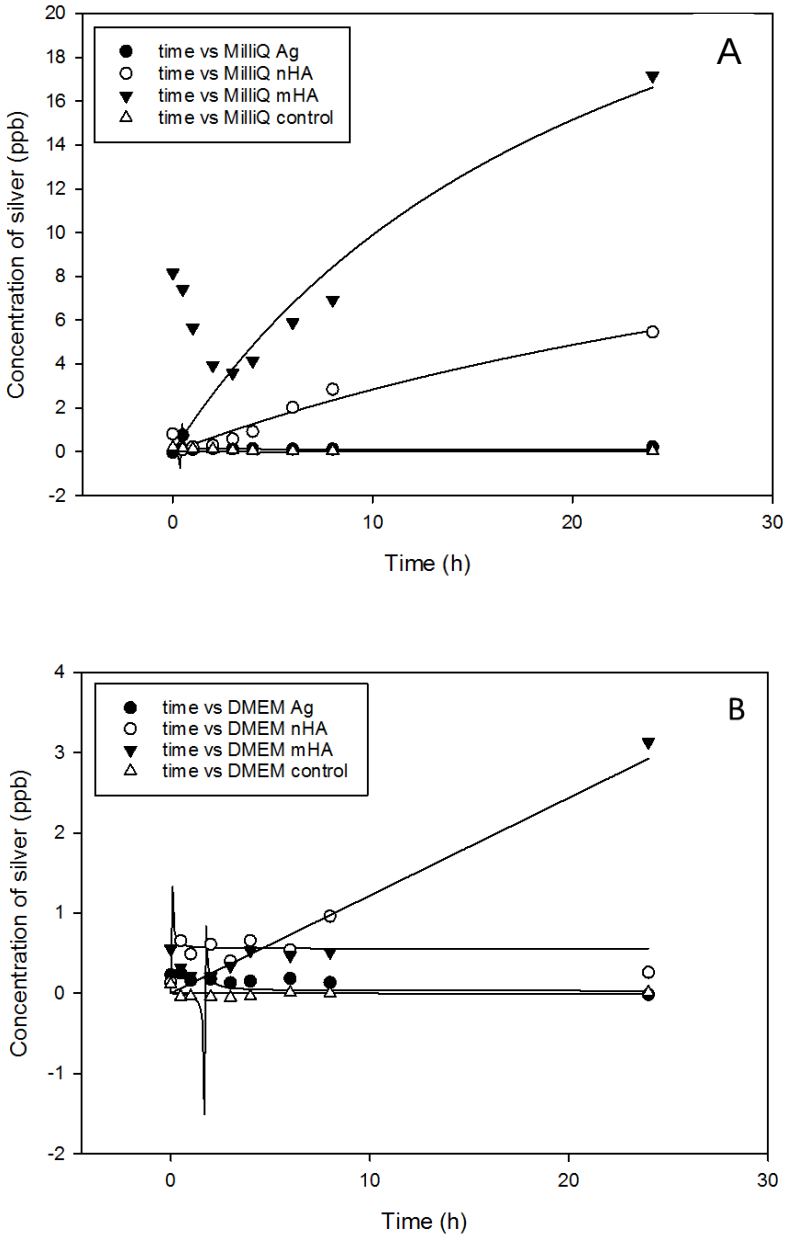

Figure 2.6. Concentration of silver ion release (ppb) from discs to the external media in the beakers (n = 3). External media was either ultrapure water (Milli-Q) (A) or cell culture medium (DMEM) (B). Curves were fitted using SigmaPlot 13 (Systat Software, Inc.) applying the legal binding one site saturation (rectangular hyperbole function). Abbreviations refer to the type of sample in a specific media.

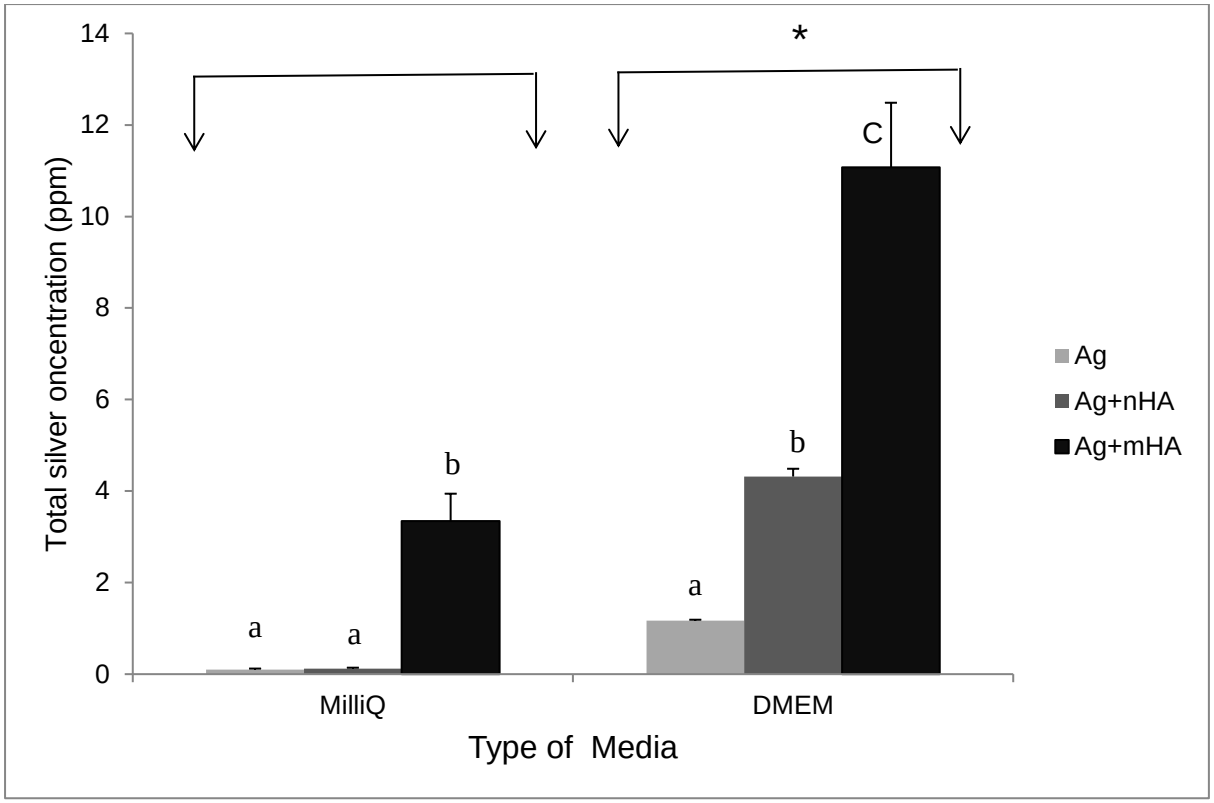

Figure 2.7. Concentration of silver (mg L^{-1}) in 4 ml solution in dialysis bags after 24 hours. Error bars represent S.E.M (n = 3). Asterisk means statistically significant difference between the treatment (DMEM) and control (Milli-Q) groups. Different letters between bars mean statistically significant difference within each media. (one way ANOVA, $p < 0.05$).

2.3.5 Dissolution of silver nanoparticles in different cell culture medium

Ag+nHA discs were soaked in different cell culture medium and silver concentration was measured after 24, 48 and 72 hours of incubation. The results in Table 2.3 reveal that DMEM + 10%FBS + 1%antimicrobial (Control) caused significantly higher silver dissolution (18.83±2.38 mg L^{-1}) at day 1 as compared to other groups ($p < 0.05$). (75%DMEM+25%physiological saline) + 10%FBS and (50%DMEM+50%physiological saline) + 10%FBS were not significantly different at all-time points. However, DMEM without FBS caused significantly less silver dissolution at all-time points as compared

to other groups (except blanks). (Physiological saline + 10% FBS) and (HOB) caused significantly less silver dissolution than other groups containing DMEM and FBS at day 1, values were 4.77±0.96 mg L^{-1} and 4.70±0.54 mg L^{-1} respectively. At day 2 and 3, silver concentration in (Physiological saline + 10% FBS) was significantly higher than other groups (7.04 ± 0.46 mg L^{-1}) and (2.67± 0.45 mg L^{1}) respectively. SEM images of the samples after the experiment showed that coatings were physically intact and FBS did not have an effect on the physical stability (Figure 2.8).

Table 2.3. The total amount of silver release from Ag+nHA discs to the external media after 72 hours of incubation

Treatment	Day1	Day 2	Day 3
	mg L^{-1}		
DMEM+10%FBS Without disc (blank 1)	< 0.03 ^{A}	< 0.03 ^{A}	< 0.03 ^{A}
Physiological saline+10%FBS without disc (blank 2)	< 0.03 ^{A}	< 0.03 ^{A}	< 0.03 ^{A}
HOB without disc (Blank 3)	< 0.03 ^{A}	< 0.03 ^{A}	< 0.03 ^{A}
DMEM + 10%FBS (Control)	18.83 ± 2.38 ^{E}	2.61 ± 0.52 $^{C\#}$	1.75 ± 0.11 $^{B\#}$
DMEM (without FBS)	0.07 ± 0.003 ^{B}	0.19 ± 0.04 ^{B}	0.17 ± 0.04 ^{E}
(75% DMEM + 25%physiological saline) + 10%FBS	10.82 ± 0.6 ^{D}	2.59 ± 0.29 $^{C\#}$	1.80 ± 0.07 $^{B\#}$
(50% DMEM + 50%physiological saline) + 10%FBS	10.85 ± 1.1 ^{D}	2.67 ± 0.38 $^{C\#}$	1.92 ± 0.17 $^{B\#}$
Physiological saline + 10% FBS	4.77 ± 0.96 ^{C}	7.04 ± 0.46 ^{D}	2.67 ± 0.45 ^{C*}
HOB	4.70 ± 0.54 ^{C}	1.68 ± 0.08 $^{C\#}$	0.96 ± 0.01 $^{D\#}$

Data are expressed as mean ± S.E.M (n = 3). Different capital letters within each column indicate statistically significant difference, asterisk (*) means significant difference within the previous time point while (#) mean significant difference within day 1 (one way ANOVA, $p < 0.05$). Two way ANOVA showed that there was a time, as well as treatment effects ($p < 0.05$). All the treatment groups were supplemented with 1% antibiotics.

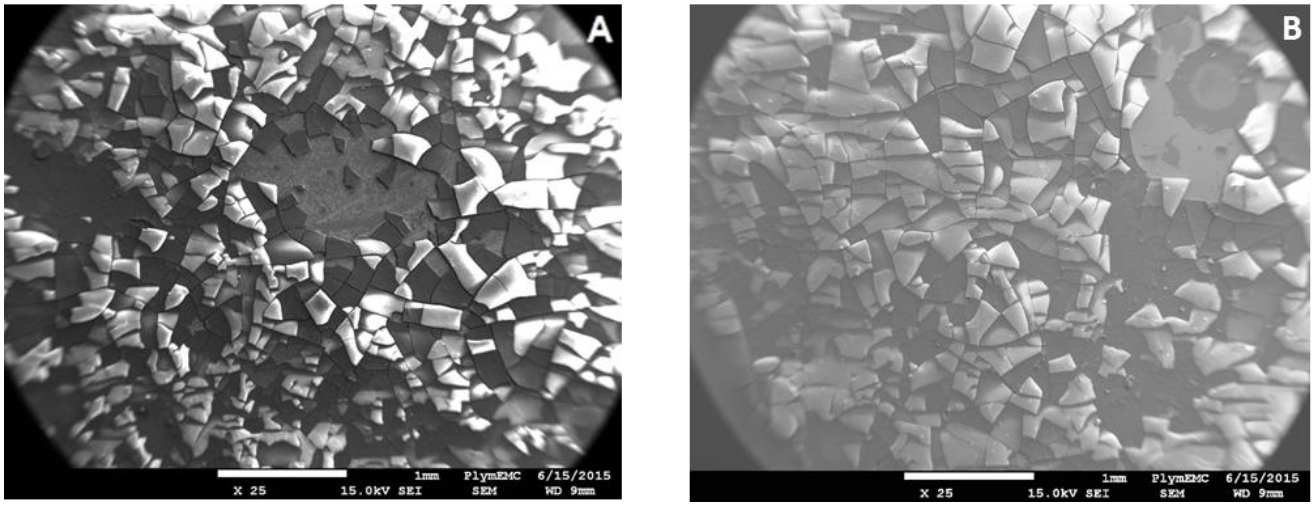

Figure 2.8. SEM images of Ag+nHA coated samples after soaking in cell culture media for 72 hours: (A) DMEM with FBS (B) DMEM without FBS, it can be noticed that the presence of FBS has not induced a physical damage to the coatings.

2.3.6 Pull-off test

Results showed that the adhesive strength of the control (epoxy resin) was at least 22.36 ± 1.43 MPa. The bonding strength of the silver nanocoating to the titanium alloy substrate (silver plated titanium; Ag) was 7.96 ±1.96 MPa (Table 2.4). EDS analysis suggested coating failure. EDS spectra obtained from the tested area after the pull-off test showed that more than 80% of the total surface consisted of titanium, which suggests that the silver nanocoating was removed (Figure 2.9). Bonding strength for the Ag+nHA specimens was at least 7.85 ± 1.31 MPa. As SEM and EDS analysis suggest, failure occurred between the adhesive and the coating and not between the coating and the titanium alloy substrate. SEM and EDS results of the specimen surface after the test showed that the coating was intact and not detached after conducting the pull off test. It could be noticed in (Figure 2.10) that the surface topography of the

tested and untested area was similar and mainly consisted of calcium and phosphorous. Similarly, the adhesive strength of the Ag+mHA coatings was higher than 20.52 ± 1.75 MPa. At that stress, the coating did not detach but failure occurred between the adhesive and the coating. SEM and EDS analysis confirmed that the composition of the tested and untested areas was similar (Figure 2.11).

Table 2.4. Bonding strength of the test coatings on the titanium alloy surface

Treatments	True stress (MPa)
Ti	22.36 ± 1.43 [a]
Ag	7.96 ± 1.96 [b]
Ag+nHA	7.85 ± 1.31 [b]
Ag+mHA	20.52 ± 1.75 [a]

Stress values (MPa) at which failure occurred. Data are mean ± S.E.M. Different letters indicate a significant difference with each other, one way ANOVA ($p < 0.05$).

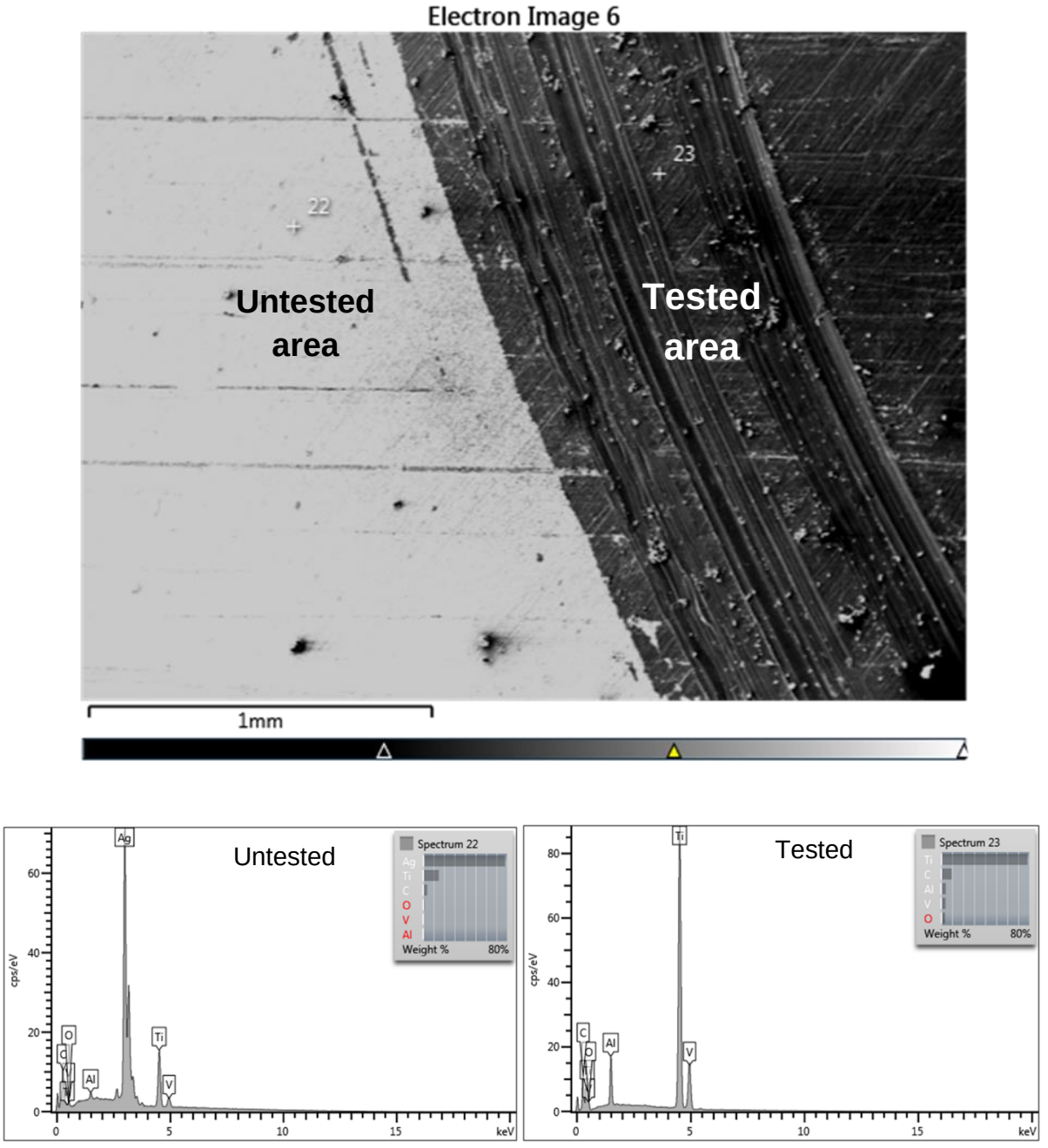

Figure 2.9. EDS spectra of Ag after the pull-off test, Note the difference between the tested and untested area, the tested area is composed mainly of titanium which means that the Ag layer has been detached after the test.

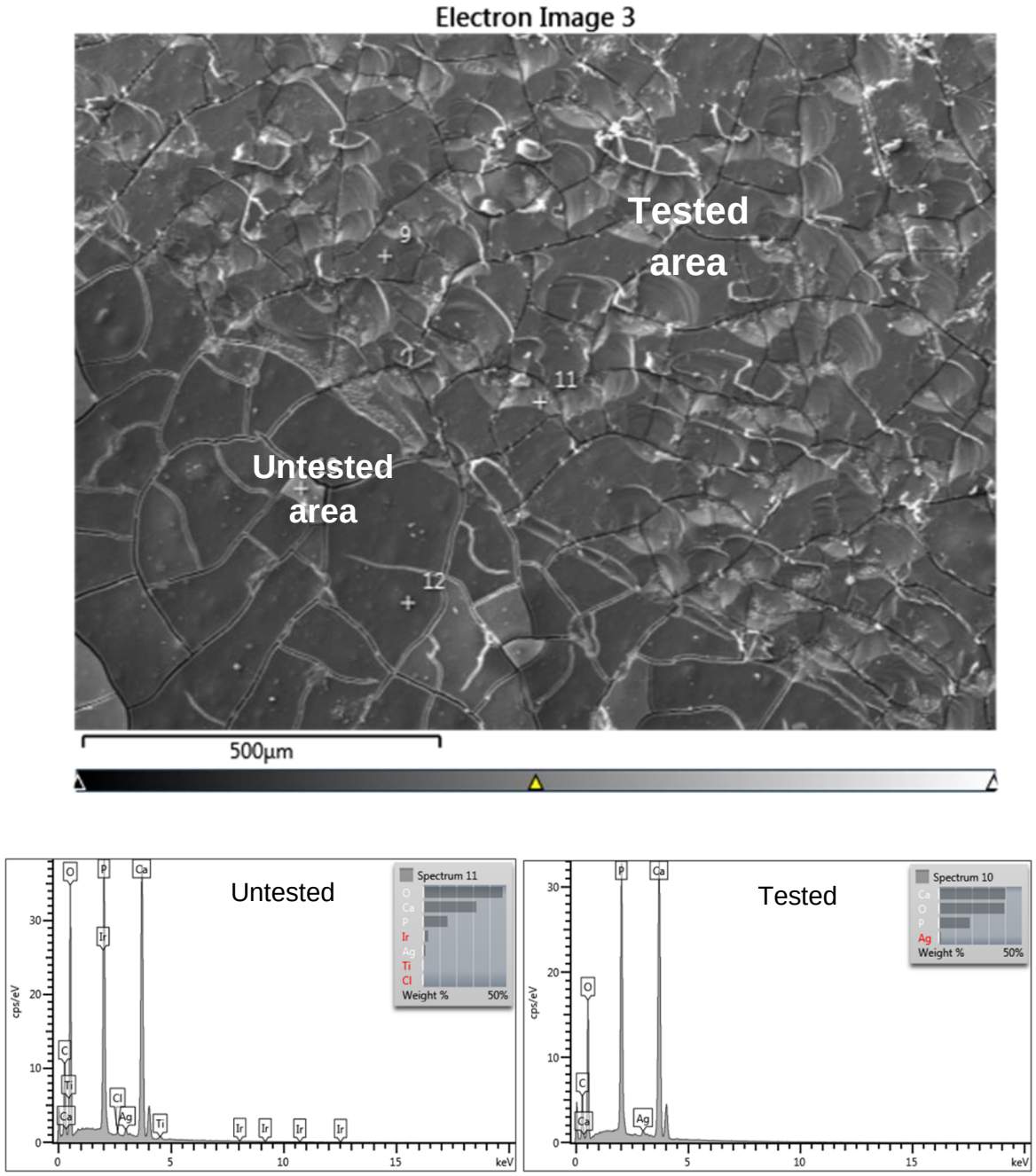

Figure 2.10. EDS spectra of Ag+nHA after the pull-off test. The composition of tested and untested area is similar indicating that the coating is intact and not detached after the test.

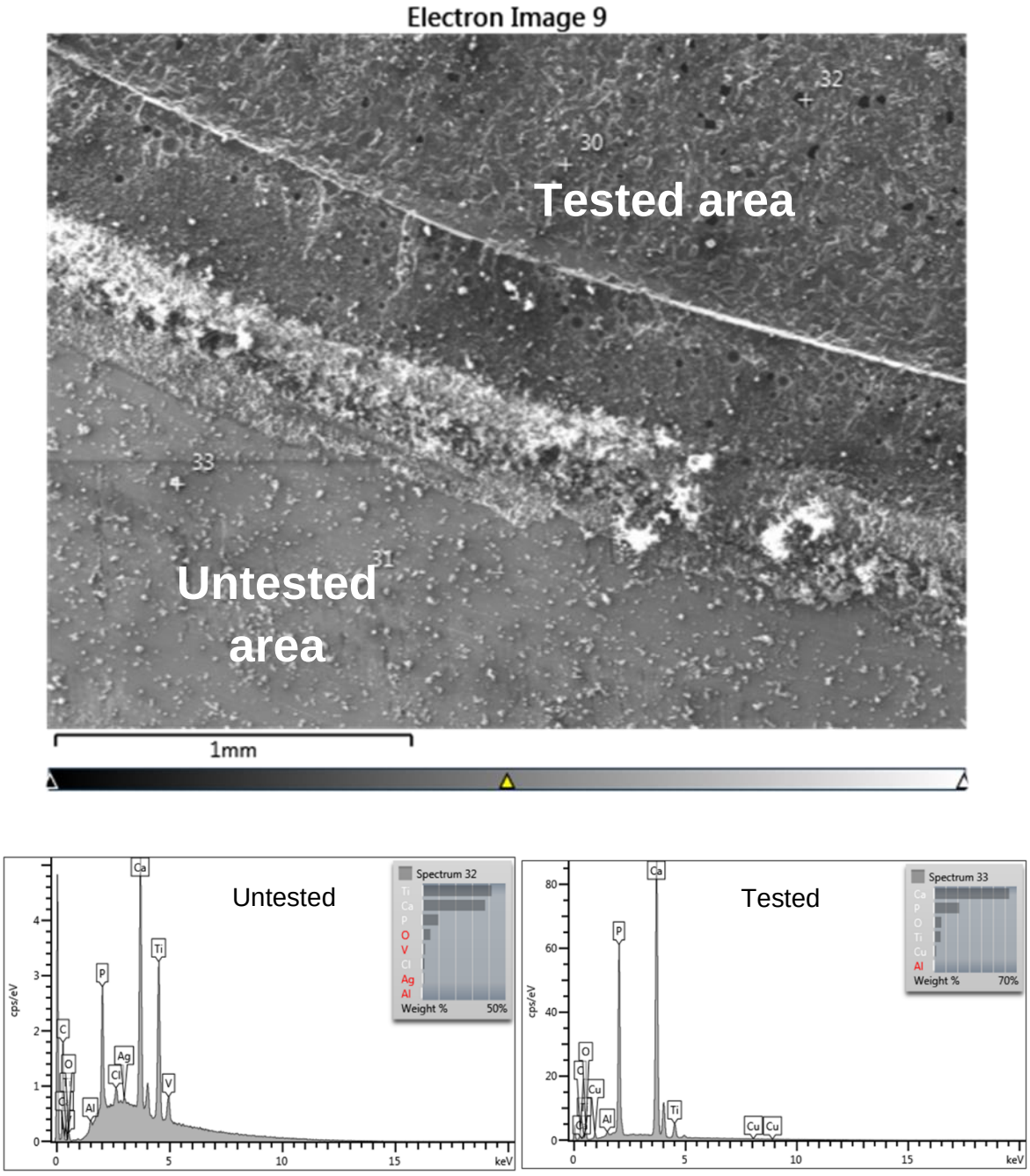

Figure 2.11. EDS spectra of Ag+mHA after the pull-off test. The composition of tested and untested area is similar indicating that the coating is intact and not detached after the test.

2.3.6 Silver interference with lactate dehydrogenase assay

Interference of silver with components of LDH assay was tested, the key finding was that silver ions dissolved from the coating to the external media did not significantly

interfere with components of LDH assay in the experimental conditions here. However, silver ions caused slightly higher absorbance than the positive control. So the total LDH activity was 0.005 higher than the positive control, although the difference was not statistically significant (Figure 2.12).

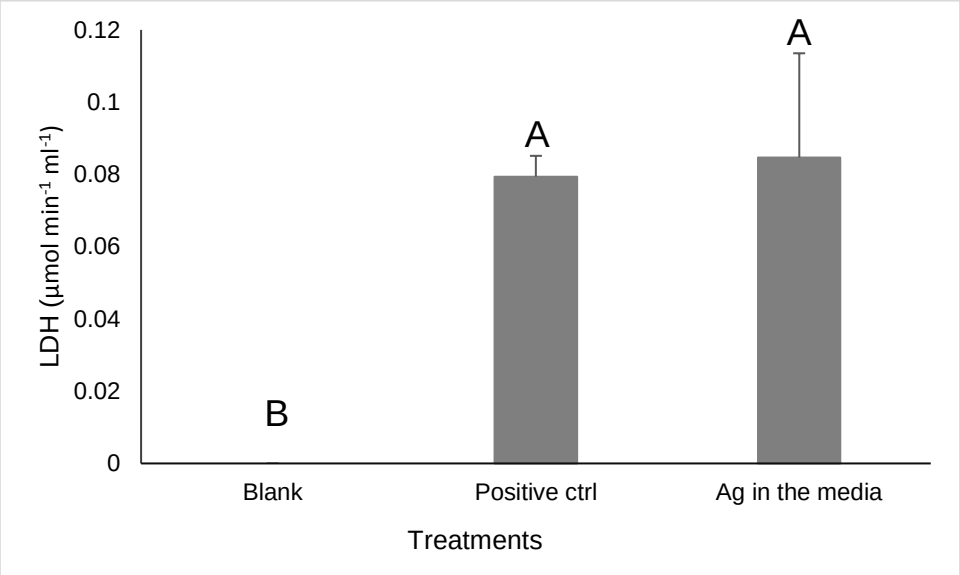

Figure 2.12. Silver interference with LDH assay, positive control is pure LDH enzyme in assay reagent and (Ag in the media) is same as the positive control but with cell culture media containing Ag. Data are expressed as mean ± S.E.M (n = 3), different letters indicate a statistically significant difference, one way ANOVA ($p < 0.05$).

2.3.7 Silver interference with protein assay

Silver nanoparticles were dissolved in Milli-Q water in concentrations of 5 and 50 mg L^{-1}. Then they were “spiked” with protein assay standards to check the interference of silver nanoparticles with the assay components. The results showed that the absorbance value of silver nanoparticles was slightly higher than the standard. 5 mg L^{-1} silver nanoparticles caused slightly higher absorbance than 50 mg L^{-1} (Figure 2.13).

This means that silver nanoparticles can cause a slight interference with a BCA protein assay kit.

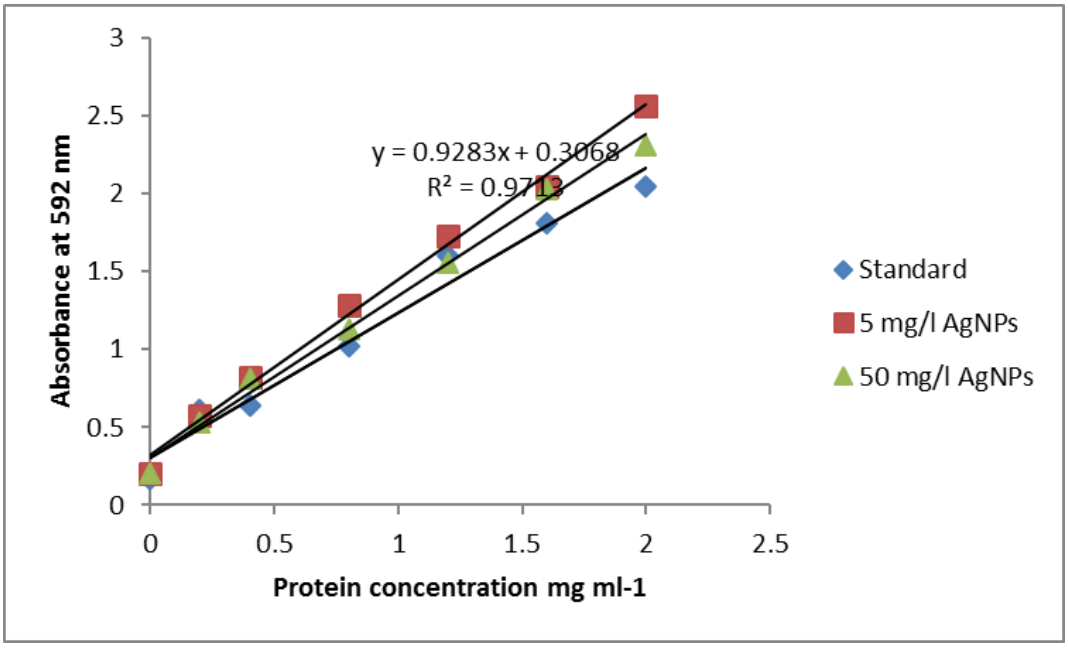

Figure 2.13. Silver nanoparticle interference with protein assay standard curve (BCA kit). (◆) is the standard curve of the BCA kit, (■) is the standard curve with 5 mg L^{-1} silver nanoparticles and (▲) is the standard curve with 50 mg L^{-1} silver nanoparticles.

2.4 Discussion

In this study, medical grade titanium alloy was successfully coated with an even and dense coverage of silver nanoparticles that were spontaneously formed in the electroplating conditions used here. Subsequently, the Ag-NP coated alloy was decorated with either a layer of nHA or mHA. In the case of the mHA, the gaps between the spherical particles meant that the underlying silver layer was partly visible, less so for the nHA. In terms of coating stability in cell culture medium, key findings showed

that the coatings were stable in cell culture medium although some silver dissolution was found which can be explained by the presence of FBS in the cell culture medium. Bonding strength of the coatings is > 7 MPa, this is clinically acceptable since maximum force needed to insert implant is 0.05 MPa. Furthermore, in contrast to what is known about silver interference with LDH and protein assay components, the results showed that silver nanoparticles do not significantly interfere with those assay components.

2.4.1 Roughness values of the specimens

Titanium discs were coated with silver nanoparticles by electroplating method and HA nano and micro particles by sintering method. The particles produced a rougher surface than titanium (Table 2.2), values obtained (0.2 to 2 μm) are considered to be a moderately rough surface. The roughness values here are also consistent with previous reports (Besinis *et al*., 2017). The particles produced a rougher surface than titanium, value resembles those results of (Bagno and Di Bello, 2004) who found that surface roughness of medical grade titanium discs after polishing was 0.23 ± 0.01. It also agrees with (Giavaresi *et al*., 2003) who measured 0.20 ± 0.01 μm as a surface roughness value of polished titanium surface.

Bacterial colonisation can be directly influenced by the degree of surface roughness, the rougher the surface the higher the risk of bacterial colonisation (Morgan & Wilson, 2001). The results suggest that the roughness values of the treatments are not appreciably different in terms of the probability of bacterial colonization. Le Guéhennec *et al*. (2007) found that the surface roughness value of lower than 2 μm is less likely to increase the risk of bacterial colonisation. Moreover,

coating the surface of titanium with HA particles increased the surface roughness by four times (nHA) and eight times (mHA), respectively, as compared to uncoated polished titanium, however, they are still less than 2 µm so they are not more prone to bacterial colonisation than the polished titanium. This result more or less corroborates with Giavaresi *et al*. (2003) who observed that coating titanium surface with HA can significantly increase the surface roughness value as compared to polished surfaces. Nevertheless, it disagrees with (Borsari *et al*., 2005) who found that deposition of further HA coating on the titanium surface can lead to decreased surface roughness.

2.4.2 Investigating quality of the coatings using SEM and EDS

Coating quality was assessed by SEM and EDS after application of the nanoparticles on their titanium substrate. The findings of figure 2.3 and 2.4 revealed that silver electroplating was successful and consistent with the previous work (Besinis *et la*., 2017) forming a dense covering of silver nanoparticles of approximately 100 nm. They also revealed that silver ions were successfully reduced on titanium forming a uniform layer of silver nanoparticles on the surface. This could be explained by the fact that electroplating method can dissolve ions from the silver source reducing them on titanium substrate on which they form nanoparticles. This finding corroborates with Li *et al*. (2010) who managed to produce silver nanoparticles on Au@SiO_2 core/shell nanomaterial by an electroplating method in $AgNO_3$ bath.

HA coatings were successfully applied to the silver plated titanium discs (Figure 2.3). For both the Ag+mHA and Ag+nHA the coatings showed densely packed particles of the relevant HA on the surface, but there were some notable differences between the nano and micron forms of HA. Firstly, the relatively large and spherical

micro HA particles formed a continuous layer, but inevitably, the geometry of the material enabled gaps in between particles, which allowed some silver release. Besinis *et al*. (2017) also observed this morphology. In contrast, for the more rod-like nano HA the gaps in the material was reduced. However, some cracks were observed on the surface of Ag+nHA coated discs (Figure 2.3). Weng and Baptista. (1999), applied HA on medical grade five titanium by sintering technique; they found that heating treatment can lead to a better development of HA but also produce cracks on the surface of the coating. Cracking of HA after heating was also noticed by Liu *et al*. (2002) who applied HA on stainless steel by sintering process; a relatively dense coating was produced but also some degree of micro cracking was observed. The formation of cracks after the sintering process can be due to the difference in thermal expansion of HA and titanium, respectively (Jarernboon *et al*., 2009). Another explanation is the possibility of HA shrinkage during the drying process which subsequently results in the formation of cracks on the final surface (Mahé *et al*., 2008). HA microparticles produced an even coating on the titanium substrate (Figure 2.3 E). It can be observed that the particle sizes are at the micro scale level. No cracks were observed on the surface and this is because microparticles did not produce a densely packed layer like nanoparticles, they rather produced an even coating but with noticeable gaps between the particles (Figure 2.3 E). However, the coatings were as expected and could be used for clinically relevant experiments.

2.4.3 Investigating the stability of the coatings in cell culture medium by dialysis experiment

Some local release of Ag was found which is desirable for bacterial killing in the first hours after surgery, the required dose of dissolved silver is around 0.2 mg L^{-1} with

S.mutans (Besinis *et al*., 2017). Dialysis experiment was conducted to study the effect of cell culture medium on the coating stability. The results showed that silver dissolution was higher in cell culture medium (DMEM + 10%FBS + 1%animicrobial) as compared to the Milli-Q (Figure 2.7). The cause of silver dissolution might be due to the high affinity of silver with the –SH group on amino acids that is present in the cell culture medium which causes silver dissolution but later “mop up” the released silver. Freshly made silver nanoparticles show some dissolution that is simply driven by an outward diffusion gradient (as observed in Milli-Q water). In the cell culture media, the dissolution gradient can be maintained by the rapid removal of dissolved Ag+ from the media. The explanation is that silver ions form insoluble silver chloride from the high concentration of Cl^- in the cell culture media (Besinis *et al*., 2014). Moreover, silver ions avidly bind to –SH groups which are available in amino acid chain of proteins. Silver dissolution from Ag+mHA discs was higher than Ag plated and Ag+nHA discs. The reason behind this could be due to the presence of gaps between HA micro particles that can facilitate silver ion release as compared to Ag+nHA discs in which the HA layer is densely packed on the silver layer. Moreover, EDS analysis of samples showed that 28.6% of the surface of Ag+mHA discs was composed of silver, whereas only 8.9% of the surface of Ag+nHA was composed of silver (Figure 2.4). Ag+mHA and Ag+nHA discs released more silver ions than Ag plated discs. This might be due to the heating process required during HA application process. The explanation is that heating process can produce silver oxide which facilitates silver ion dissolution, (Pal *et al*., 1997) found that the presence of oxygen is essential for conversion of silver particle to silver ion.

The concentration of released silver from the discs to the cell culture medium in dialysis bags was significantly higher than in Milli-Q water in all treatment groups.

The explanation is that cell culture medium contains components that can dissolve silver ions from the surface of nanoparticles on the discs. This result supports the conclusion drawn by Loza *et al*., 2014 who found that the presence of organic molecules in the cell culture medium can accelerate silver ion dissolution which is due to forming a complexation of silver ions. In contrast, silver concentration in beakers was higher in Milli-Q water than in cell culture medium over 24 hours. The latter can have three possible explanations; either silver particles had not been dissolved or released silver ions but they had physically detached from the surface and accumulated in the dialysis bag as the bag is only permeable to the ions, or silver was dissolved to ionic form and the ions aggregated to one another or had bound to chloride ions and produced a poorly soluble silver chloride salt. Another explanation is that the dissolved silver ions had attached to the proteins in cell culture medium forming a protein corona that cannot pass the membrane. The most likely explanation is that the silver ions had attached to the chloride ions and produced a poorly soluble salt which is not able to pass the membrane. To some extent, it was difficult to measure the exact amount of silver concentration in the beaker, this is because a tiny amount of silver cannot be easily detected by ICP-MS. It could be noticed that silver release from Ag+mHA samples in Milli-Q water in the beaker was 8 ppb initially, and then it decreased gradually over 4 hours then increased again after 24 hour. Since Milli-Q water is not expected to contain components which might at some point interfer with silver ion and biasing the actual silver measurement, so the gradual decrease in silver concentration could be due to silver disappearance as a result of possible silver adherence to the glass. In the current study, silver concentration in the beakers was gradually increased over 24 hours in all treatment groups. This finding disagrees with

Kittler et al., 2010 who reported that the diffusion of silver ion out of the dialysis tube is very fast at the beginning then slows down after few hours.

2.4.4 Dissolution of silver nanoparticles in different cell culture medium

To further investigate the effect of cell culture medium and its components on silver stability and chemical dissolution and to follow up with the results of dialysis experiment, another experiment was conducted using different biological media with different components. The difference between this experiment and the dialysis is that this experiment was run in 24-well micro plates for three days in an incubator. The results showed that the cause of high silver dissolution in cell culture medium was the presence of FBS (Table 2.3). The presence of 10% FBS in DMEM caused almost 200 fold more silver release than DMEM without FBS. FBS is a very heterogenous colloid with many different macromolecules including several large proteins, so a precise ligand-based explanation for the effect of serum on silver nanoparticle dissolution cannot be derived. However, other studies have demonstrated that the presence of FBS can accelerate the dissolution of nanoparticles. For example, Shi and co-workers. (2012) found that presence of FBS can cause 17.7% and 0.35% dissolution of Zno and TiO_2 nanoparticles, respectively, while only 12.3% and 0.02% dissolution was found in the absence of FBS. Silver release in (DMEM without FBS) was significantly lower than all other groups at all time points. The reason behind this could be the presence of cysteine in DMEM which can prevent silver ion dissolution from the surface of particles. Loza *et al*., 2014 found that cysteine has a clearly inhibiting effect with almost no dissolution of the silver nanoparticles. Silver release in (75% DMEM + 25% physiological saline) + 10% FBS and (50% DMEM + 50% physiological saline) + 10% FBS was lower than the control (DMEM + 10% FBS) at day 1 but not significantly different at day 2 and 3. This indicates that diluting DMEM with physiological saline (at

the same FBS concentration) can only cause a decrease in silver release after 24 hours. This finding might be due to the presence of high amount of glucose in physiological saline. Loza *et al*., 2014 reported that the presence of reducing sugars (glucose) can slow down but not prevent the dissolution of silver nanoparticles.

From the clinical point of view, preconditioning the implants surface with the cell culture medium ensures that any excess silver is washed away and any fragments lost, so only the durable surface of the implant remains, hence rapid silver dissolution inside the socket can be avoided. This can minimise the immediate cell death by a silver "shock" which might occur in the case of massive silver dissolution.

2.4.5 Pull-off test

Since dental implants are screw shaped devices that are mechanically installed into the jawbone, so for any dental implant coating, the adhesion between the coating and the substrate must carefully be addressed. In this study, the bonding strength between the silver and titanium was approximately 7 MPa; EDS showed that the coating was detached after the test indicating that the failure has occurred between the silver coating and titanium resulting in detachment of the coating. while the bonding strength between the hybrid coating and the substrate in Ag+nHA and Ag+mHA was higher than that of Ag. This is due to the heating step required to process the HA coating which can lead to a diffusion adhesion between the substrate and the metal coating that subsequently results in a better adhesion between the coating and the substrate (J.R. Davis, 2001). From a clinical point of view, maximum loading torque that can be applied during implant insertion without damaging the surrounding bone is 0.05 MPa (Maluf *et al*., 2015). The force which is applied on the coatings during implant insertion

is called shear force, according to Budynas and Nisbett. (2008), shear force is 0.6 of the tensile strength. Thus, the tensile strength that is required to break the coating is higher than the maximum force applied during implant insertion. Therefore, the coatings possess an acceptable mechanical adhesion with the substrate. Similar studies have been conducted testing the adhesion between the HA and titanium, for example, Tsui *et al*. (1998) tested the bonding strength of the plasma sprayed HA coating on titanium, it was found that adhesion between HA and substrate after heat treatment at 1 hour 600 °C for was 15 MPa. Moreover, Liu *et al*. (2002) coated the stainless steel substrate with HA deposits using water-based sol-gel technique followed by annealing in air at 500 °C, the adhesion between the coating and the substrate was tested and found to be higher than 20 MPa. Kwok *et al*. (2009) found that the adhesion between spherical HA coating of medical grade titanium discs is 10.7 MPa.

2.4.6 Silver interference with lactate dehydrogenase and protein assays

In the current study, silver ions released from silver coated discs to the cell culture media did not seem to interfere with LDH assay components (Figure 2.12). This result disagrees with Gliga *et al*. (2014) which incubated silver nanoparticles (particle size 10 nm) with the cell lysate and detected LDH after 0, 4 and 24 hours. The reduction in LDH enzyme activity was pronounced which indicates that silver nanoparticles can interfere with LDH assay. It has been found recently that incompatibility of LDH assay for silver nanoparticle toxicity may be due to: (1) silver nanoparticles can adsorb LDH enzyme which in turn leads to under estimation of the actual LDH level; (2) reactive oxygen species (ROS) that are produced by silver nanoparticles inside the cell are

able to inactivate LDH (Oh *et al*., 2014). Silver interference with LDH assay can be different with different cells, particle chemistry and the form of which silver contacts with LDH enzyme or assay components. In the current study, the form of silver that possibly contacted with LDH enzyme and components of the assay was ionic.

The possibility of silver interference with the protein assay components by the formation of what is called “protein corona” must always be excluded in the studies that use silver nanoparticles with the protein assay. In the current study, slight interference was reported which caused slightly increased absorbance in groups that contain silver particles as compared to the standard curve, there was not a detectable difference at the beginning, but a slight difference was noticed with an increase in the protein concentration as shown in Figure 2.13. The increase in the absorbance might be due to the light absorption by silver particles at the same wave length used in the assay.

2.4.7 Conclusions

Silver and HA nano and micro particles were successfully coated on medical grade titanium discs. The HA nanoparticles were at nano-scale and produced an even coating on silver plated titanium with the presence of some expected cracks on the surface. The coating stayed intact when treated with cell culture medium after 72 hours; no physical damage was noticed on the surface of coatings when examined under SEM after 72 hours treatment with cell culture media. However, some silver dissolution in the ionic form was noticed especially with DMEM+10%FBS+1%antimicrobial. FBS was found to be the cause of silver release from the specimens to the external media. Sintering process which was required for HA deposition was found to cause an

increased silver dissolution as silver release was higher in Ag+mHA and Ag+nHA discs as compared to the silver plated ones. Coatings showed a desirable bonding strength with the substrate which is clinically acceptable in terms of coatings stability upon implant placement. The dissolved silver ions surprisingly did not interfer with LDH assay components when tested. The coatings were deemed ready for the biocompatibility experiments, although some limitations such as a rapid dissolution of silver ions in the media can create obstacles, but with careful design this problem can be overcome.

Chapter 3

Biocompatibility of the silver coated titanium discs with rapidly growing human primary osteoblast cells

3.1 Introduction

The concept of retaining artificial teeth with the so-called surgically installed titanium dental implants is becoming widely accepted among dentists and patients. This is due to several advantages such as: improved appearance, speech, self-esteem, durability, comfort and convenience. However, although the incidence rate is low in most surgeries, the surface of dental implants can be subject to bacterial colonisation and infection with subsequent implant failure. To overcome this problem, coating the implant surface with an antibacterial agent can be effective. Besinis *et al*. (2014) found that metal nano particles (eg., silver) can have potential antibacterial activity against oral pathogens. Coating dental implants with silver nanoparticles may therefore be effective at preventing bacterial colonisation on the surface. Taking into account the clinical safety requirements of low human toxicity and biocompatibility with human tissue one issue that arises with using silver nanoparticles as antimicrobial agents, is whether the dose of silver which is required to kill the bacteria can have detrimental effects on osteoblast cells in the vicinity of the dental implant surface.

There are various factors that can affect silver toxicity including particle size, shape, chemical composition, solubility, (see Chapter One). Concerns include the ability of silver nanoparticles to interfere with mitochondrial function as well as compromising the integrity of cell membranes (Carlson *et al*., 2008). In addition, it is still uncertain whether the toxic effect of silver nanoparticles belongs to the particles itself or the dissolved silver ions from it (Albers *et al*., 2013). However, in some circumstances silver ion release inside cells may occur. Singh *et al*. (2012) argued in favour of the intracellular presence of silver ions released from silver particles which had been trafficked into the cytoplasm. Nano sized silver particles may also release significantly

more ions than micro sized particles, possibly due to high surface area to volume ratio (Hajipour *et al*., 2012).

The biocompatibility of nano silver coating on titanium to human primary osteoblast cells should be tested before use of the materials in clinical practice, as the human primary osteoblast cells are in direct contact with dental implants inside the jaw. In order to decrease the potential toxic effect of silver nanoparticles on the osteoblasts, the surface can be coated with another material on top of the silver layer. For examples, Samberg *et al*. (2010) reported that carbon-coated silver nanoparticles were significantly less toxic to keratocytes than uncoated particles. Since HA particles resemble the inorganic constituent of the living bone, coating the silver layer with HA nanoparticles may decrease the contact toxicity of the silver and also enhance osseointegration. HA is regarded as a biocompatible and osteoconductive material (Woodard *et al*., 2007). Nano scale HA has been found to have positive effects in promoting osteoblast cell adhesion to the surface, proliferation and calcium deposition as well as improved bioactivity and biocompatibility as compared to micro-meter scale grains (Shi *et al*., 2009). Consequently, the hypothesis in this chapter is that coating the dental implant surface with silver and HA nanoparticles may potentially decrease the incidence of peri-implant infection without impairing peri-implant osteoblast cells. The aims of the chapter are to investigate the biocompatibility of the coatings with rapidly growing human primary osteoblast cells and to determine the effect of dissolved silver on cell health and electrolyte balance.

3.2 Materials and methods

3.2.1 Cell Culture

The experiment was performed using primary human osteoblast cells (Hob) obtained from ECACC (European Collection of Cell cultures) which were cultured in 75 cm^2 flasks (Sterilin, Newport, UK) with vented caps containing 15 mL of DMEM (Dulbecco's Modified Eagle's medium) with L-Glutamine, 10 % foetal bovine serum (FBS), and 1 % penicillin-streptomycin (100 IU Penicillin- 100 µg/ml Streptomycin) purchased from Invitrogen. The media were changed whenever needed as indicated by the quantity of dead cells (every 4 days roughly). Growing cells were sub-cultured into new flasks when the confluence reached 80-85%. For the latter, the media was removed first and the cells were washed twice with phosphate buffer saline, D-PBS, (Fischer scientific, without added calcium and magnesium), then trypsinised with 2 ml of 0.25% trypsin and EDTA and re-suspended in fresh culture medium, then counted with a haemocytometer; trypan blue dye was used to check the cell viabiltiy. The cells were maintained at 37 °C in an incubator with a humidified atmosphere of 5 % CO_2 and 95 % air. Cells used in the present experiment were at Passage 12 and 13.

3.2.2 Sample (titanium disc) preparation

Titanium samples were prepared according to the protocol being discussed in Chapter 2. For this experiment, 9 samples of each group were prepared and sterilised via gamma (radiation dose 36.42-40.72 kGy for 10 hours). The samples were pre-treated with the cell culture medium for 2 days to get rid of the rapidly dissolved silver ions that could have toxic effects on the cells.

3.2.3 Experimental design

The purpose of this experiment was to investigate the biocompatibility of primary human osteoblast cells (Hob) that were in direct contact with a titanium alloy surface coated with silver nanoparticles and HA. The experiment was done in 24 well-microplates, and the microplate was the unit of replication in the experimental design (n = 6 plates/treatment). 12000 cells/well were used in this experiment, (20000 cells/ml and 0.6 ml of media was added to each well), (Frandsen *et al*., 2014). Controls included a reference consisting of cells plus the culture media, but without the alloy disc, which will be referred as a reference control; and uncoated titanium disc plus cells and media (Ti). The treatment groups were silver plated titanium plus media and cells (Ag), silver plated plus nano HA coated titanium plus media and cells (Ag+nHA) and silver plated plus micro HA coated titanium plus media and cells (Ag+mHA). The cells were incubated with the appropriate treatment or control for 7 days in 95% air and 5% CO_2 incubator and the cell culture medium was replaced on days 1, 4 and 7 with fresh media.

After 7 days of incubation, the cells were washed with 2 ml washing buffer (300 mmol L^{-1} sucrose, 0.1 mmol L^{-1} EDTA, 20 mmol L^{-1} HEPES buffered to pH 7.4 with few drops of trizma base) and then 1 ml of a lysis buffer (the same as the washing buffer above, except hypotonic with a sucrose concentration of 30 mmol L^{-1}, and containing 0.001 % of Triton-X 100 (Sigma Aldrich). The subsequent detatched/lysed cells in the lysis buffer were homogenised for 10 to 15 minutes to ensure the complete detachment of the cells from the surface. The crudely homogenised cells were used for biochemical assays, the determination of protein content of the cells and also to determine the silver and electrolytes concentration (see below). The stock cell culture medium was also used for biochemical assays (LDH and ALP) and also to measure the

concentration of Ag and electrolytes (Ca^{2+}, Na^{+} and K^{+}) by inductively coupled plasma - optical emission spectrometry (ICP-OES, iCAP 7400 RADIAL, Hemel Hempstead, UK). The experiment was repeated again with the same design and treatment groups as above (n = 3). For the latter, the cells were fixed after 7 days and investigated under SEM for morphology (see below).

3.2.4 Biochemical assays

3.2.4.1 Alkaline Phosphatase

ALP, optimum pH 9-10, is a protein found in organisms from bacteria to humans. It can be found in all body tissues and is particularly high in the liver, bile ducts, and bone. ALP is a biomarker which is widely recognized as a measure of osteoblast activity, differentiation and mineralization (Sabokbar et al., 1994). ALP activity can be easily measured using a colourimetric assay at 405 nm. The assay is based on the hydrolysis of para-Nitrophenylphosphate (pNPP) which is colourless to slightly yellow substrate which respresents p-Nitrophenol (PNP) in the presence of ALP enzyme giving a distinct yellow colour detectable at 405 nm. The progress of the enzyme catalysed reaction can be followed kinetically by measuring the change in absorbance at 405 nm over time.

ALP activity was measured in the external culture media on each day of the experiment and also in the cell homogenates at the end of the experiment (7 days) to determine evidence of biological functionality in the cells. For the cell homogenates, 30 µl of sample were added to 96 well micro plates, after that, 105 µl of glycine buffer were added. Finally, 145 µl pNPP were added to the wells with multi-channel pipettes, then the plate was shaken twice and read immediately in a plate reader (VersaMax,

molecular devices, Berkshire, UK) for 300 seconds at 405 nm at room temperature. For the blank, glycine was added (instead of the sample) to the assay reaction mixture. The reagents were 100mM glycine buffer in Milli-Q ultrapure water (18.2 MΩ), 500µM pNPP (Acros organics) dissolved in glycine buffer and ALP (Sigma Aldrich) in glycine buffer. ALP activity curve is shown in Appendix 2, Figure 3.

3.2.4.2 Lactate dehydrogenase

LDH is an enzyme which is normally found in the cytoplasm of animal cells and has been implicated in cell biology/toxicology as a biomarker of cell injury. The basis of this assay in the current experiment is that osteoblast cells contain LDH, while cell culture media normally does not. The presence of LDH in the culture media is therefore interpreted as a release of LDH enzyme from the cells through a compromised cell membrane. LDH activity was measured every day in the external media, and after 7 days in the cell homogenate. The method followed Campbell *et al*. (1999) who used 100 µl of sample added to the reacting mixture (2800 µl of 6 mmol L^{-1} sodium pyruvate in 50 mmol L^{-1} phosphate buffer at PH 7.4, plus 100 µl of 6 mmol L^{-1} NADH solution), mixed directly in a 3 ml cuvette and the change in absorbance was measured over 2 minutes at 340 nm (Jenway 7315 spectrophotometer). LDH activity was expressed as IU mg L^{-1} (µmol min^{-1} ml^{-1}) for the media and µmol min^{-1} mg^{-1} cell protein for the cell homogenate. LDH activity curve is shown in Appendix 2, Figure 4.

3.2.4.3 Protein assay

Crudely homogenised cultured cells contain fairly high amount of proteins. Several commercially available colorimetric kits are available which could be used to measure the protein content of samples. The Bicinchoninic assay (BCA) (MC155208, Pierce,

Rockford, USA) is one of the colorimetric kits that offer speed and convenience for routine protein measurements. The method works by reducing copper ions by peptide bonds in the protein in alkaline conditions. The produced Cu ions bind to the bicinchoninic acid and this will result in a colour change of the dye. The procedure used 10 µl of each sample (cell homogenate or bovine serum albumin) into a 96-well microplate with 200 µl of fresh colour reagent, the plate was then mixed thoroughly on a shaker for few seconds then covered and incubated in 37˚C for 30 minutes. Absorbance of the samples were read at 592 nm (VersaMax, molecular devices, Berkshire, UK). To plot a calibration curve, the protein assay standards (bovine serum albumin) were diluted with phosphate buffer saline (phosphate buffer tablet (Sigma Aldrich) was dissolved in 100 ml of ultrapure deionised water) to give final protein concentrations of 2, 1.6, 1.2, 0.8, 0.2, 0.1 and 0 mg L^{-1}.

3.2.5 Metal and electrolyte analysis

Concentration of silver (Ag), sodium (Na^{+}), calcium (Ca^{2+}) and potassium (K^{+}) were determined both in homogenised cells at 7 days and in media after 1, 4 and 7 days. The purpose of measuring silver in the media was to investigate the amount of silver released from the coatings. Measuring the silver concentration in the cell homogenate was performed to determine the amount of silver which have been released from the coating but subsequently trapped/associated with the cell monolayer. The electrolyte composition of the cell homogenates were also measured with respect to osmotic health. For metal and electrolyte analysis, 400 µl of the external media from each sample were acidified with 20 µl of 70% nitric acid. For the cell homogenate, 800 µl from each sample were taken and acid digested with 1 ml of 70% nitric acid and left

overnight for complete acid digestion. Ag, Na^+, K^+ and Ca^{2+} of each sample were determined using ICP-OES. The concentration of silver was expressed as mg L^{-1}, whereas the concentrations of Na^+, K^+ and Ca^{2+} were expressed as mmol L^{-1}.

3.2.6 Investigation of osteoblast morphology by Scanning Electron Microscope

SEM was used to visualise the morphology of cells which have been grown on the discs over 7 days. Cells were fixed with 1 ml of 2.5% glutaraldehyde in sodium cacodylate buffer. Then cells were immersed in a series of different concentrations of ethanol (30, 50, 70, 95 and 100%) to dehydrate the cells. For further dryness, the cells were immersed in 50% of ethanol - 50% hexamethyldisilazane (HMDS) solution for 30 min then in 100% of HMDS for 60 minutes. The specimens were removed from the HMDS and left in a fume cupboard to dry overnight.

3.2.7. Protein adsorption test

Results of this study showed that there was significantly higher protein on the specimens compared to the reference control. This was argued to be an adsorbed protein from the external media. To confirm this, protein adsorption test was conducted by adding the cell free media to the discs for 7 days and then measuring the adsorbed protein.

3.2.7.1 Sample preparation

Medical grade titanium discs were used for this experiment. The specimens were polished and silver plated then coated with nano HA and micro HA, finally, they were sterilised by gamma radiation (Chapter 2).

3.2.7.2 Experimental design

The experiment was conducted in 24 well micro plates, n = 3 and the micro plate was the unit of replication. Control of the experiment was uncoated titanium (Ti), treatments were silver plated titanium (Ag), silver plated plus nano HA (Ag+nHA), silver plated plus micro HA (Ag+mHA). All the specimens were treated with the cell culture medium for 2 days prior to the experiment. At the experiment, cell free culture medium (DMEM + 10%FBS + 1%antimicrbial) was added to the discs for 7 days, media was changed at day 1, 4, and 7. At the end of the experiment, the specimens were washed with 2 ml washing buffer (300 mmol L^{-1} sucrose, 0.1 mmol L^{-1} EDTA, 20 mmol L^{-1} HEPES buffered to 7.4 with few drops of trizma base) and then 1 ml of a lysis buffer (the same as the washing buffer above, except hypotonic with a sucrose concentration of 30 mmol L^{-1}, and containing 0.001 % of Triton-X 100 (Sigma Aldrich). The lysis buffer was left on the discs for 15 minutes (same as the experiment above) and then removed to conduct the protein assay. Basically, the experimental condition was exactly the same as the biocompatibility experiment above but without cells. Protein assay was performed for the samples using exactly the same method as described earlier in this chapter.

3.2.8 Statistical analysis

All data are expressed as mean ± S.E.M. data were analysed using Statgraphics 16, out layers were removed using Box and Whisker plot, then the data were subjected to normality test. To investigate the treatment effect, the values were subjected to an analysis of variance (ANOVA) using the Tukey test to analyse the difference, for non-

parametric data, Kruskal Wallis test was used and the differences were determined using Box and Whisker plot. To investigate the time dependent changes, two way ANOVA was used. Values of $p < 0.05$ were considered as significant difference.

3.3 Results

3.3.1 Silver release to the external media and exposure to the cell monolayer

Results showed that there was a constant silver ion release from the Ag+nHA to the external media over 7 days, silver release was lower in Ag+nHA than Ag and Ag+mHA samples (Table 3.1), silver exposure to the cell homogenate was also confirmed (Table 3.1). Silver concentration in the external media showed significantly higher values (one way ANOVA, $p < 0.05$) in Ag group as compared to other groups in all time points. It was also noticed that silver concentration was steadily increased over 7 days in Ag, Ag+nHA and Ag+mHA groups. However, time points did not significantly affect silver release in Ag+nHA, while it can be noticed that time has a significant effect on silver release in both Ag and Ag+mHA groups (Table 3.1).

Table 3.1. Concentration of silver in the external media over 7 days and in the cell homogenate at the end of the experiment

Treatment	Day 1	Day 4	Day 7	Homogenate
	Silver (mg L^{-1})			
Reference control	0.10 ± 0.00 ^{b}	0.06 ± 0.00 ^{c} *	0.01 ± 0.00 ^{c} *#	8.01 ± 0.40
Ti	0.16 ± 0.06 ^{b}	0.06 ± 0.02 ^{c}	0.01 ± 0.00 ^{c} #	6.21 ± 1.20
Ag	1.12 ± 0.08 ^{a}	2.14 ± 0.08 ^{a} *	2.09 ± 0.11 ^{a} #	5.19 ± 1.89
Ag+nHA	0.98 ± 0.26 ^{a}	1.07 ± 0.22 ^{b}	1.19 ± 0.20 ^{b}	6.91 ± 3.61
Ag+mHA	0.60 ± 0.03 ^{ab}	1.37 ± 0.08 ^{b} *	1.16 ± 0.18 ^{b} #	19.38 ± 7.37

Data are expressed as mean ± S.E.M, (n = 6), different letters within the column indicate a significant difference, asterisk means significant different with the previous time point and (#) means a significant difference with day 1 (one way ANOVA, or Kruskal Wallis test, $p < 0.05$).

3.3.2 Cell health and morphology on the coatings

Cell morphology at the end of the experiment is shown (Figure 3.1). SEM images of the cells after 7 days on uncoated titanium discs (Ti) showed that they were confluent, attached to each other and with normal morphology (stellate appearance with extensive filopodia). There was no evidence of cell membrane damage or loss of cell volume. Cells grown on the Ag+nHA discs showed the same features as on the titanium alloy control, except the cell density was lower. It was difficult to find healthy cells on the Ag+mHA coating, but some cellular debris and protein substances were found. Moreover, only a few surviving cells were found on silver-coated surface without added HA. The cells were stellate with extensive filopodia, but because they were sparse no cell to cell contact was observed.

Cell health was also assessed biochemically in the cell homogenates. The ALP activity in the cells was low, as expected, since it is mainly induced later in cell differentiation (Figure 3.2). However, Ag+mHA measured higher ALP activity compared to others but the difference was not significant. There were time-dependent changes in the media ALP activity in all treatments except in reference control and Ag+mHA which did not show any significant difference over 7 days (Table 3.2). Consequently, the LDH enzyme activity in the cell homogenate was higher in the cells grown on culture plates without any alloy discs, followed by the Ti, then the silver-coated groups (Figure 3.3). LDH activity in the cell culture medium was highest in the reference control on Day 1 but the difference with others was not significant. In Day 4, the highest value was recorded in Ag group which was significantly higher than other groups and also than the group itself in the previous time point (Day 1), (Table 3.3). The protein content of the cell homogenate showed that the cell growth was better on Ti alloy than just on the culture plate, regardless of the type of coating on the alloy

(Figure 3.4). The major electrolytes were also measured in the cell homogenates (Table 3.4). The Na^+ concentration in the homogenates was higher in all treatments grown on Ti alloy compared to the culture plate surface. There were no changes in homogenate K^+ concentration. However, the Ca^{2+} concentration in Ag+nHA and Ag+mHA treatments were significantly higher than any of the other groups (Table 3.4).

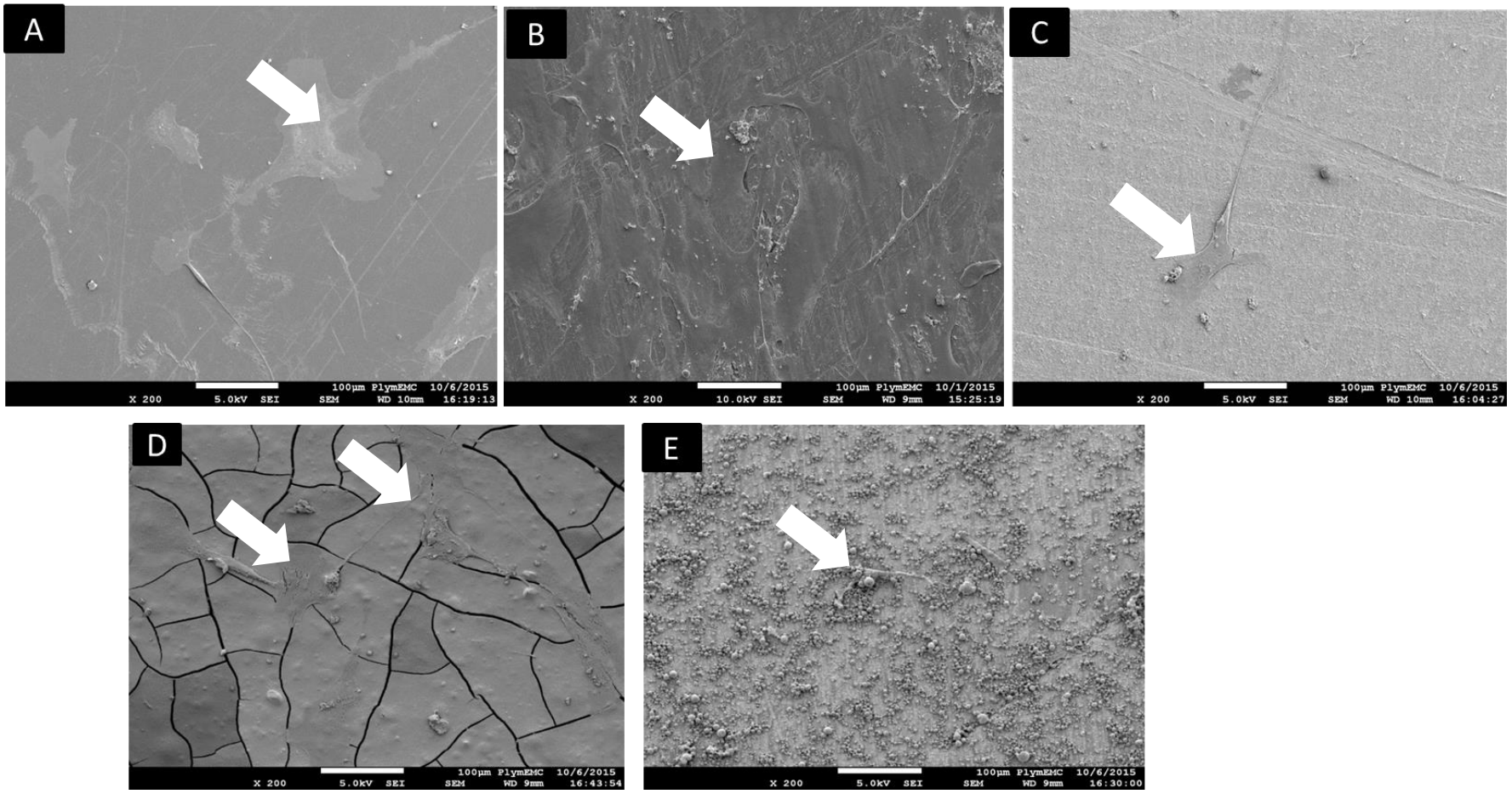

Figure 3.1. SEM images showing the morphology of primary osteoblast cells grown on different surfaces over 7 days. (A) 24-well microplates (x 200); (B) uncoated titanium disc (x 200); (C) silver plated titanium (x 200); (D) Ag+nHA (x 200); (E) Ag+mHA (x 200). The cells exhibited a stellate shape with extensive filopodia. There was more cell covernge on the Ag+nHA compared to the Ag and Ag+mHA treatments, but less than the reference control and Ti. All the scale bars are 100 µm.

Table 3.2. ALP enzyme activity in the cell culture media over 7 days

Treatment	Day 1	Day 4	Day 7
	ALP (nmol min^{-1} ml^{-1})		
Reference control	0.057 ± 0.019	0.054 ± 0.011 [b]	0.057 ± 0.019 [a]
Ti	0.041 ± 0.018	0.023 ± 0.040 [b] *	0.040 ± 0.014 [a] *
Ag	0.054 ± 0.017	0.071 ± 0.026 [a] *	0.047 ± 0.016 [a] *
Ag+ nHA	< 0.004	0.074 ± 0.001 [a]	0.052 ± 0.003 [a] *
Ag+ mHA	< 0.004	< 0.004	0.026 ± 0.001 [b]

Data are expressed as mean ± S.E.M (n = 6). Different capital letters within each column indicate statistically significant difference, asterisk (*) means significant difference within the previous time point while (#) mean significant difference within day 1 (Kruskal wallis test, $p < 0.05$).

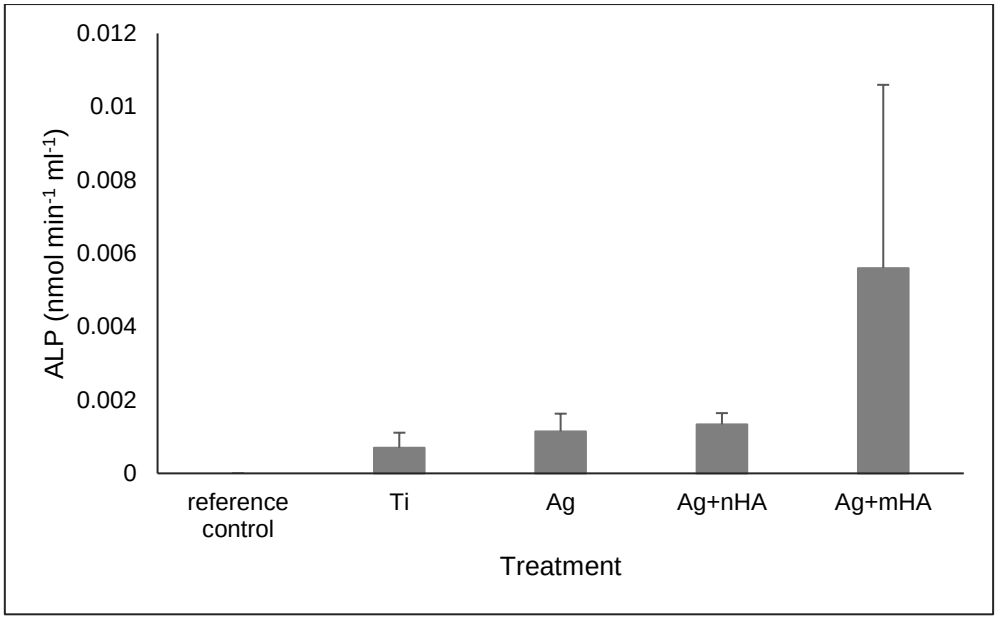

Figure 3.2. ALP enzyme activity in the cell homogenate after 7 days. Data are expressed as mean ± S.E.M (n = 6). Statistical analysis (Kruskal Wallis test, $p < 0.05$) showed no significant differences between groups.

Table 3.3. LDH enzyme activity in the cell culture media

Treatment	Day 1	Day 4	Day 7
	LDH (nmol min^{-1} ml^{-1})		
Reference control	1.95 ± 1.01	0.84 ± 0.45 [b]	0.89 ± 0.26 [a]
Ti	0.66 ± 0.53	0.63 ± 0.21 [b]	0.87 ± 0.27 [a]
Ag	0.66 ± 0.31	2.64 ± 1.12 a [*]	0.47 ± 0.16 [a *]
Ag+nHA	1.87 ± 1.46	0.47 ± 0.08 [*]	0.44 ± 0.20 a [#]
Ag+mHA	0.66 ± 0.20	0.60 ± 0.14	0.18 ± 0.13 b [* #]

Data are expressed as mean ± S.E.M (n = 6). Different capital letters within each column indicate statistically significant difference, asterisk (*) means significant difference within the previous time point while (#) mean significant difference within day 1 (Kruskal Wallis test, $p < 0.05$). Detection limit is 0.004 nmol min^{-1} ml^{-1}.

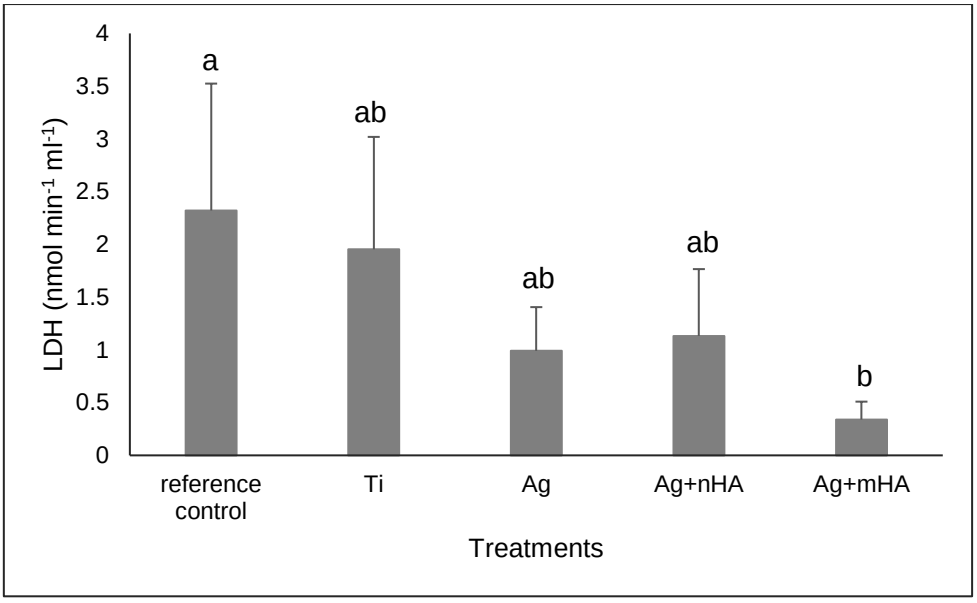

Figure 3.3. LDH enzyme activity in the cell homogenate after 7 days. Data is expressed as mean ± S.E.M (n = 6). Different letters with bars indicate Statistical significant difference between the groups (Kruskal Wallis test, $p < 0.05$).

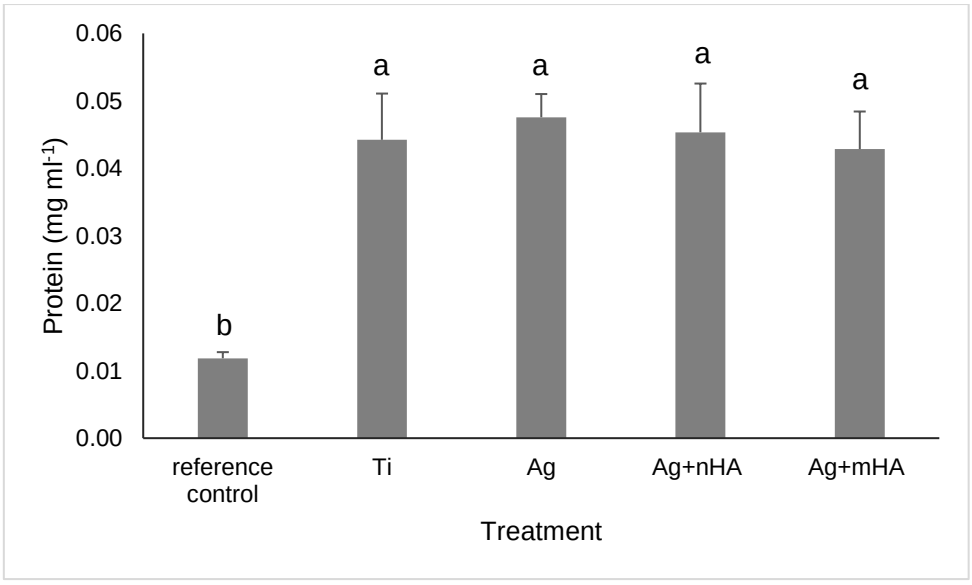

Figure 3.4. Protein content of the cell homogenate after 7 days exposure. Data are expressed as mean ± S.E.M (n = 6). Different letters within bars indicate statistically different from each other (one way ANOVA, $p < 0.05$).

Table 3.4. Total concentration of electrolytes (Ca^{2+}, Na^{+} and K^{+}) in cell homogenate.

Treatment	Ca^{2+}	Na^{+}	K^{+}
	mmol L^{-1}		
Reference control	0.01 ± 0.00 [b]	0.10 ± 0.01 [b]	0.02 ± 0.00 [b]
Ti	0.11 ± 0.02 [b]	1.10 ± 0.18 [a]	0.09 ± 0.01 [a]
Ag	0.09 ± 0.02 [b]	1.21 ± 0.12 [a]	0.10 ± 0.02 [a]
Ag+nHA	0.30 ± 0.01 [a]	1.04 ± 0.24 [a]	0.13 ± 0.04 [a]
Ag+mHA	0.42 ± 0.09 [a]	0.75 ± 0.13 [ab]	0.05 ± 0.00 [ab]

Data are expressed as mean ± S.E.M (n = 6). Different letter within the column indicate significant difference (one way ANOVA, $p < 0.05$).

3.3.3 Changes of electrolytes in the cell culture media over the coatings

Concentration of electrolytes (Ca^{2+}, Na^{+} and K^{+}) was measured in the cell homogenate and the external media over 7 days. Ca^{2+} values in the external media in Ag+nHA and Ag+mHA were significantly lower than other groups in (one way ANOVA, $p < 0.05$). While in Day 4, Ag+nHA showed a significantly lower value than others. Time points did not have an effect on Ca^{2+} in all groups except Ag+mHA which showed a significant difference at all time points (Table 3.5).

Na^{+} level in the external media in Day 1 did not show any significant difference between groups. While the value significantly decreased in Day 4 in Ag, Ag+nHA and

Ag+mHA groups. The level continued to decrease in Ag and Ag+mHA groups while Ag+nHA showed an increase in Day 7 (Table 3.5).

Regarding the K^+ level, a gradual decrease over 7 days was noticed in reference control and Ti (Table 3.3), however, other groups showed an increase in K^+ level over 7 days. To compare the groups with each other, the Ti showed highest value in Day 1, while the reference control measured highest K^+ in the following time points. Lowest K^+ value in all time points was measured in Ag+nHA which was significantly lower (one way ANOVA, $p < 0.05$) than other groups (except Ag+mHA in day 7).

Table 3.5. Concentration of Na^+, K^+ and Ca^{2+} in the external media over 7 days.

Element	Treatment	Day 1	Day 4	Day 7
		mmol L^{-1}		
Na^+	Reference control	143.08 ± 1.89 ^{a}	158.75±14.37 ^{a}	139.68 ± 3.85 ^{a}
	Ti	143.90 ± 7.31 ^{a}	131.90±1.76 ^{ab}	129.27 ± 3.24 ^{ab}
	Ag	138.59 ± 1.51 ^{a}	122.70±3.70 ^{b*}	120.31 ± 1.55 $^{b\#}$
	Ag+nHA	137.23 ± 4.57 ^{a}	113.10±6.66 ^{b*}	126.74 ± 1.69 ^{ab}
	Ag+mHA	145.97 ± 3.89 ^{a}	124.58±2.26 ^{b*}	120.81 ± 2.13 $^{b\#}$
K^+	Reference control	6.48 ± 0.13 ^{ab}	7.23±2.95 ^{a}	6.35 ± 0.19 ^{a}
	Ti	6.92 ± 0.20 ^{a}	5.96±0.10 ^{ab*}	5.83 ± 0.14 $^{ab\#}$
	Ag	6.41 ± 0.05 ^{ab}	5.53±0.16 ^{ab*}	5.44 ± 0.05 $^{b\#}$
	Ag+nHA	6.24 ± 2.54 ^{b}	4.87±0.50 ^{b*}	5.78 ± 0.07 ^{ab}
	Ag+mHA	6.68 ± 0.14 ^{ab}	5.69±0.10 ^{ab*}	5.48 ± 0.08 $^{b\#}$
Ca^{2+}	Reference control	1.88 ± 0.02 ^{a}	2.20 ± 0.18 ^{a}	2.01 ± 0.06 ^{a}
	Ti	2.15 ± 0.17 ^{a}	1.89 ± 0.02 ^{ab}	1.87 ± 0.04 ^{a}
	Ag	1.93 ± 0.05 ^{a}	1.76 ± 0.04 ^{bc}	1.78 ± 0.06 ^{a}
	Ag+nHA	0.76 ± 0.04 ^{c}	0.67 ± 0.08 ^{d}	0.74 ± 0.05 ^{b}
	Ag+mHA	1.41 ± 0.06 ^{b}	1.45 ± 0.03 ^{c}	1.02 ± 0.14 $^{b*\#}$

Data are expressed as mean ± S.E.M (n = 6). Different letters within the column indicate significant difference from each other. Asterisk (*) means significant difference within the previous time point while (#) mean significant difference within day 1 (one way ANOVA, $p < 0.05$). Two way ANOVA showed that there were both time and treatment effect on Ag, Ca^{2+}, Na^+ and K^+ concentration.

3.3.4 Protein adsorption test

Results showed that the amount of protein was ranging from 0.02 to 0.07 mg ml^{-1} (Figure 3.5). The differences between the groups were not significant (Kruskal Wallis test, $p > 0.05$).

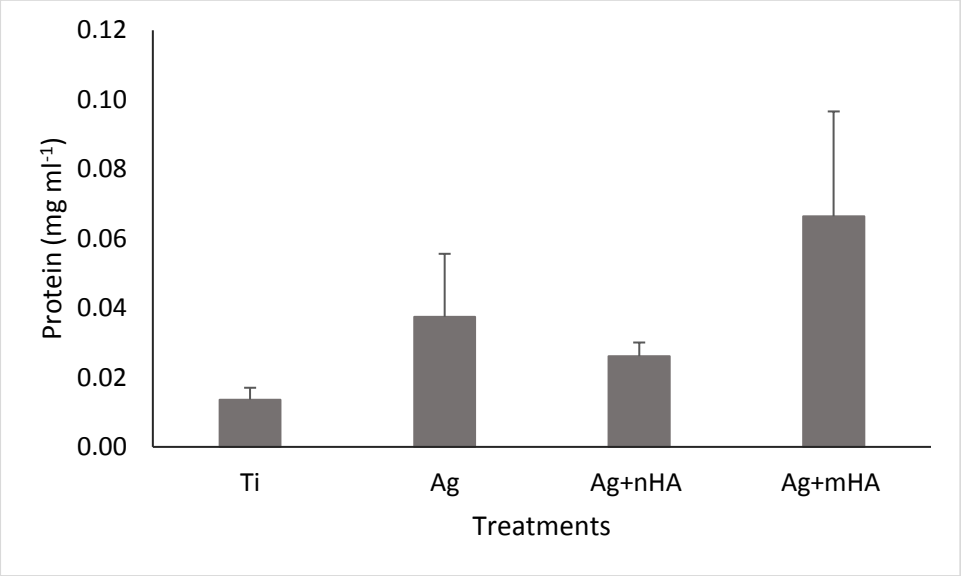

Figure 3.5. Concentration of protein on the specimens after 7 days exposure to the cell free culture medium. Data are mean ± S.E.M, (n = 3), there was no significant difference between the treatments (Kruskal Wallis test, $p > 0.05$).

3.4 Discussion

Clinical demand on dental implants is growing over the last few years, possibly due to the several advantages over traditional tooth/teeth replacements. Researchers have always tried to modify the implant surface so that to improve antibacterial activity and biocompatibility. For any new material to be used in clinical practice, there are serval tests that must be performed to confirm the biocompatibility with the surrounding living cells. Silver nanoparticles coating on titanium dental implants can effectively inhibit bacterial growth on the surface of the implant, however, concerns are increasing regarding the cytotoxic side effects of ionic silver and silver nanoparticles (Foldbjerg

et al., 2009; Ahamed *et al*., 2010). Results of the present study demonstrated that Ag+nHA can allow osteoblast cell survival and growth but with lower density and confluency as uncoated titanium discs. Furthermore, Ag and Ag+mHA were less biocompatible than Ag+nHA. This result can be elucidated by the fact that HA nanoparticles can allow for more osteoblast cell growth and proliferation than micro-sized particles (Shi *et al*., 2009). Although HA is more biocompatible than titanium and rough surfaces can perform better than smooth surfaces in enhancing osteoblast cell proliferation (Bachle *et al*., 2004), so the reason of less confluent cells on Ag+nHA than those on titanium can be due to the presence to free silver ions that to some extent had detrimental effects on cell proliferation.

3.4.1 Effect of the coatings on cell morphology and growth

Cells were allowed to grow and spread for 7 days. SEM images revealed that reference control and Ti cells were healthy, confluent and looked as exprected, cells on Ag+nHA were healthy and contacting with each other without having a noticeable membrane rupture (Figure 3.1). From the osseointegration point of view, cells were well attached to the nHA layer, however, they were less confluent than the control but more confluent than Ag and Ag+mHA, cell shrinkage was observed on Ag and Ag+mHA but not on Ag+nHA this finding indicates that silver causes cell shrinkage but cells on Ag+nHA were healthier. This indicates that the surface topography and chemistry of Ag+nHA was appropriate for the cells to survive and grow better than Ag and Ag+mHA, this is the first study to compare between nan HA and micro HA in terms of cell growth and morphology. In addition, cell health was investigated metabolically, there was no adverse anaerobic metabolism and not significant cell membrane rupture

as LDH in the media was low, the dissolved silver did not seem to induce a significant toxicity to the cells (Table 3.3, Figure 3.3). There was no evidence of change in cell volume and osmotic stress as the Na^+ and K^+ were not damaged. This result was also validated by Kawata *et al*. (2009) who found that more than 1 mg L^{-1} of silver for 24 hours had cytotoxic effects against Human hepatoma cells. However, another study found that minimum concentration of released silver to kill osteoblast cells was 5.1 mg L^{-1} (Albers *et al*., 2013). The latter disagrees with the results of this study, as it was found here study that silver release was less than 5 mg L^{-1} in both Ag and Ag+mHA and the dissolved silver ions were probably toxic to the primary osteoblast cells. The converse results can clarify the fact that not only released silver ions (or particles themselves) can have impact on cell viability; the surface chemistry and whether silver nanoparticles were coated or not, can also affect the cell viability. In the current study, there was no significant difference in the silver release to the external media in Ag, Ag+nHA as well as Ag+nHA (Table 3.1). Nonetheless, Ag+nHA exhibited more biocompatibility than others, the presence of HA nanoparticles which prevented the direct contact between the cells and the silver layer could be the reason of a better biocompatibility demonstrated by Ag+nHA. This result supports Samberg *et al*. (2010) who found that coated silver particles exhibit less cytotoxicity than the bare ones. It also supports the fact that HA nanoparticles are more biocompatible than HA micro particles.

ALP assay was performed to investigate the activity and function of osteoblast cells. The high ALP enzyme in the external media indicates that cells are active metabolically and they are growing and also high ALP enzyme in the cell homogenate indicates that there were a high number of surviving cells in the monolayer before homogenization. In the current study, ALP activity in external media was as low as it

was close to the background levels of the instrument (Table 3.2). This result shows that 7 days is not enough for 12000 cells/well to produce detectable ALP enzyme. However, values in the cell homogenate were also close to the background level which can also be the result of low quantity of cells resulting in undetectable ALP enzyme.

Regarding LDH activity, values in the external media was close to the background levels of the machine (Table 3.3) which means that membrane integrity of the cells was intact and LDH was not released out of the cells. This can give a conclusion that cells were surviving during the experimental period. Same results were found in the homogenate indicating that quantity of the cells was not enough to produce measurable LDH activity. Protein assay results of the cell homogenate revealed that the protein density was significantly higher in all treatment groups as compared to the reference control (Figure 3.4). This result indicates that the cells were surviving on all discs, however, SEM images do not agree with this finding as it was shown that no cells were surviving on Ag+mHA and only few were surviving on Ag group. It could be argued that high protein content in Ag+mHA and Ag groups might be the result of the formation of a protein layer on the coating coming from FBS in the culture media. Hellstrand *et al*. (2009) demonstrated the attraction of proteins by silver nanoparticles resulting in the formation of a protein corona on the particles.

3.4.2 Total silver release from the coatings and possible effects on the electrolyte balance

Silver and electrolytes were measured in the external media over 7 days (Table 3.1 and Table 3.5) and in the cell homogenate (Table 3.4). The results showed that the concentration of Ca^{2+} in the external media was lower in Ag+nHA and Ag+mHA than other groups over 7 days, this might be the result of chemical reaction between calcium

in the media and hydroxide ions present in the HA which results in the formation of calcium hydroxide $Ca(OH)_2$. This finding was also supported by (Harding, Rashid *et al*., 2005) who demonstrated that the surface of HA is able to adsorb Ca^{2+}. The concentration of Ca^{2+} in the cell homogenate indicated that there was significantly higher Ca in Ag+nHA and Ag+mHA than other groups. There are two explanations for this finding, either Ca^{2+} ions were released from the coating and settled in the cell monolayer, or it might be due to homogenisation which can result in detaching HA particles from the surface.

Silver release to the external media was significantly increasing over 7 days in Ag and Ag+mHA, while silver release from Ag+nHA was constant and not significantly different over 7 days. This result indicates that Ag+nHA can release a constant amount of silver for a long time which could be sufficient to retain antibacterial activity without having any adverse effects to the cells. Moreover, as the sintering process results in higher silver release due to the formation of silver oxide (see the discussion in chapter 2). Therefore, the explanation of the lower silver release in Ag+nHA and Ag+mHA as compared to Ag might be due to the sintering process which was mandatory during HA application that has probably caused higher silver release in Ag+nHA and Ag+mHA during the disc pre-treatment with the cell culture media prior to the experiment.

Furthermore, it was noticed in the cell homogenate that the concentration of Na^+ and K^+ (normalised to protein) was lower in Ag+mHA as compared to others. This could be due to the presence of high amount of silver in the cells which is known to block Na^+, K^+ -ATPase membrane bound transport system (Hussain *et al*., 1994). Silver can prevent Na^+ and K^+ entry from the media to the cells, also results in normal

outward movement of Na^+ and K^+ ions from the cells which leads to slowly depleting the cell of Na^+ and K^+.

3.4.3 Conclusions

The aim of this study was to determine the biocompatibility of silver plated discs (Ag, Ag+nHA and Ag+mHA) with human primary osteoblast cells. Ag+nHA was more biocompatible than Ag and Ag+mHA. Comparing to the control, there were more cells on uncoated titanium compared to Ag+nHA. Moreover, silver release in this study was less than that of dissolution experiment (chapter 2.3.5), which is due to the disc pre-treatment with the cell culture media for 2 days prior to the experiment. HA nanoparticles in Ag+nHA, enhanced osteoblast cell viability and growth compared to Ag and Ag+mHA. Furthermore, there were some experimental challenges in this study; there was difficulty in detecting cellular enzymes (LDH and ALP) because of using low number of cells initially which resulted in limited enzyme production. Thus, it is useful to increase the number of cells initially to produce high amount of enzymes and better interpret the results. In addition, it was found that protein adsorption from the media to the specimens were masking the actual protein content of the cells, so it is not recommended to normalise enzyme activity and electrolyte concentration in the cell homogenate per amount of proteins in the cell homogenate.

Chapter 4

Toxicity of Dissolved Silver from Silver-coated Titanium Implants to Human Primary Osteoblast Cells

4.1 Introduction

The release of dissolved silver from silver-containing materials used in medical implants can potentially be beneficial as a biocide for infection control immediately after surgery. However, dissolved silver can also be toxic to mammalian cells. The target organs for dissolved silver include the liver and kidney in rodents and humans. In rats, the lethal dose (LD_{50}) is around 400 mg kg^{-1} body weight of silver nitrate (Tamimi *et al*., 1998). In humans, there is no lethal concentration value of silver, but the lethal toxic dose rate of silver is estimated to be higher than 0.5 µg/kg of body weight/day (Hadrup and Lam. 2014).

The toxicity of dissolved silver is dependent on the exposure concentration and time (i.e., the total dose), but also on the chemistry of the cell culture medium; and how it alters bioavailability, the type of cells used, and the cell density in the culture system (i.e., the dose delivered per cell). For example, for silver nitrate, 5 mg L^{-1} $AgNO_3$ in cell culture media (DMEM + 10%FBS + 1% antibiotic) was found to induce significantly more LDH leak to the external media compared to unexposed controls in human fibroblast cells after 24 hours (Meran *et al*., 2013). For silver nanoparticles, it is unclear what the dose metric should be, but on a mass concentration basis, Ahamed *et al*. (2010) found that the tolerance of different cell lines to silver varied, even though the cells were exposed to similar amount of silver. For example, the PC-12 cell line in a supplemented RPMI-1640 media and exposed to 50 mg L^{-1} of silver nanoparticles (15 nm in size) showed significantly reduced mitochondrial function and dopamine level after 24 hours (Hussain *et al*., 2006). While, Meran *et al*. (2018) showed that exposure to 50 mg L^{-1} of silver nanoparticles (size not defined) did not induce a significant damage to the human fibroblast cell morphology and there was no appreciable leak of LDH release after 24 hours exposure.

The mechanisms of dissolved silver toxicity are partly understood. For silver salts (or silver coatings made by electroplating), the silver may dissolve to yield the Ag^+ ion. The free silver ion can bind to –SH groups on proteins and enzymes (Yang *et al*., 2011). Ag^+ ions inhibit the Na^+ K^+-ATPase especially (Hussain *et al*., 1994) and also interferes with Na homeostasis. Dissolved silver can also cause oxidative stress when enzymes involved in defence against reactive oxygen species are damaged (Carlson *et al*., 2008). In body fluid or culture medium where high concentrations of Cl^- ions are present, the Ag rapidly forms a poorly soluble silver chloride complex which is less bioavailable (Hansen *et al*., 2015). So the bioavailability of Ag depends on the presence of Cl^- ions, -SH groups on proteins and other organic molecules. However, for cultured cells on silver plated discs, it is unclear whether the cell damage is caused by direct contact toxicity between the cells and the silver layer, or if it is indirect via the release of dissolved silver into the media. Results of the previous experiments (chapter 2 and 3) showed that there was a constant silver dissolution from the coatings into the external media. Moreover, there was a silver toxicity which led to a significant loss of cells and an inability of the cells to proliferate, especially on Ag and Ag+mHA surfaces. The aim of this experiment was to investigate the toxicity of silver released from the silver plated titanium implants to human primary osteoblast cells; and also to investigate the effect of cell culture medium on bioavailability of dissolved silver. The specific objectives were to expose the silver coated specimens (without cells present) to the cell culture medium (DMEM + 10FBS + 1% antimicrobial) so as to condition the media with dissolved silver from silver plated titanium discs; and then transfer the conditioned media to the growing cells in culture plates. A second objective was to measure the dissolved silver uptake by the cell monolayer, and the total silver release to the external media. Then finally, to study the toxic effect of dissolved silver on the

cells by measuring the LDH release, protein content of the cells and also examining the cells in situ under the microscope after exposure.

4.2 Materials and methods

4.2.1 Cell culture

Human primary osteoblast cells were cultured in DMEM plus 10% FBS and 1% antimicrobials (antibiotic and antimycotic). The culture conditions were the same as described in Chapter 3. Cells at passage 7 and 8 were used for this experiment.

4.2.2 Experimental design

The control for the experiment was untreated cells in normal culture media (hereafter termed the 'reference control'). The treatments were cells exposed to media from silver plated titanium discs (Ag), silver plated titanium disc plus nano HA (Ag+nHA), and silver plated titanium discs plus micro HA (Ag+mHA). All the discs, as prepared for the treatments above, were sterilised by gamma radiation prior to the experiment (see chapter 2). The discs without any cells were then covered with 1 ml of cell culture medium (DMEM , supplemented with 10% FBS and 1% antimicrobial) and incubated in 5% CO_2 with 95% air in an incubator at 37 °C (HETO-HOLTEN cell house 170) for 2 days, then the media was discarded and the discs were ready for the actual experiment. This step enabled the removal of any rapidly exchangeable silver from the coatings that might damage the cells (see Chapter 2).

The experiment was run in 24 well microplates (n = 6 plates/treatment). The microplate was the unit of replicate in the experiment and the experiment was run on

two separate occasions with different batches of the cells, and each run was triplicated (x3 plates/treatment/run). The cells were grown directly on cell culture dishes and in parallel, the discs were incubated with culture media without the cells for this initial part of the experiment. Breifly, while the discs were incubating in the cell culture medium, at the same time, cells were grown in a second series of plates (n = 6 plates/treatment, seeded with 30,000 cells/well). To initiate exposure of the cells, the now conditioned media from the incubation of the discs was added to the cell cultures. The media for the cells were replaced by the conditioned medium from the discs on days 1, 4 and 7 (Figure 4.1). Samples of the conditioned media were collected before adding it to the cells (termed 'before exposure') and then after exposing the cells to it for fixed durations (termed 'after exposure'). The silver concentration in the conditioned media was measure before and after the exposure using ICP-MS. The media (after exposure) was also analysed for Na^+, Ca^{2+} and K^+ using ICP-OES, as well as for LDH and ALP activities. The media was sampled from cell growing plates at days, 1, 4 and 7. At the end of the experiment, the cell were photographed *in situ* under the light microscope (OLYMPUS, CK30-F200) using (Galaxy s6 camera) to examine the cell morphology and confluence of the dishes. Then, the cells were washed with 2 ml of washing buffer (300 mmol L^{-1} sucrose, 0.1 mmol L^{-1} EDTA, 20 mmol L^{-1} HEPES buffered to 7.4 with few drops of Trizma base) and then 1 ml of a lysis buffer [the same as the washing buffer above, except hypotonic with a sucrose concentration of 30 mmol L^{-1}, and containing 0.001 % of Triton-X 100 (Sigma Aldrich) to lyse the cells. The resulting cell homogenate was analysed for total protein content, and LDH and ALP activities. The concentration of total Ag, Na^+, Ca^{2+} and K^+ were also measured by ICP-MS or ICP-OES as appropriate.

4.2.3 Lactate dehydrogenase and alkaline phosphatase enzyme activity

LDH and ALP enzyme activities were measured in the cell culture medium and the cell homogenate. For the former, 100 µl of the sample was added to 2800 µl assay reagents in a 1 ml cuvette and absorbance was read at 320 nm wavelength. For the later, 30 µl of sample was added to 250 µl assay reagent in 96 well microplates and the absorbance was read at 405 nm. The procedures are described in detail in Chapter 3.

4.2.4 Protein assay

The protein assay was conducted to measure the protein content of the cell homogenate to normalise the LDH and ALP activity, as well as allowing the metal or electrolyte analysis to be expressed per mg of protein. Briefly, 10 µl of the sample was added to 200 µl assay reagents and then the absorbance measured at 592 nm. The protocol is discussed in Chapter 3.

4.2.5 Metal and electrolyte analysis

The total silver concentration in the external media and the cell homogenate was measured using by ICP-MS (X series, 0475, UK). The Na^+, K^+ and Ca^{2+} concentrations in the external media and the cell homogenate was also determined using ICP-OES (iCAP 7400 RADIAL, Hemel Hempstead, UK). The procedure is exactly the same as described in Chapter 3.

4.2.6 Statistics

Statgraphics version 16 was used for the statistical analysis. All data were subjected Box and Whisker plot to remove the outliers, if present. Standard skewness and standard kurtosis were used to determine whether the data were normally distributed. For the data which were normally distributed, data were subjected to one way analysis of variance (ANOVA) for treatment or time-effects within treatment, followed by Tukey's multiple range test to determine the locations of any significant differences. For non-parametric data, the Kruskal Wallis test was used and significant differences were found using Box and Whisker plot. However, for multifactor analysis (treatment x time), a two way ANOVA was used. The default 95% confidence interval was used for all statistical analysis. All data are expressed as mean ± S.E.M.

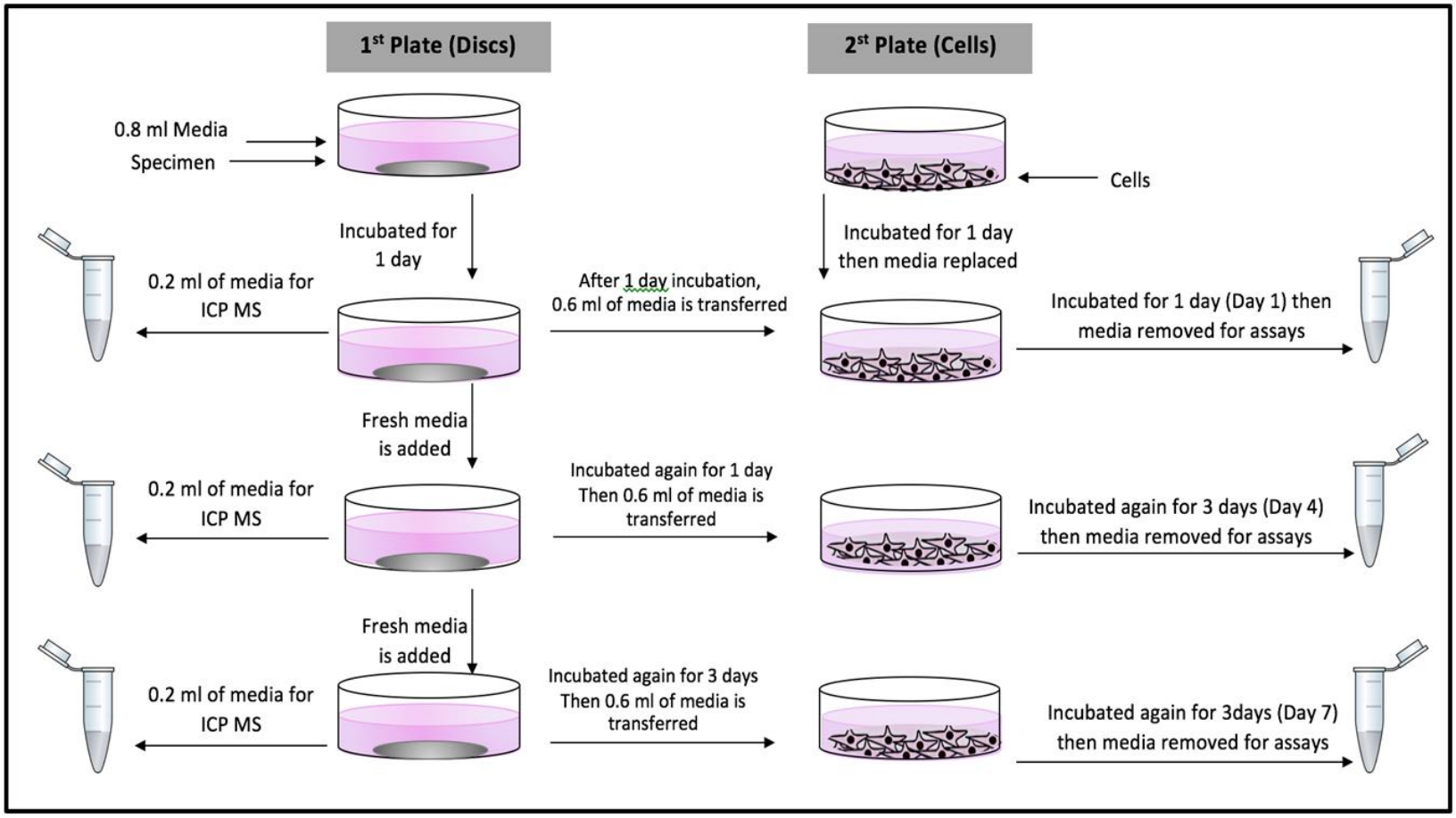

Figure 4.1. The experimental design, the approach to the experiment involved seeding the cells in one culture plate and treating the samples with the cell free culture medium in another plate. Note the time points on which the conditioned media was exposed to the cells.

4.3 Results

4.3.1 Release of silver to the external media

Silver release to the external media was assessed by measuring the total silver in the media by ICP-MS before and after additions to the cells. The silver concentration in the media of the reference control was close to the detection limit, as expected (Table 4.1). All the treatments containing added silver, were significantly higher than the reference control (one way ANOVA, $p < 0.05$). Silver release from all the silver plated discs to the external media (conditioned media before exposure) was approximately 1 mg L^{-1}. No significant difference was found between the groups and/or between the time points in those treatments that contained silver (Table 4.1). Cumulative silver release over 7 days was approximately 3 mg L^{-1} in all treatments (Figure 4.2), and no statistically significant difference was located between the treatments (one way ANOVA, $p < 0.05$).

Silver concentration in the external media (after exposure) was lower than 1.4 mg L^{-1} in all time points. Release of Ag into the media gradually increased over 7 days and it was significantly higher at day 7 compared to day 4 and day 1 (one way ANOVA, $p < 0.05$). There was no significant difference in silver release from Ag+nHA over 7 days, however, silver release in Ag+mHA was significantly lower in day 1 compared to others (one way ANOVA, $p < 0.05$) , then significantly increased in day 4 and 7 (Table 4.1). Since there was two factors affecting the silver release (treatment and time), a two way analysis of variance (ANOVA) was performed and showed that both factors have a significant effect on silver release.

Table 4.1. Total silver concentration in the conditioned media (mg L^{-1}) before and after adding the media to the cells.

Treatment	Day 1		Day 4		Day 7	
	(before)	(After)	(before)	(After)	(before)	(After)
Reference control		0.009 ± 0.006 ^{C}		0.012 ± 0.004 ^{B}		0.008 ± 0.005 ^{B}
Ag	0.783 ± 0.037 $^{z\,A}$	0.669 ± 0.082 $^{z\,A}$	0.779 ± 0.071 $^{z\,A}$	0.738 ± 0.078 $^{z\,A}$	1.667 ± 0.049 $^{y\,A}$	1.374 ± 0.123 $^{y\,A}$
Ag+nHA	1.335 ± 0.334 ^{Za}	1.017 ± 0.305 ^{zA}	0.678 ± 0.058 ^{zAB}	0.871 ± 0.11 ^{xA}	1.169 ± 0.074 $^{z\,A}$	1.105 ± 0.153 $^{z\,A}$
Ag+mHA	0.705 ± 0.071 ^{zyA}	0.406 ± 0.074 $^{z\,B}$	0.490 ± 0.053 ^{zB}	0.674 ± 0.048 ^{zyA}	1.282 ± 0.085 $^{y\,A}$	1.002 ± 0.196 $^{y\,A}$

Data are mean ± S.E.M. (n = 6). Different capital letters within the column indicate significant difference between treatments, while different small letters within the row indicate a significant difference between time points within treatment. One way ANOVA, p value < 0.05. Two way ANOVA showed that there is time and treatment effect on silver release ($p < 0.05$). Reference control only shows (after) values as it was not pre-conditioned with silver to have (before) values.

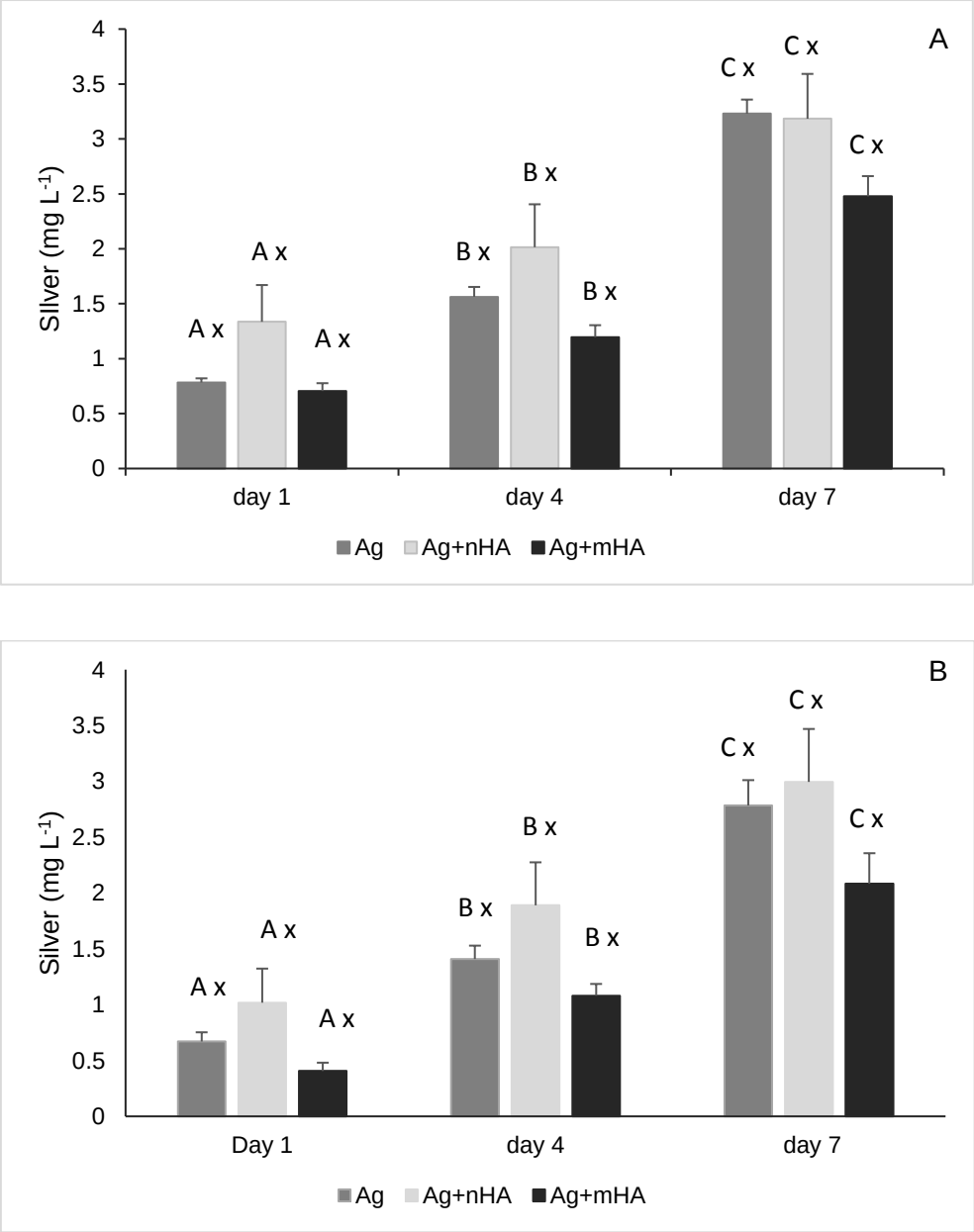

Figure 4.2. Cumulative silver release from the discs to the external media over 7 days (A) before exposure (B) after exposure. Data are mean ± S.E.M, different letters between the time points of the same treatment indicate a significant difference, while different small letters between the treatments in the same time point indicate a significant difference (one way ANOVA, $p < 0.05$).

4.3.2 Cell health and morphology after 7 days exposure

The cells were examined under the light microscope after 7 days (Figure 4.3). The osteoblasts were confluent and appeared healthy in all treatments, with no obvious signs of membrane damage or cell swelling. In addition, there was no significant difference (one way ANOVA, $p > 0.05$) in protein content between the treatments (Figure 4.4). Although the silver exposure was confirmed in the cell homogenate, there was not an appreciable LDH leak to the external media (Table 4.2) and there was no significant difference (one way ANOVA, $p > 0.05$) in the LDH activity in the cell homogenate between the reference control and the others (Figure 4.5). ALP activity was close to the background level in both cell culture medium and cell homogenate (Table 4.3, Figure 4.6). The concentration of silver in the cell homogenates was lower than 0.1 µg mg protein^{-1} in all groups, indicating that only small fraction of the silver was accumulated in the cells (Figure 4.7). The cell homogenate from the Ag+mHA treatment showed a trend of higher silver concentrations (0.08 ± 0.01 µg mg^{-1} protein), relative to the Ag and Ag+nHA treatments which were 0.07 ± 0.01 µg mg^{-1} protein and 0.05 ± 0.01 µg mg^{-1} protein, respectively. However, this trend was not statistically significantly (Figure 4.7).In the cell homogenate, Na^+ concentration was significantly higher in reference control compared to other groups (one way ANOVA, $p < 0.05$), while there was not a significant difference between the groups regarding Ca^+ and K^+ level (Figure 4.7).

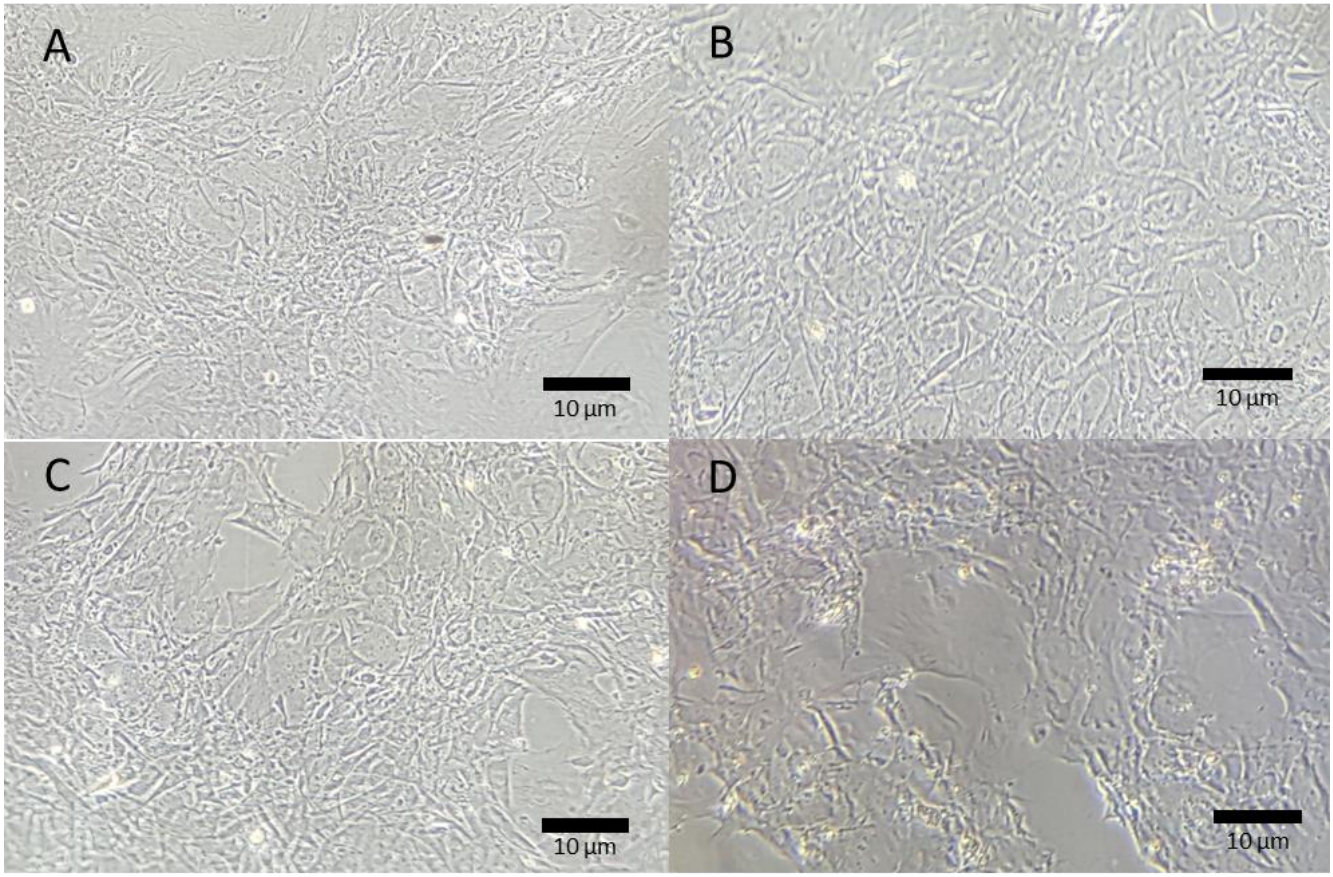

Figure 4.3. Microscopical images of the osteoblast cells after 7 days exposure to silver. (A) reference control (B) Ag (C) Ag+nHA (D) Ag+mHA. Note the cells are healthy and confluent, they are attached to each other without a noticeable membrane.

4.3.3. Protein content, ALP and LDH activity

The BCA method was used to measure the cellular protein content after 7 days growth. There was no significant difference between the treatments (Figure 4.4). Protein content showed a trend of being higher in the homogenates of the reference control cells, measuring 0.14 mg mL^{-1} and the lowest values in the homogenates from the Ag+nHA treatment measuring 0.126 mg mL^{-1}, although this was not statistically significant (Figure 4.4). The LDH activity assay worked as expected. In the cell homogenate, the activity was around 0.05 µmol min^{-1} mg $protein^{-1}$ in all treatments

and the control (Figure 4.5). There was not a significant difference between the control and the treatments, nor between the treatments (Kurskal wallis, $p > 0.05$). This indicates that the cells were not leaking an appreciable amount of LDH into the external media (Table 4.2).

ALP activity was measured as a functional biomarker of bone cells, given the importance of ALP activity in bone formation. As expected for immature cells, a small background of ALP activity was detected with values being slightly higher than the detection limit in the cell homogenates (Figure 4.6); but no treatment effect was observed. The ALP activity in the external media was also low but above the detection limit (Table 4.3).

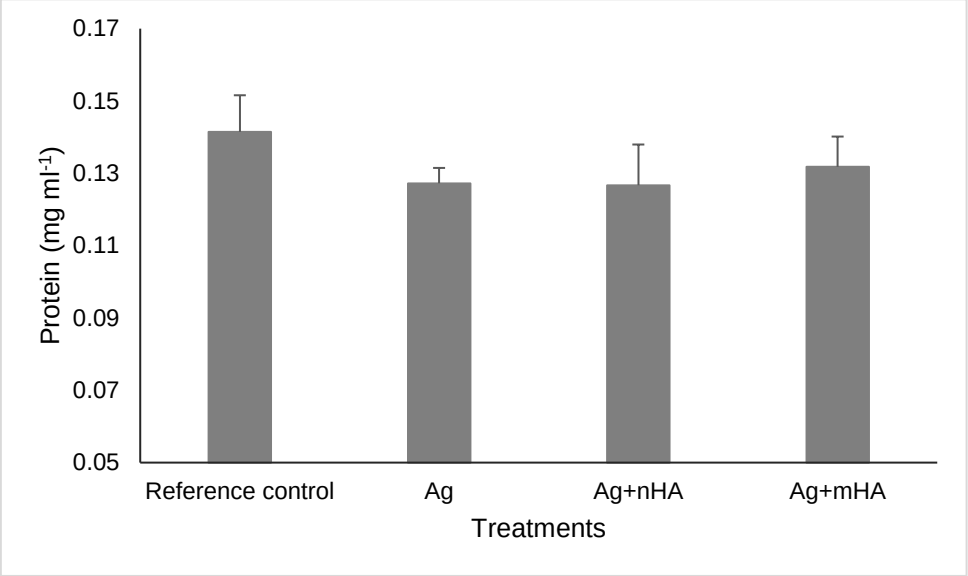

Figure 4.4. Protein content of the cell homogenates after 7 days. Data are mean ± S.E.M., (n = 6). Unlabelled means there was no significant difference between the treatments (one way ANOVA, $p > 0.05$).

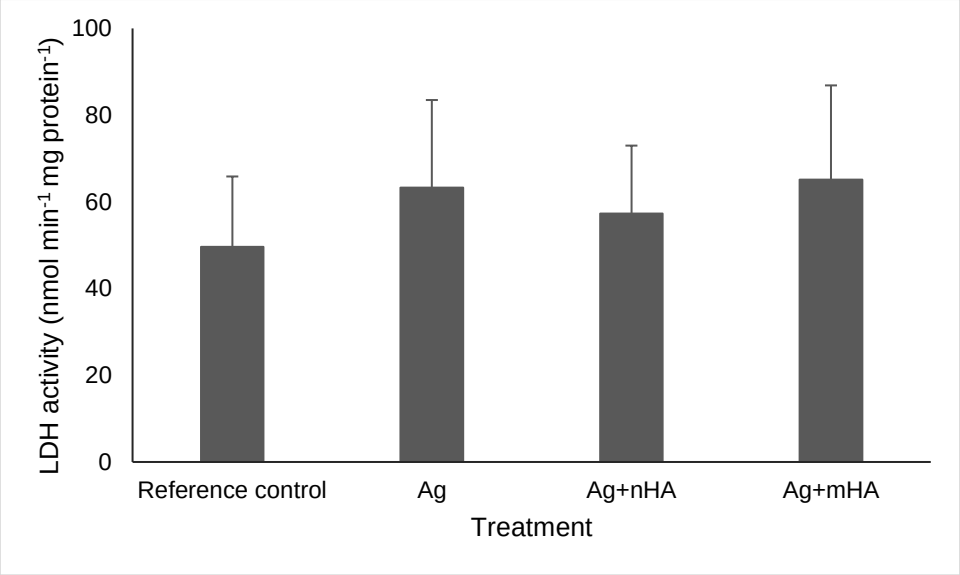

Figure 4.5. LDH enzyme activity in the cell homogenates after 7 days. Data are mean ± S.E.M., (n = 6). Unlabelled means there was no significant difference between the treatments (Kruskal Wallis test, $p > 0.05$).

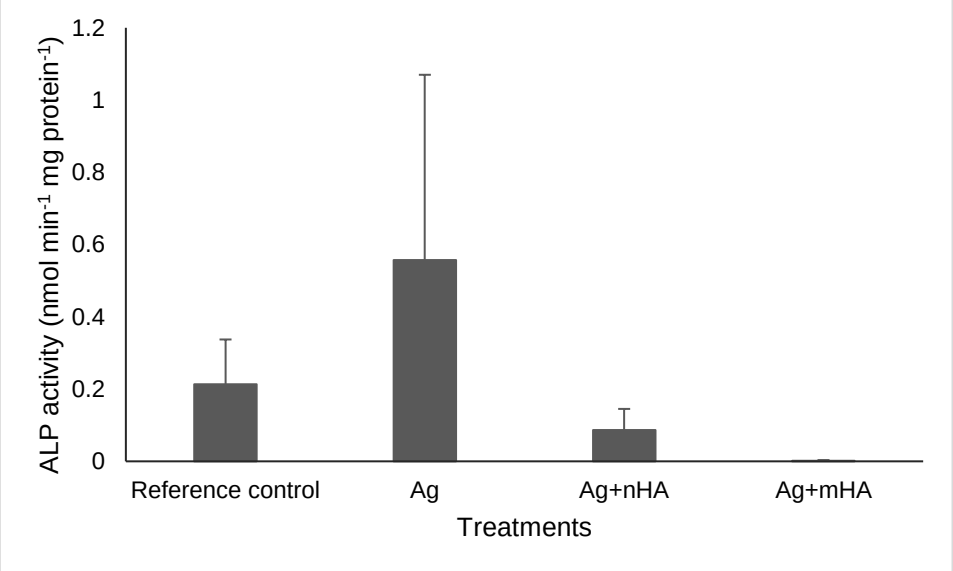

Figure 4.6. ALP enzyme activity in the cell homogenates after 7 days. Data are mean ± S.E.M., (n = 6). Unlabelled means there was no significant difference between the treatments (Kruskal Wallis test, $p > 0.05$).

Table 4.2. LDH enzyme activity in the external media over 7 days.

Treatment	Day 1	Day 4	Day 7
	LDH (nmol min^{-1} ml^{-1})		
Reference control	0.343 ± 0.198	0.317 ± 0.158	0.582 ± 0.291
Ag	0.449 ± 0.206	0.925 ± 0.383	0.899 ± 0.546
Ag+nHA	0.476 ± 0.224	3.201 ± 2.037	0.608 ± 0.341
Ag+mHA	0.185 ± 0.132	0.476 ± 0.312	0.793 ± 0.332

Data are mean ± S.E.M, (n = 6). There were no significant difference between the treatments and treatments with the control, also no time effect (Kruskal Wallis test, $p > 0.05$), Detection limit was 0.549 nmol min^{-1} ml^{-1}. No label means no significant difference.

Table 4.3. ALP activity in the external media over 7 days.

Treatment	Day 1	Day 4	Day 7
	ALP (nmol min^{-1} mL^{-1})		
Reference control	0.155 ± 0.043	0.209 ± 0.070	0.055 ± 0.026
Ag	0.092 ± 0.023	0.093 ± 0.025	0.066 ± 0.029
Ag+nHA	0.035 ± 0.011	0.053 ± 0.008	0.007 ± 0.003
Ag+mHA	0.064 ± 0.021	0.059 ± 0.020	0.006 ± 0.001

Data are mean ± S.E.M, (n = 6). There were no significant difference between the treatments and treatments with the control, also no time effect (Kruskal Wallis test, $p > 0.05$). Detection limit was 0.004 nmol min^{-1} ml^{-1}.

4.3.4 Concentration of Na^+, K^+ and Ca^{2+} in the external media

Concentration of Na^+, K^+ and Ca^{2+} was measured in the external media over 7 days. Results showed that there was a significant reduction in Ca^{2+} concentration in all time points in Ag+nHA compared to the reference control (Table 4.4), (one way ANOVA, $p < 0.05$). Moreover, calcium concentrations in all groups was significantly higher in day 4 and 7 compared to day 1 (one way ANOVA, $p < 0.05$). The Na^+ concentration in the external media gradually increased over 7 days, however, the differences were not statistically significant (one way ANOVA, $p < 0.05$). Potassium level in the external media was also slightly increased in all groups, but the differences were not statistically significant (Table 4.4).

Table 4.4. Concentration of Ca^{2+}, Na^{+} and K^{+} in the external media over 7 days.

Element	Treatment	Day 1	Day 4	Day 7
		mmol L^{-1}		
Ca^{2}	Reference control	1.15 ± 0.12 [a]	1.83 ± 0.07 [a] *	1.72 ± 0.09 [a]
	Ag	0.76 ± 0.18 [b]	2.01 ± 0.07 [a] *	1.97 ± 0.15 [a]
	Ag+nHA	0.64 ± 0.05 [b]	1.11 ± 0.07 [b] *	0.85 ± 0.13 [b]
	Ag+mHA	1.18 ± 0.08 [a]	1.78 ± 0.09 [a] *	1.59 ± 0.20 [a]
Na^{+}	Reference control	140.75 ± 4.17	159.81 ± 9.08	148.10 ± 2.42
	Ag	115.51 ± 13.24	146.58 ± 4.75	137.67 ± 11.30
	Ag+nHA	121.91 ± 2.30	146.39 ± 7.90	132.04 ± 14.58
	Ag+mHA	123.65 ± 2.50	160.78 ± 3.12	141.53 ± 13.86
K^{+}	Reference control	6.23 ± 0.14	7.25 ± 0.39	6.64 ± 0.09
	Ag	5.53 ± 0.62	7.12 ± 0.22	6.62 ± 0.52
	Ag+nHA	5.80 ± 0.10	7.09 ± 0.40	6.35 ± 0.68
	Ag+mHA	5.89 ± 0.10	7.70 ± 0.15	6.80 ± 0.66

Data are mean ± S.E.M (n = 6). Different letters within the row indicate statistically significant difference from each other, asterisk indicates a significant difference from the previous time point (one way ANOVA $p < 0.05$). Unlabelled means no significant difference. Two-way ANOVA showed that there was a significant time and treatment effect on Ca^{2+} concentration.

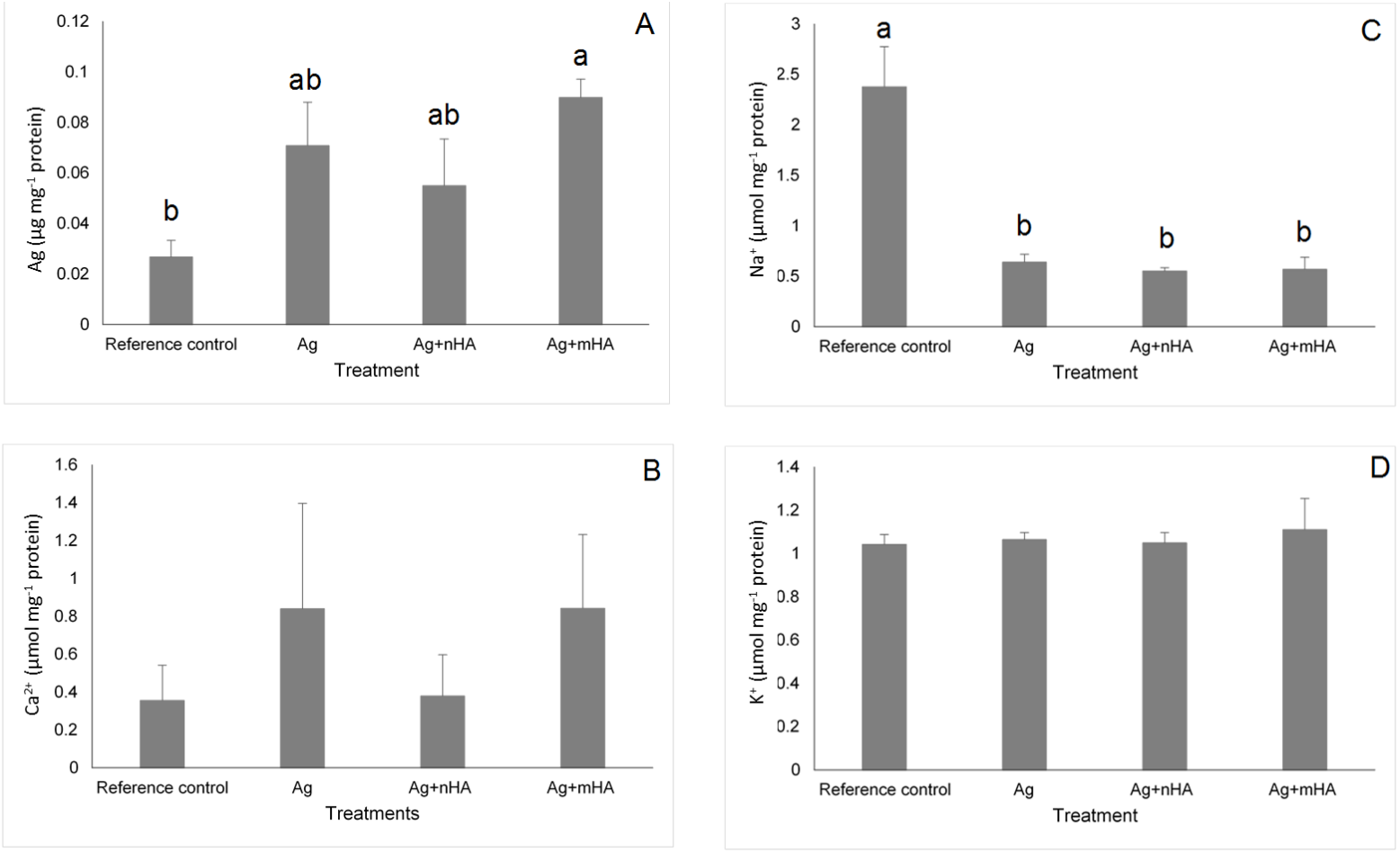

Figure 4.7. Concentration of (A) silver, (B) Ca^{2+}, (C) Na^{+}, and (D) K^{+}, after 7 days in the cell homogenate. Data are mean ± S.E.M, (n = 6) different letters indicate significant difference with each other (one way ANOVA, $p < 0.05$). Unlabelled means no significant difference between the treatments.

4.4 Discussion

In this study, the potential toxicity of dissolved silver in conditioned media derived from silver coated titanium discs was explored. The experimental approach exposed human primary osteoblast cells to the conditioned media so that any direct toxicity of silver could be identified, and separated from any contact toxicity associated with cells grown directly onto the silver-coated titanium alloy discs (Chapter 3). The Silver release into the conditioned media was demonstrated, with a consistent concentration of silver of around 1 mg L^{-1} from the discs over 7 days. Cumulative silver release over 7 days was around 3 mg L^{-1}. This amount of silver over 7 days is acceptable, since it is still higher than the required antibacterial dose which is around 0.2 ppm (Besinis *et al*., 2017). All the treatment groups (except reference control) released almost the same amount of silver to the external media. However, when osteoblasts were exposed to this conditioned media, there was no evidence of adverse cell morphology compared to the reference control. The control cells showed healthy, confluent cells with normal morphology and a negligible background of silver in the cells throughout the experiment. After 7 days exposure to the relevant conditioned media, regardless of the type of silver treatment, the cells accumulated a small amount of total silver. However, the cells showed the same protein concentrations as the reference control, and with no evidence of LDH release into the external media. Taken together, these data suggest that silver exposure via conditioned media from silver-coated discs is of negligible toxicity to osteoblasts in the conditions used here.

4.4.1 Physiochemical properties of the conditioned media

The silver plated titanium discs were treated with the cell culture medium 2 days prior to the experiment. This was to get rid of any excess silver from the manufacturing process of the new discs and any associated fast dissolving silver that might have a significant toxic effects on the cells. Subsequently, the discs were placed in culture media for a further seven days. In this experiment, silver release from the discs was consistent and remained at around 1 mg L^{-1} over 7 days. This steady, slower release of silver indicates that the fast dissolving silver had been removed in the initial media washing steps, and further leaching of silver slowed due to the presence of FBS and other macromolecules in the culture media that would likely form a protein corona on the surface on initial contact with the discs. The significance of this step for experimental design was to prevent false positives in the results of *in vitro* toxicity tests, and from drawing a conclusion that the material is hazardous when it is not. So it is highly recommended to immerse implants in the cell culture medium used to pre-condition the specimens in this study (DMEM + 10%FBS + 1%antibiotic) to remove the excess silver and provide a protein corona on the surface. There were also some other physical effects of the disc surface on the electrolyte composition of the media. Calcium concentration in the external media showed a significant reduction in Ag+nHA compared to others (Table 4.4). This is best explained by adsorption phenomena. The Ag+nHA, which is made of the nano HA layer on titanium, likely was able to absorb Ca^{2+} leading to the formation of $Ca(OH)_2$. This phenomena is well-known and previously reported for HA-containing materials (Harding *et al*., 2005; Besinis *et al*., 2017).

4.4.2. Absence of silver toxicity to osteoblasts from conditioned media

There was no substantial appearance of LDH activity overtime in the external media, and this confirms that there was negligible damage to the cell membranes to release LDH. In the cell homogenate, there was no significant differences in the LDH activity between the reference control and the other treatments. This observation reveals that the cells were not using anaerobic metabolism and had no need to induce high amounts of LDH activity. LDH is primarily induced in low oxygen conditions where lactate is fermented for ATP generation (Heiden *et al*., 2009). Therefore, the absence of increased LDH activity in the cell homogenate may imply the cells were not requiring to use anaerobic metabolism, this is expected since the media was bubbled with 95% air. Moreover, the absence of increased LDH also suggests that mitochondria were working normally for an aerobic metabolism. Alternative explanations such as; Ag inhibiting LDH and preventing an inducible activity are excluded because it was found that dissolved silver from the discs does not significantly inhibit or induce LDH activity (see Chapter 2). Moreover, cell growth in terms of the protein content of the cell homogenates was unaffected, and the cells remained viable and attached over 7 days exposure to silver. Together, these observations suggest that cells were healthy and biocompatible with the surfaces over 7 days in the conditions used here. This result is consistent with the finding of Meran *et al*. (2018) who measured 1.04 ± 0.22 mg L^{-1} of total silver after conditioning the media (DMEM) with 5 mg L^{-1} silver nanoparticles (size not known) and found that silver did not induce a significant toxicity to the confluent primary human fibroblast cells after 24 hour exposure, as there was no appreciable LDH release to the media and also cell morphology was not altered. However, Albers *et al*. (2011) found that the lC_{50} value of osteoblast viability after 72 hours was 0.063 mM (6.80 mg L^{-1}) silver ions dissolved from silver nanoparticles (size 50 nm) in alpha-

MEM supplemented with 10% FBS. Since 10% of the IC_{50} is regarded as sublethal and the silver release in the current study was close to 10% of silver release measured by Albers *et al*. (2011), so the amount of silver release in the current study can be regardred as sublethal. Moreover, Hadi *et al*. (2014) was unable to find attached viable cells after exposure to 10.99 mg L^{-1} dissolved silver from the silver coated titanium disc after 3 days; also, LDH activity in the homogenate was significantly less than the control. The difference in the results can be explained by that fact that several factors are affecting toxicity including cells type and seeding density before the exposure, experiment duration and silver (metal) chemistry. Moreover, it is challenging to compare different toxicological experiments, this is because not all the studies have measured the silver release to the cell culture medium. In this case it will not be possible to correlate the cell survival and the silver dose.

ALP activity was low in the cell homogenate and the external media, this is because the osteoblast cells were at an early stage of growth and immature cells do not produce large amounts of ALP. ALP activity values of the cell homogenate resembles Rawadi *et al.* (2003) who observed that the ALP activity in the osteoblast cell homogenate after 3 days culture was less than 1 nmol min^{-1} mg protein-^{1}.

The silver was detected in the cell homogenate (Figure 4.7) and also in the external media (Table 4.1), however, no significant toxicity was observed. This finding suggests that the silver was not bioavailable inside the cells. This is likely due to the presence of metal binding proteins (-SH groups) and also high amount of chloride inside the cells (or the media) leading to insoluble silver chloride formation. It could be argued that the silver forms insoluble chloride complexes in chloride containing solutions (Ha and Payer., 2011). The concentration of Cl^- in DMEM is higher than 100 mmol, in this study, around 1 mg L^{-1} (0.0092 mmol) silver release was detected which

is far lower than the concentration of Cl^- in DMEM. Thus, it is highly likely that the presence of high amount of chloride in the cell culture media has turned all the silver into silver chloride particles as seen in Besinis *et al*. (2014). In addition, high amount of proteins and other organic molecules in the media have mopped up silver as a result of high affinity between silver and –SH groups present in proteins. Therefore, there is plenty of buffering capacity in the media compared to 1 mg L^{-1} of silver, thus, it is very unlikely that any free silver ions are in the cytoplasm of the cells. This has resulted in a small fraction of silver in/on the cells confirming low bioavailability and hence low toxicity.

Silver is also known as an ionoregulatory toxicant that inhibits the Na^+ K^+-ATPase in cells (Hussain *et al*., 1994). The K^+ concentration in the cell homogenates did not show any significant difference between the groups; and this might be expected given the ample K^+ content of mammalian cells to mask any small changes. However, the Na^+ content of the cell homogenates from the reference control was significantly higher than Ag, Ag+nHA and Ag+mHA (Figure 4.7). A likely explanation is that the normal outward leak of Na^+ down the electrochemical gradient was occurring, but silver-dependent inhibition of the Na^+ pump was preventing the intracellular Na^+ from being replenished; thus slowly depleting the cells of Na^+. Values of Na^+ and K^+ in the cell homogenate resemble those described by Gitrowski *et al*. (2014) who measured Na^+ and k^+ level in the cell homogenate of Caco-2 intestinal cells after exposure to TiO_2 nanoparticles. Moreover, the values were similar to Hadi *et al*. (2014) who found that the concentration of Na^+ in the cell homogenate of primary human osteoblast cells after 3 days growth was around 1 mmol L^{-1}.

4.4.3. Conclusions and clinical perspective

Silver was released from the discs to the external media over 7 days, the dissolved silver was higher than the required antibacterial dose. Silver did not induce a significant toxic effect to the human primary osteoblast cells and no significant damage to the cells was observed. Moreover, since wound healing of freshly installed dental implant requires several days after surgery, the first few days of implant placement is vulnerable for bacterial colonisation and infection. Thus, an antibacterial silver release from the implant during this first period is crucial and can potentially prevent the incidence of infection. However, for any new dental material to be used in clinics, there are some criteria which need to be met prior to clinical use: the material must be better than the existing one, also biocompatibility is crucial to ensure the safety of material to the patient. This experiment showed that the antibacterial released silver is biocompatible with human primary osteoblast cells. Furthermore, it is highly recommended to immerse the silver coated dental implants in cell culture medium so as to get rid of the excess silver which might disturb the biocompatibility of the dental implant material.

Chapter 5

Biocompatibility of the Silver and Hydroxyapatite Nanoparticle Coating on Titanium Dental Implants with Primary Human Osteoblast Cells

5.1 Introduction

Designing biocompatibility experiments usually requires some optimisation and often pilot studies prior to the main experiments. This may be to resolve practical issues such as the logistics of sampling as well as range finding on the appropriate doses or time scales. Issues arise including the initial cell number or density, the biomaterials to use and their most appropriate controls, the size of any such material specimens, the ability to measure the amount of released enzyme or other endpoints from the cells and deciding which cell viability assay to choose are crucial. Conducting experiments with nanomaterials has a number of extra practical challenges compared to experiments with soluble chemicals. For example, Goss *et al*. (2011) have found that engineered nanomaterials can interfere with the LDH assay and colorimetric dyes used in colour endpoint-style assays (e.g., the MTT assay), (Kroll *et al*., 2012; Ong *et al*., 2014; Selck *et al*., 2016). Moreover, there can be difficulty in detecting the total metal from metal nanoparticles in tissue or cell homogenates, due to analyte losses during digestion protocols and/or subsequent measurement methods. For example, Shaw *et al*. (2013) experienced difficulties in determining TiO_2 nanoparticles in fish gut homogenate and reported on the necessary adaptations of analytical procedures to achieve reliable results.

In the first biocompatibility study (Chapter 3), there were only 12,000 cells at the beginning of the experiment. The reason for choosing this cell density was to study the cells in a log phase, where the cells were still dividing until confluence was reached on the discs. However, there were some experimental difficulties that created uncertainty and limited the interpretation of the data. For example, it was difficult to measure LDH activity in the external media and the cell homogenate, this is due to the low number of cells at the beginning which resulted in an insufficient enzyme

production to precisely determine the cell health. In addition, it was unclear whether the toxicity was caused by the released silver to the external media, or if it was from the direct contact with the surface of the disc. Moreover, the influence of surface geometry of the biomaterial specimens to the cell health was not well understood, so it was necessary to better elucidate this with additional control experiments.

The aim of this study was to address the biocompatibility of silver and HA coatings with human primary osteoblast cells, it was repeating the experiment in Chapter 3, but with more cells, extra controls and also extra endpoints to assess the cell viability. Critically, this experiment intended to use confluent cells compared to the still rapidly dividing cells (i.e., still growing to reach confluence) used in Chapter 3. It could be argued that confluent cells are resting, and less vulnerable to insult than a cell culture that is actively dividing. Thus, the objectives in this current chapter were to use a higher number of cells at the beginning of the experiment to ensure confluence, but also to achieve enough biomass for reliable biochemical measurements at the start of the experiment and throughout. Moreover, it was difficult to assess the cell viability in the previous study with reliance on the LDH assay (Chapter 3), and so, the Alamar blue assay was also used to assess the cell viability. The Alamar blue assay is frequently used to assess the metabolism and proliferation of cells (O'Brien *et al*., 2000), and has also been used for exposures to nanomaterials (Ong *et al*., 2011). Another objective was to add two more controls to the experimental deign, so that the effect of surface geometry on cell viability and activity could be explored. The controls were nano HA coating on titanium and micro HA coating on titanium.

5.2 Materials and methods

5.2.1 Cell culture

Primary Human osteoblast cells were used in this experiment. The cell culture conditions for growing the stock of cells were the same as in Chapter 3. Cells at passage 8 and 9 were used in this experiment.

5.2.2 Experimental design

This experiment was conducted to investigate the biocompatibility of the various coatings (see below) with a confluent culture of human primary osteoblast cells. The experiment was carried out in 24 well-microplates, and the microplate was the unit of replication in this experiment (n = 6 plates/treatment). The experimental design included osteoblast cells grown on the microplate directly without any alloy disc; hereafter referred to as the 'reference control'. Other treatments were: uncoated titanium discs plus cells and media (referred to as 'Ti' hereafter); titanium discs coated with nano HA plus media and cells (nHA); titanium coated discs with micro HA plus media and cells (mHA). A series of discs were also prepared by silver plating to create a silver layer on the surface of titanium. The silver treatment groups included: silver-coated titanium discs plus media and cells (referred to as 'Ag' hereafter), Ag plus nano HA coated titanium plus media and cells (Ag+nHA) and Ag plus mHA coated titanium plus media and cells (Ag+mHA). All the discs (without any cells) were pre-treated with the cell culture medium and incubated in 95% air and 5% CO_2 incubator (HETO-HOLTEN Cell House 170) at 37 ^{o}C for 48 hours to allow stabilisation of the biocorona on the surface of the coating and to wash out any labile fraction of silver arising from the manufacture of the composites. The discs were then seeded with 30000 cells/

each well. To achieve this cell density, the cells were suspended in the culture media in a ratio of 50000 cells/ml, and then 0.6 ml of the media (30000 cells) was added to each well to set up the experiment. The experiment was then conducted for 7 days exactly as described in Chapter 3, except that the Alamar blue assay was also conducted to assess cell viability. For the latter, Alamar blue was added to the media on day 1, 4 and 7 (see below).

5.2.3 Biochemical assays

ALP and LDH enzyme activity assays were performed on samples of the cell culture medium at each time point (days 1, 4 and 7) and also in the cell homogenates after 7 days. For LDH activity, briefly, 100 µl of the test sample was added to 2800 µl LDH assay reagent in a cuvette and then the absorbance was measured at 340 nm wavelength. For the ALP activity, the sample volume was 30 µl and the test reagent volume was 250 µl. The assay was conducted in 96 well microplates and the absorbance was measured at 405 nm wavelength. The procedure and instruments used are exactly the same as explained in detail in Chapter 3.

5.2.4 Alamar blue assay

Cell viability and mitochondrial function was assessed using an Alamar blue assay. The Alamar blue assay is based on an indicator dye incorporating an oxidation-reduction (REDOX) indicator. Alamar blue in oxidised form is blue in colour, the colour reduces and changes to red as a result of metabolic activity and cell growth. The Alamar blue assay was carried out at each time point (days 1, 4 and 7). An adequate volume of the alamar blue dye (purchased from abD serotec) equal to 10% of the cell

culture medium in the well was aseptically added to each well and the cells were incubated for 6 hours. After that, 200 µl of the cell culture medium (with the alamar blue dye) in each well was transferred to 96 well plates and then the absorbance was measured at 600 nm wavelength using a plate reader (VersaMax, molecular devices, Berkshire, UK). The technique is not destructive sampling, as the cells were fed with fresh media after transferring the existing media (with the dye) to 96 well plates for absorbance reading. As the dye is sensitive to light, the procedure was followed in a dark room. Cell viability of the treatments were normalised with the untreated control cells. Cell viability of the treatments was expressed as a percentage viability of the reference control.

5.2.5 Concentration of Ag, Na^+, K^+, Ca^{2+} and P in the external media and the cell homogenate

The concentration of Ag and the electrolytes was measured in the external media at each time point and in the cell homogenate at the end of experiment, using ICP-OES (iCAP 7400 RADIAL, Hemel Hempstead, UK). The volumes of samples collected and the procedure for sample preparation and analysis were exactly as described in Chapter 3.

5.2.6 Investigating the cell morphology using the scanning electron microscopy

A separate run of the experiment (a triplicate / treatment) having a micro plate as a unit of replication was conducted to assess the cell morphology after 7 days, cell attachment, confluence and membrane integrity were examined under SEM at the end

of experiment. The procedure of cell fixation, dehydration and imaging technique was the same as described in Chapter 3.

5.2.7 Statistical analysis

Statgraphics version 16 was used for the statistical analysis. All data are expressed as mean ± S.E.M. Data were subjected the Box and Whisker plots to check for the presence of out layers, which were then excluded from the data. Standard skewness and kurtosis were performed to check the normality of the data. Normally distributed data were subjected to one way Analysis of Variance (ANOVA) and Tukey's test was used to locate the difference. Two way ANOVA was also used to investigate the time and treatment effect. In the case of non-parametric data, the Kruskal-Wallis test was used and the differences were located using Box and Whisker plot with notches. Any difference having a P value < 0.05 was considered statistically significant.

5.3 Results

5.3.1 Silver release to the external media

Results of this study showed that there was a consistent silver release (around 2 mg L^{-1}) from the silver coated titanium discs to the external media (Table 5.1). Cell exposure to the silver was also confirmed by the concentration of silver in the cell homogenates, which was around 0.4 mg L^{-1} (Table 5.1). In the external media, silver showed a significantly lower concentration in the reference control (as expected); and in the Ti, nHA and mHA compared to other treatments in all the time points (one way ANOVA, $p < 0.05$). The silver concentration in Ag, Ag+nHA and Ag+mHA increased in day 4 and 7; with the highest silver release was from Ag+mHA treatment at day 4 (7.002 ± 2.375 mg L^{-1}), (Table 5.1). There were no significant differences between the silver coated groups (Ag, Ag+nHA and Ag+mHA) in any time points, also, no significant difference was observed between time points of the same treatment (one way ANOVA, $P < 0.05$) (Table 5.1). Two way ANOVA showed that both factors (time and treatment) have a significant effect on silver release ($p < 0.05$).

Table 5.1. Concentration of silver in the external media over 7 days and in the cell homogenate at the end of the experiment.

Treatments	Day 1	Day 4	Day 7	Homogenate
	Concentration of silver (mg L^{-1})			
Reference control	0.057 ± 0.009 [b]	0.093 ± 0.009 [b]	0.080 ± 0.007 [b]	0.068 ± 0.017 [b]
Ti	0.092 ± 0.013 [b]	0.073 ± 0.017 [b]	0.079 ± 0.014 [b]	0.038 ± 0.008 [b]
Ag	2.508 ± 0.419 [a]	3.552 ± 0.226 [a]	4.044 ± 0.527 [a]	0.517 ± 0.125 [a]
Ag+nHA	2.851 ± 0543 [a]	3.480 ± 0.640 [a]	2.608 ± 0.553 [a]	0.455 ± 0.169 [a]
Ag+mHA	2.039 ± 0.527 [a]	7.002 ± 2.375 [a]	3.841 ± 0.617 [a]	0.299 ± 0.072 [a]
nHA	0.150 ± 0.019 [b]	0.244 ± 0.60 [b]	0.276 ± 0.037 [b]	0.075 ± 0.011 [b]
mHA	0.290 ± 0.173 [b]	0.167 ± 0.021 [b]	0.138 ± 0.012 [b]	0.049 ± 0.008 [b]

Data are mean ± S.E.M, (n = 6). Different letters within the column indicate a significant difference (one way ANOVA, or Kruskal Wallis test, $p < 0.05$).

5.3.2 Assessing the cell viability and morphology

Osteoblast cells were examined under SEM after 7 days of the experiment (Figure 5.1). Images showed that the cells grown on the titanium, alloy discs without any HA or silver (Ti) were attached to the substrate and covered most of the surface (Figure 5.1A). The Ti-treated cells also appeared healthy without any noticeable membrane rupture. The cells from this treatment were confluent, contacted to each other (confluent), and there were no visible signs of cellular shrinkage. Cells grown on nHA and mHA treatments were also confluent, and appeared attached to the substrate and with each other. There was no visual evidence of membrane damage in these latter cells. The level of confluence was higher in nHA compared to mHA (Figure 5.1E and F). In contrast, cells grown on the Ag coated Ti alloy discs were sparser. However, the cells that were present did not show overt pathology with the absence of membrane blebs on the cell membrane or rupture of the membrane. The cells still showed the typical extending filopodia of osteoblasts, although shrinkage was noticed in some cells (Figure 5.1B). The cells grown on the Ag+nHA discs were almost 90% confluent, and appeared to be attached to the surface and to each other. There were no noticeable signs of cell membrane damage and no noticeable evidence of cell shrinkage (Figure 5.1C). Cells on the Ag+mHA discs exhibited similar characteristics with those grown on Ag. The cells from the Ag+mHA treatment were the most sparse, and with poor contact with each other despite having filopodia (Figure 5.1D). There was noticeable cell shrinkage, but there was no morphological evidence of cell membrane damage.

The Alamar blue assay was used to assess cell viability at days 1, 4 and 7 (Figure 5.2). Results of the Ti treatment for the alamar blue assay were entirely consistent with the morphology on the SEM images (Figure 5.1). The Ti control

showed around 100% viability at all time points (Figure 5.2). Cell viability in the nHA treatment was higher than 80%, and not significantly different from the Ti or silver plated groups (one way ANOVA, $p < 0.05$). Cell viability on the mHA treatment was not significantly different from the Ti treatment at day 1 or day 4, but it was significantly lower than the Ti treatment at day 7 (one way ANOVA, $p < 0.05$, Figure 5.2). However, cell viability in Ag group was approximately 65% in day 1 and 4, but it was less than 60% at day 7, however, the differences were not significant (Figure 5.2). Cell viability in Ag+nHA treatment was approximately 70% at all time points and with no significant differences between the time points (one way ANOVA, $p < 0.05$). In contrast, there was a slight trend of decreased cell viability over time in Ag+mHA treatment, although this was not statistically significant. Nonetheless, the cell viability at day 7 in the Ag+mHA treatment was less than 60% of the reference control (Figure 5.2) which was significantly less than Ti (one way ANOVA, $p < 0.05$).

Regarding the cell electrolyte balance, there were no evidence of disturbances that would lead to the cell shrinkage or cell swelling and membrane rupture due to the change in salt concentrations (Figure 5.3). There was no significant difference in the Na^+ concentration between the Ti, Ag, Ag+nHA and Ag+mHA treatments (one way ANOVA, $p < 0.05$). However, the concentration of Na^+ in the cell homogenate was significantly lower in the reference control compared to all other treatments (one way ANOVA, $p < 0.05$). The Na^+ concentration was 0.47 ± 0.1 mmol L^{-1} in the reference control, while it was around 1.5 mmol L^{-1} in all the other treatments (Figure 5.3). There was no significant difference in K^+ concentration between the treatments (one way ANOVA, $p < 0.05$), and values were around 0.4 mmol L^{-1} (Figure 5.3).

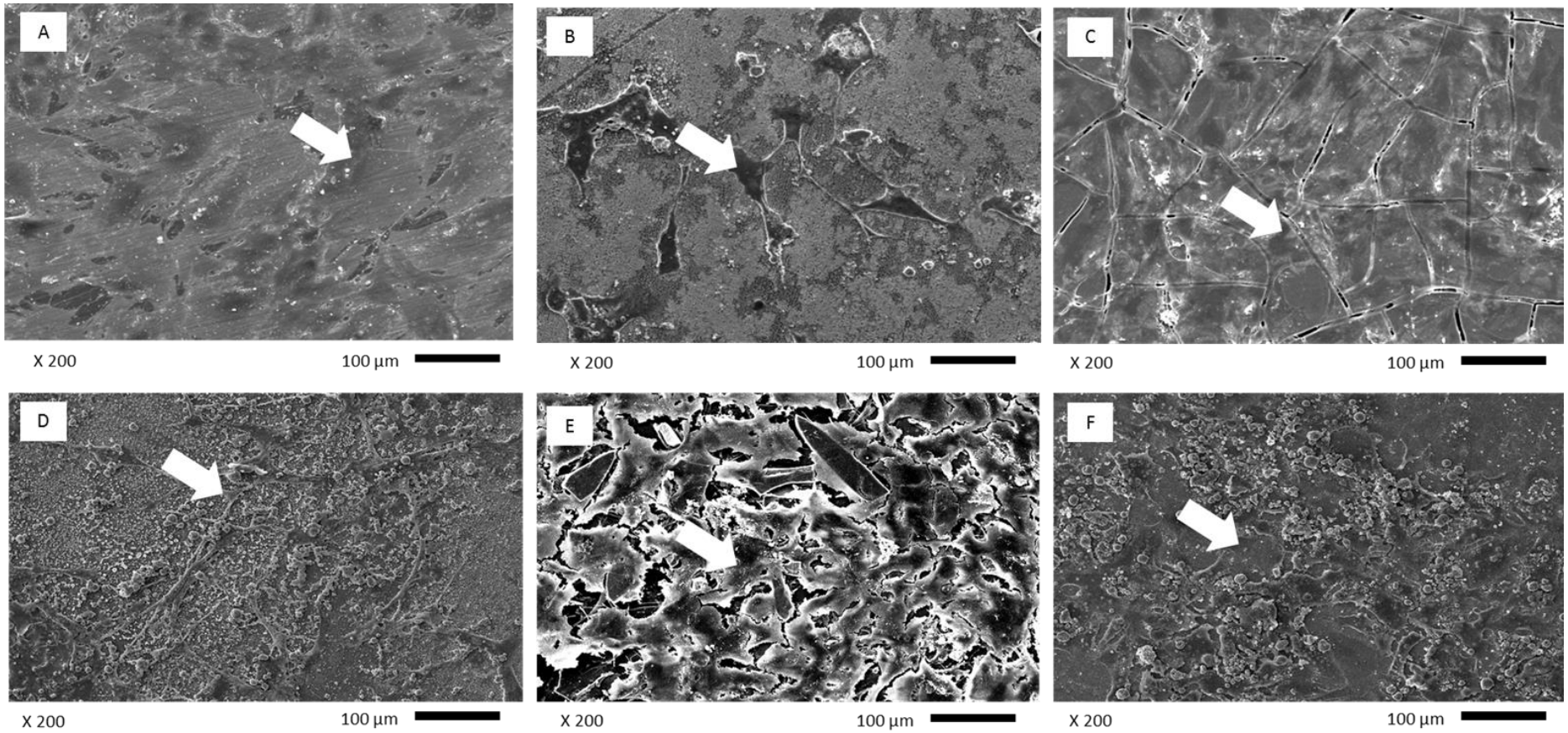

Figure 5.1. SEM images of human primary osteoblast cells grown on titanium discs after 7 days. (A) uncoated Ti, (B) Ag, (C) Ag+nHA, (D) Ag+mHA, (E) nHA, (F) mHA. Arrows show the cells grown on the surface. Note the membrane integrity, cell confluence and attachment with each other. Also, note the apparent cell shrinkage on Ag and Ag+mHA. All magnifications and scale bars are x200 and 100 µm respectively.

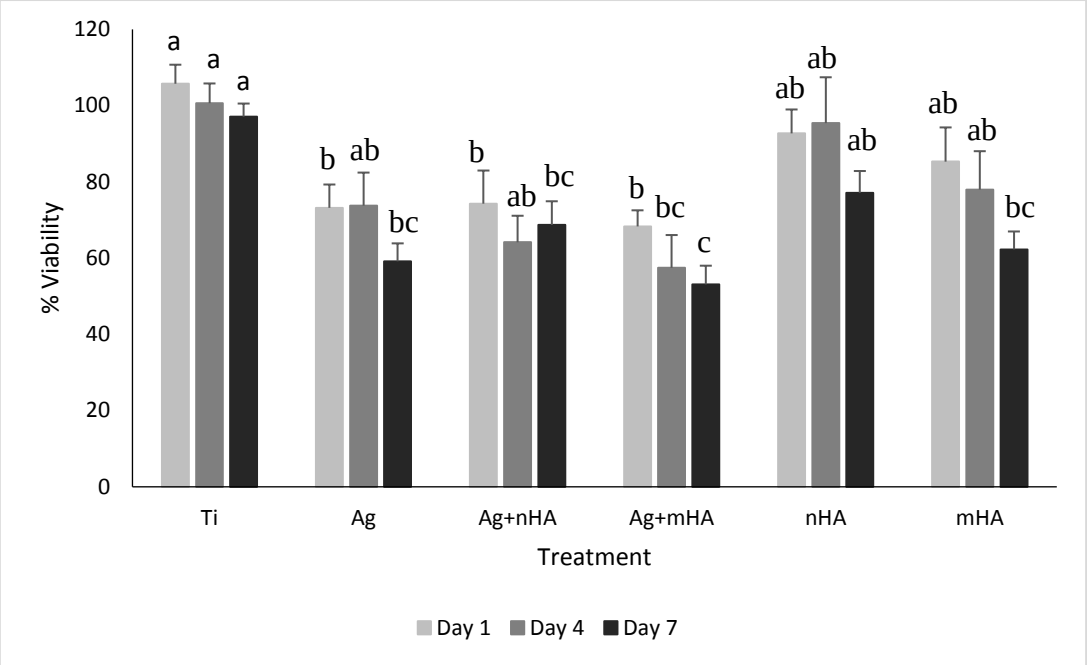

Figure 5.2. Cell viability over 7 days using an alamar blue assay. Data are mean ± S.E.M, (n = 6). Different letters between the treatments within the same time point indicate a significant difference (one way ANOVA, $p < 0.05$). There was not a significant difference between the time points of any group.

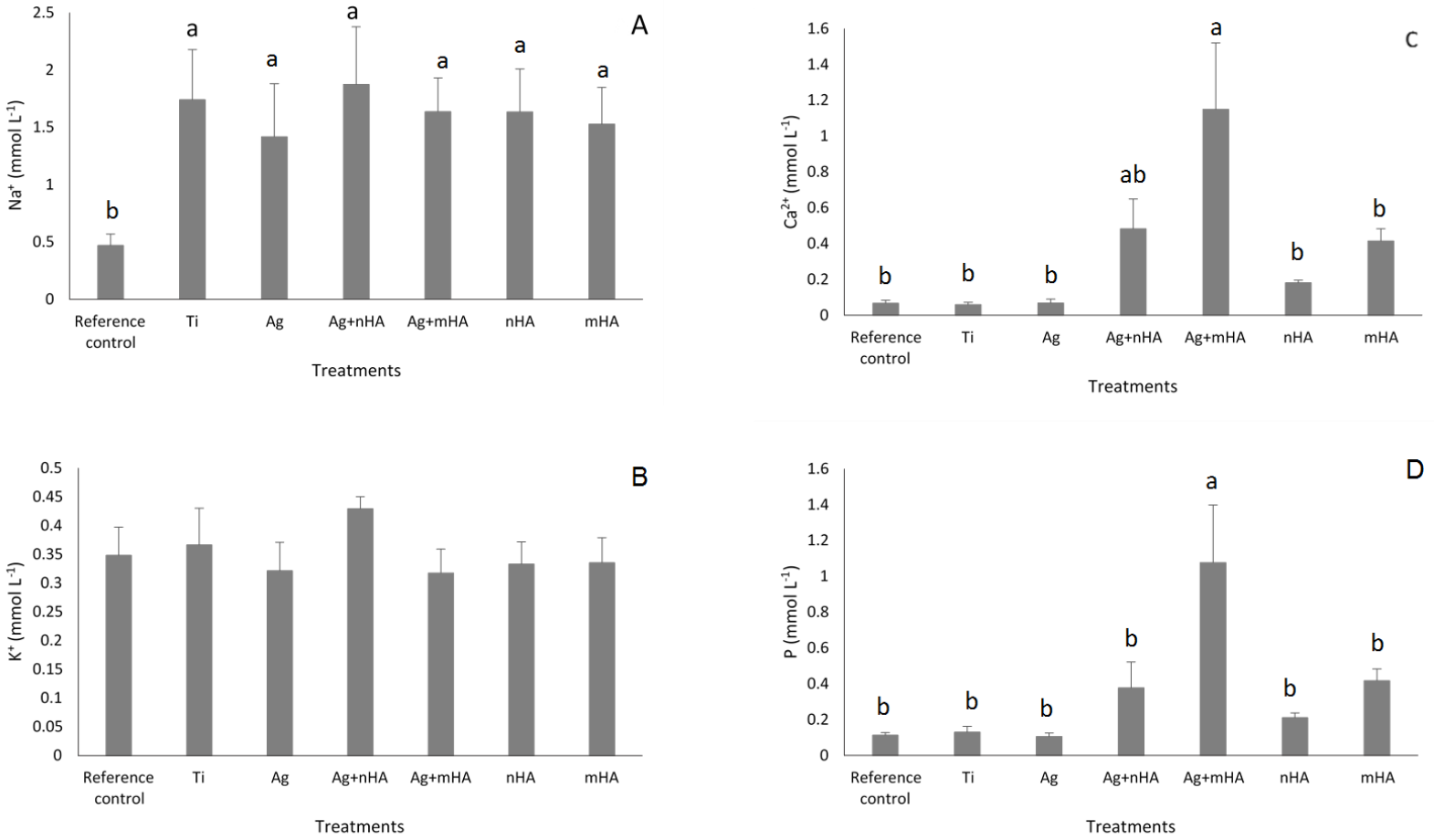

Figure 5.3. Concentration of (A) Na^+, (B) K^+, (C) Ca^{2+} and (D) P, in the cell homogenate. Data are mean ± S.E.M, (n = 6). Different letters between the bars indicate a significant difference with each other (one way ANOVA, $p < 0.05$). Unlabelled means there is no significant difference.

5.3.3 Alkaline phosphatase and lactate dehydrogenase enzyme activity

The ALP assay worked as expected (see the positive control curve in Appendix 2, Figure 3), however, very low enzyme activity was detected in both the cell homogenate and the external media (Figure 5.4 and Table 5.2). No significant differences between the treatments were observed (Kruskal Wallis test, $p < 0.05$), two way ANOVA showed that there was time effects on ALP activity in the media ($p < 0.05$, Table 5.2). Values for the cell homogenates were around 0.01 nmol min^{-1} ml^{-1}, while they were around 0.1 nmol min^{-1} ml^{-1} in the external media (Figure 5.4 and Table 5.2). LDH enzyme activity was assessed in both cell homogenate after 7 days and cell culture medium at days 1, 4 and 7. The assay worked as expected, and LDH activity was detected in the cell homogenate in all treatment groups (Figure 5.5). Results showed that there was no significant difference in LDH activity between the treatments (Kruskal Wallis test, $p < 0.05$), with LDH activity being between 2 – 5 nmol min^{-1} ml^{-1} in all groups (Figure 5.5). In the cell culture medium, the LDH leak to the external media was 2 nmols or less, but within that, there was some small, but statistically significant effects (Kruskal Wallis test, $p < 0.05$, Table 5.3). Two way ANOVA showed that there was both time and treatment effects on LDH activity in the media ($p < 0.05$, Table 5.3).

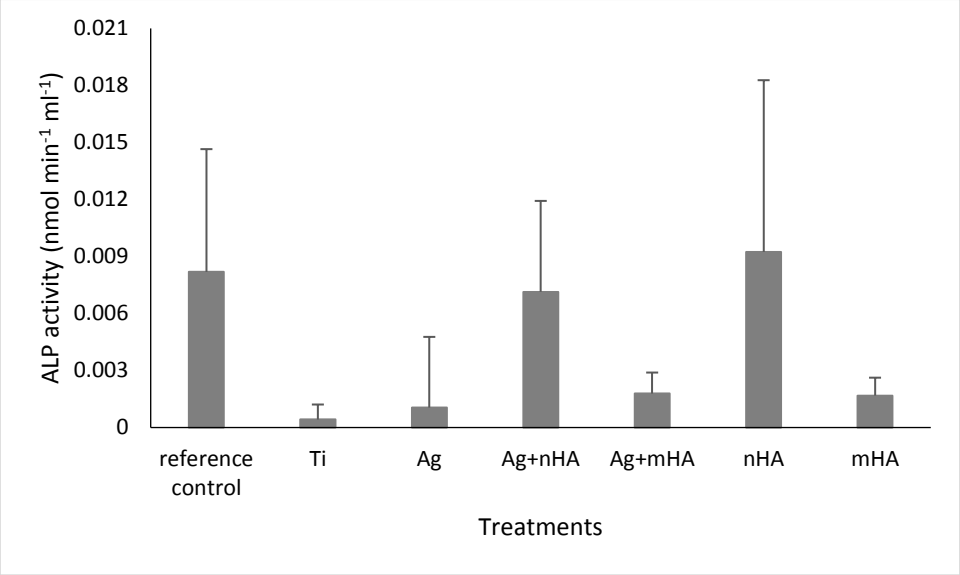

Figure 5.4. ALP enzyme activity in the cell homogenate at the end of the experiment (day 7). Data are mean ± S.E.M, (n = 6). There were no statistically significant difference between the groups (Kurskal Wallis test, $p > 0.05$). Unlabelled means there is no significant difference.

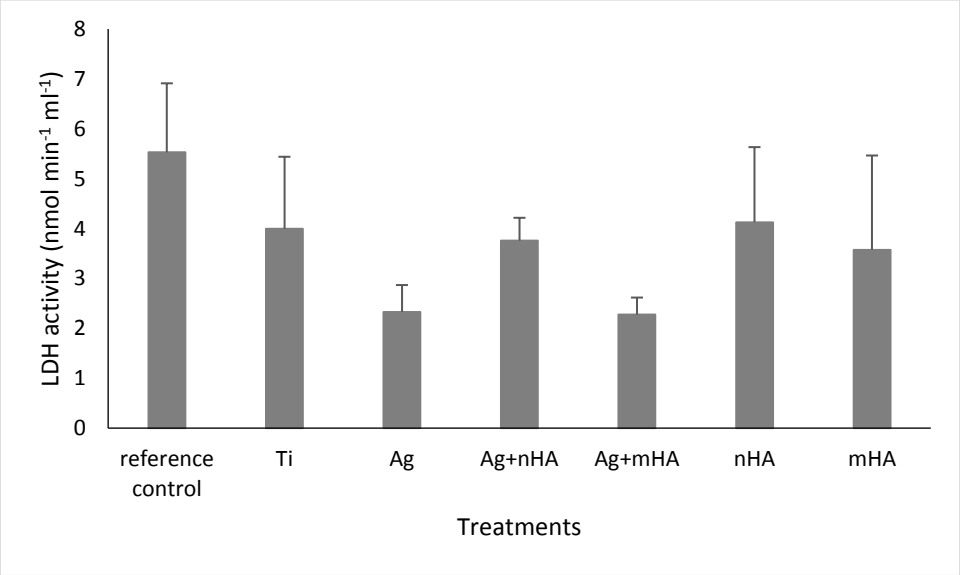

Figure 5.5. LDH enzyme activity in the cell homogenate at the end of the experiment (day 7). Data are mean ± S.E.M, (n = 6). There were no statistically significant difference between the groups (Kurskal Wallis test, $p > 0.05$). Unlabelled means there is no significant difference.

Table 5.2. ALP enzyme activity in the external media over 7 days.

Treatments	Day 1	Day4	Day7
	ALP enzyme activity (nmol min^{-1} ml^{-1})		
Reference control	0.071 ± 0.027 [b]	0.092 ± 0.023	0.120 ± 0.030
Ti	0.092 ± 0.023 [b]	0.087 ± 0.019	0.113 ± 0.036
Ag	0.067 ± 0.022 [b]	0.064 ± 0.022	0.115 ± 0.028
Ag+nHA	0.070 ± 0.017 [b]	0.069 ± 0.023	0.066 ± 0.021
Ag+mHA	0.075 ± 0.022 [b]	0.082 ± 0.018	0.082 ± 0.034
nHA	0.065 ± 0.016 [b]	0.048 ± 0.016	0.059 ± 0.017
mHA	0.252 ± 0.217 [a]	0.080 ± 0.021 *	< 0.004

Data are mean ± S.E.M, (n = 6). Different letters within the column indicate a significant difference. An asterisk indicates a significant difference with the previous time point, (one way ANOVA or Kruskal-Wallis test, $p < 0.05$). Unlabelled means there is no significant difference. The detection limit was 0.004 (nmol min^{-1} ml^{-1}).

Table 5.3. LDH enzyme activity in the external media over 7 days.

Treatments	Day 1	Day4	Day7
	LDH enzyme activity (nmol min^{-1} ml^{-1})		
Reference control	< 0.549	1.058 ± 0.660 ^{b*}	0.661 ± 0.374 ^{b*}
Ti	1.005 ± 0.440	< 0.549 *	0.687 ±0.319 ^{b*}
Ag	0.634 ±0.357	1.005 ± 0.829 ^{b*}	2.883 ± 1.182 ^{a*}
Ag+nHA	< 0.549	0.687 ± 0.190 ^{b*}	2.328 ± 0.597 ^{a}
Ag+mHA	1.216 ± 0.748	1.534 ± 0.722 ^{b}	2.566 ± 1.495 ^{a}
nHA	1.190 ± 0.586	0.793 ± 0.439 ^{b}	1.666 ± 0.793 ^{ab}
mHA	0.714 ± 0.255	3.809 ± 1.593 ^{a*}	1.746 ± 0.150 ^{ab}

Data are mean ± S.E.M. (n = 6). Different letters within the column indicate a significant difference between treatments and within time point. An asterisk shows a significant difference with the previous time point (one way ANOVA or Kruskal-Wallis test, $p < 0.05$). Unlabelled means there is no significant difference. The detection limit was 0.549 nmol min^{-1} ml^{-1}.

5.3.4 Concentration of Na^+, K^+, Ca^{2+} and P in the external media

The concentration of electrolytes was measured in the external media over 7 days. Generally, electrolytes in the media did not show significant changes (Table 5.4). Na^+ and K^+ concentrations in the external media were stable and neither the time points nor the treatments showed any statistically significant changes (one way ANOVA, $p < 0.05$). The values for Na^+ concentration were higher than 100 mmol L^{-1}, as expected, while K^+ concentrations were around 8 mmol L^{-1}. The Ca^{2+} concentrations remained around 1-2 mmol L^{-1} regardless of treatment. However, there were some statistical differences in the latter (one way ANOVA, $p < 0.05$). The Ca^{2+} concentration was

significantly lower in Ag+nHA and nHA compared to others in all time points (one way ANOVA, $p < 0.05$), (Table 5.4). P in the external media showed values of around 1 mmol L^{-1} in all treatments, and the P concentration in the media was significantly lower in the HA coated groups compared to all the others (one way ANOVA, $p < 0.05$,Table 5.4). Moreover, nHA exhibited a significantly lower P concentration in the media compared to all the other treatments; Ag+nHA, Ag+mHA and mHA also showed a significant reductions in P concentration compared to the others, except the nHA treatment (one way ANOVA, $p < 0.05$). Two way ANOVA showed that there was both time and treatment effect on Ca^{2+} and P concentration ($p < 0.05$, Table 5.4).

Table 5.4. Concentration Na^+, K^+, Ca^{2+} and P measured by ICP-OES in the external media over 7 days.

Element	Treatment	Day 1	Day 4	Day 7
		mmol L^{-1}		
Na^+	Reference control	128.59 ± 3.48	163.69 ± 11.18	174.17 ± 8.58
	Ti	153.51 ± 9.15	179.83 ± 15.19	168.35 ± 8.38
	Ag	158.91 ± 9.63	163.73 ± 21.42	154.32 ± 10.15
	Ag+nHA	155.77 ± 9.79	167.27 ± 12.28	152.80 ± 4.82
	Ag+mHA	171.59 ± 19.37	209.98 ± 34.36	160.52 ± 9.58
	nHA	156.03 ± 9.37	171.53 ± 21.86	151.58 ± 9.73
	mHA	149.32 ± 8.64	171.08 ± 9.42	165.79 ± 14.33
K^+	Reference control	6.04 ± 0.16	7.63 ± 0.55	8.02 ± 0.40
	Ti	7.17 ± 0.50	8.34 ± 0.73	7.73 ± 0.39
	Ag	7.57 ± 0.60	7.73 ± 1.04	7.08 ± 0.48
	Ag+nHA	7.52 ± 0.44	7.99 ± 0.53	7.09 ± 0.18
	Ag+mHA	8.17 ± 1.03	9.70 ± 1.65	7.38 ± 0.45
	nHA	7.36 ± 0.55	7.92 ± 0.99	7.09 ± 0.49
	mHA	6.96 ± 0.52	7.95 ± 0.49	7.50 ± 0.66
Ca^{2+}	Reference control	1.88 ± 0.04 ^{a}	2.11 ± 0.06 ^{a}	2.34 ± 0.13 ^{a}
	Ti	2.00± 0.06 ^{a}	2.28 ± 0.09 ^{a}	2.28 ± 0.10 ^{a}
	Ag	2.00 ± 0.04 ^{a}	2.09 ± 0.20 ^{a}	2.02 ± 0.06 ^{ab}
	Ag+nHA	0.72 ± 0.06 ^{c}	0.68 ± 0.05 ^{b}	0.75 ± 0.06 ^{c}
	Ag+mHA	1.61 ± 0.19 ^{ab}	1.14 ± 0.18 ^{b}	1.53 ± 0.15 ^{b}
	nHA	0.86 ± 0.04 ^{c}	0.87 ± 0.16 ^{b}	0.92 ± 0.15 ^{c}
	mHA	1.44 ± 0.09 ^{b}	1.78 ± 0.04 ^{a}	1.84 ± 0.08 ^{ab}
P	Reference control	1.33 ± 0.08 ^{a}	1.46 ± 0.06 ^{ab}	1.65 ± 0.18 ^{a}
	Ti	1.36 ± 0.10 ^{a}	1.42 ± 0.10 ^{ab}	1.54 ± 0.16 ^{a}
	Ag	1.43 ± 0.09 ^{a}	1.32 ± 0.09 ^{abc}	1.35 ± 0.08 ^{ab}
	Ag+nHA	0.78 ± 0.09 ^{bc}	0.56 ± 0.03 ^{bc}	0.55 ± 0.04 ^{c}
	Ag+mHA	1.15 ± 0.08 ^{ab}	1.79 ± 0.52 ^{a}	1.02 ± 0.11 ^{bc}
	nHA	0.62 ± 0.03 ^{c}	0.48 ± 0.05 ^{c}	0.60 ± 0.03 ^{c}
	mHA	1.07 ± 0.11 ^{ab}	1.13 ± 0.07 ^{abc}	0.95 ± 0.10 ^{bc}

Data are mean ± S.E.M (n = 6). Different letters within the column in each element indicate a significant difference (one way ANOVA or Kruskal-Wallis test, $p < 0.05$). Unlabelled means there is no significant difference.

5.4 Discussion

Dental implants like any other biomaterial require thorough investigations before being introduced to patients. The first tier of biocompatibility experiments are usually conducted *in vitro* using human primary cells. However, there are some methodological challenges regarding the experimental design, the types of controls, cell density, and the endpoints measured which need to be thoroughly addressed. In this study, 30,000 cells were used at the beginning. It was found that the cell viability was more than 95% in the Ti treatment over 7 days and this was not significantly different from the other treatments without added silver (the nHA and mHA controls). Also, cells were confluent, attached to each other, and showed no signs of membrane rupture in these controls without silver (Figure 5.1). Where silver was present, the silver release to the external media was constant and there was silver exposure in the cell monolayer after 7 days (Table 5.1). Cells did not experience shrinkage on Ti, nHA, mHA and Ag+nHA, but there was a noticeable shrinkage in cells covering Ag and Ag+mHA (Figure 5.1). Despite having a slight shrinkage in some treatments, there was not a devastating cell mortality (i.e., complete loss of cells) since cell viability was above 60%, or much higher in all treatments (Figure 5.2). Biochemistry and electrolyte balance also confirmed that there was no significant damage to the cells as no (or only little) LDH leakage was measured in the external media (Table 5.3), and the Na^+ and K^+ pump in the homogenates or media were unaffected.

5.4.1 Effect of silver release and the silver coated surface on cell viability

Total silver release from the coatings into the cell culture media and the cell homogenate was measured by ICP-OES. In the various controls without added silver,

the silver concentration was at a background concentration, and significantly lower than silver coated groups, as expected (Table 5.1). In contrast, the release of silver from the silver plated treatments (Ag, Ag+nHA and Ag+mHA) was around 2 mg L^{-1} at day 1. Notably, the, alamar blue showed that the cell viability in Ag+nHA and Ag+mHA at day 1 was around 70% which was slightly lower than nHA and mHA, but the differences were not significant (Figure 2). This indicates that 2 mg L^{-1} silver did not induce a significant toxicity to human primary osteoblast cells compared to controls having similar surface geometry (nHA and mHA). In addition, silver exposure to the cell homogenate after 7 days was also confirmed. The absence of toxicity in the presence of silver can be explained by the fact that the presence of high Cl^- in the cell culture medium can take up the dissolved silver and form poorly soluble silver chloride. Moreover, the proteins available in the cell culture medium can mask the toxicity of dissolved silver through silver ion binding to –SH group in proteins (Besinis *et al*., 2014; Hansen *et al*., 2015). Similar studies have been conducted looking at the biocompatibility of silver coating on titanium. Mei *et al.* (2014) tested the cell viability after exposure to 1 mg L^{-1} of released silver from silver incorporated in titania nanotubes. MTT cell viability assay showed no significant toxicity to human fibroblast and epithelial cells (in DMEM + 10%FBS) after growing on the silver coating over 7 days.

The role of surface chemistry and geometry of crystals on the surface must not be neglected, this is because osteoblasts are known to prefer moderately rough surfaces compared to smooth ones, also, prefer surfaces that are chemically composed of calcium and phosphorus (Wennerberg 1998; Jonge *et al*., 2008). The SEM images showed that cells on the nHA surface (whether from Ag+nHA or nHA group) have a better cell-to-cell attachment and confluence compared to those on

micro HA coated specimens (Figure 5.1). This can be explained by the fact that nano HA resembles the mineral constituent of the living bone and the size enhances osteoblast cell attachment and growth (Wang *et al*., 2007; Mendoca *et al*., 2008). While micro HA, consists of large particles that might interfere with cell-to-cell contact; thus despite having filopodia, these latter cells cannot attach with each other easily. Moreover, it was found that the presence of silver causes cell shrinkage (Figure 5.1), for example, cells on Ag+mHA showed a significant shrinkage while this phenomenon was not observed on Ag+nHA. This result corroborates Tian *et al*. (2016) who observed human bone marrow stem cell shrinkage after 3 days growth on silver nanoparticle-doped HA coating on titanium. Furthermore, Gunputh *et al*. (2018) observed similar finding after culturing primary human osteoblast cells on silver coated titanium nanotubes, SEM images showed a cell shrinkage and poor cell-to-cell attachment on silver coated specimens compared to uncoated titanium. The explanation is that the HA particles on the surface of Ag+mHA are sparse, so most of the cells were adhered to the silver layer rather than the HA layer. While the surface of Ag+nHA mainly consists of nano Ha particles fused to each other, so cells in the later were attached to the HA layer. The explanation of cell shrinkage belongs to the fact that the silver is known to interfere with Na^+ K^+-ATPase. As a result of this, the concentration of electrolytes inside the cell becomes less than the external media, this may lead to the cellular water loss and shrinkage.

LDH enzyme activity in the external media was low in all treatments (Table 5.3), and this indicates that the cells were intact over 7 days, with no appreciable leak. There was some LDH activity detected in the homogenates (Figure 5.5), and at a background activity suggesting no induction of LDH activity arising from anaerobic metabolism (see Chapters 3 and 4). ALP enzyme activity was low and close to the

detection limit in both cell culture median and the cell homogenate (Table 5.2, Figure 5.4). However, this finding is expected since the ALP activity starts at a later stage of the cell differentiation process (Yamaguchi *et al*., 2000) and was the same finding as observed in the previous chapters (Chapters 3 and 4).

Electrolytes were measured in the cell homogenate to assess the osmotic health of the cells. There was no obvious changes in the electrolyte concentrations in the homogenates that would infer osmotic distress or cell lysis. The Na^+ concentration was significantly lower in the reference control compared to the others (Figure 5.3). Similar results have been found in previous experiments (Chapter 3), where the Na^+ level in the homogenate was significantly lower in the reference control. This finding could be explained by the Na^+ being adsorbed from the media to the surface of the discs along with the adsorbed proteins in the media. Furthermore, no difference was found between Ti and others (except reference control), this may be explained by two facts; either the silver has not caused any change in the electrolyte balance of the cells, or the adsorbed Na^+ from the media might have masked the Na^+ content of the cells. K^+ level in the cell homogenate did not show significant alteration, this result shows that the cellular osmotic swelling and membrane rupture due to the presence of silver were not likely. Ca^{2+} and P level in the cell homogenate were higher in HA coated discs compared to others as expected, this is due to the Ca^{2+} and P adsorption from the media to the coating surface (see Chapter 4).

5.4.2 Effects of the coatings on DMEM media

The level of Na^+ and K^+ in the media remained constant over time and there was no significant difference between the treatments, this is because the excessive Na^+ and

K^+ in DMEM cell culture medium that masks Na^+ and K^+ fluxes from the cells. This result is comparable with Hadi *et al*. (2014) and Meran *et al*. (2013) who exposed primary human osteoblast and fibroblast cells, respectively, to silver nanoparticles in DMEM+10%FBS media and found quite similar Na^+ and K^+ concentration in the external media. In contrast, the Ca^+ and P in the external media from treatments having HA coated discs were significantly lower compared to all the others. This can be explained by the fact that the -OH group in the HA coatings can attract Ca^+ and P^+ from the external media to form calcium hydroxide $Ca(OH)_2$ on the coating surface (Harding *et al*., 2005). This results agrees with the finding of Besinis *et al*. (2017) who tested antibacterial activity of silver coated titanium and found that Ca^+ and P in the physiological saline (Kerbs ringer) adsorb to the HA surface, so in turn, the Ca^+ and P level in the media in HA coated groups were significantly reduced.

5.4.3 Conclusions and clinical significances

The use of new materials to coat dental implants require a series of experiments to confirm the compatibility with the surrounding tissues, the experiments start with testing the compatibility with the cultured cells (*in vitro*) and finally to clinical trials on humans. Moreover, designing the biocompatibility experiments (especially with nanomaterials) require some optimisations. This current study showed that culturing high number of cells initially could give better results to more clearly and confidently identify biocompatibility compared to using low number of cells. In addition, having more than one material control can give a clearer idea on the effect of surface geometry on the cells. Regarding the biocompatibility, this experiment showed that Ag+nHA is biocompatible with human primary osteoblast cells after 7 days, so it is

recommended to use Ag+nHA in favour in Ag+mHA in clinics. In addition, the released silver was higher than the antibacterial concentration, thus, the benefit for the patients is preventing (decreasing) the incidence of peri-implantitis without impairing osseointegration process. This finding can create a path for this coating to be used in dental clinics to decrease the incidence of early dental implant failure hence saving the dentist and the patient from recurrent dental visits. However, more experiments are needed to be conducted to ensure the ability of the cells to differentiate and mineralise on the coating surface.

Chapter 6

Studying the Differentiation, Mineralisation and Gene Expression of Primary Human Osteoblast Cells Cultured on Silver and Hydroxyapatite Nano Coatings

6.1 Introduction

The primary stability of dental implant arises from the mechanical bond between the implant and the jawbone immediately after implant placement. A few weeks after implant placement, peri-implant bone resorption occurs and at the same time osteoblast cells adhere to the implant surface; they then proliferate and differentiate to produce new bone around the implant. This is called ossoeintegration or secondary stability (Romanos and Johansson, 2005; Natali *et al*., 2009). Thus, the strategy for biocompatibility testing to ensure the safety of any dental implant material or coating must include studies that demonstrate osteoblast differentiation, and the associated mineralisation process that produce calcified mineral phases. For it is the latter processes that inform on successful implantation. Osteoblast cell differentiation can be tracked by using targeted gene expression measurements. For example, osteoblast cell differentiation is mediated by an essential transcription factor protein called RUNX-2 (Ducy *et al*., 1997). RUNX-2 is an important gene in regulating the skeletal development of numerous mammalian organisms (Kirkham and Cartmell, 2007). Osteocalcin is an osteoblast cell specific gene which is most expressed during osteoblast cell differentiation and calcium deposition to the extra cellular matrix (Ducy and Kartensy, 1995; Masaki *et al*., 2005). The expression of osteocalcin peaks in both extra cellular matrix synthesis and mineralisation. Moreover, ALP is also an important osteoblast cell differentiation marker because it is essentially involved in extra cellular matrix mineralisation (Hessle *et al*., 2002; Rawadi *et al.*, 2003). ALP hydrolyses pyrophosphate to produces inorganic phosphate and promote matrix mineralisation (Orimo, 2014). Medical grade titanium alloy is regarded as a biocompatible material which allows osteoblast cell growth and differentiation on the surface (Marinucci *et al*., 2005; Olivares-Navarrete *et al*., 2010).

Some studies have been conducted to investigate the effect of dental implant surface topography on osteoblast gene expression and cell differentiation. For example, Tîlmaciu *et al*. (2015) found that silver-containing phosphate monolayer coatings on titanium did not interfere with osteoblast cell differentiation or gene expression, as ALP, osteocalcin and RUNX2 gene expression were not significantly different from an uncoated Ti substrate control. Moreover, Schneider *et al*. (2003) concluded that implant surface roughness was an abiotic factor involved in altering the expression of osteogenic regulatory genes. This was through finding that Cbfa1 gene expression (which regulates osteoblast cell differentiation and mineralisation) is enhanced in osteoblast cells grown on roughened titanium implant surfaces compared to grooved ones. Yang *et al.* (2015) investigated the influence of HA surface topography on osteogenic differentiation of human osteoblast cells and found that osteogenic differentiation and gene expression was enhanced on an HA layer. While much research has been conducted on the effect of titanium, HA and their surface topography on human primary osteoblast (or osteoblast-like) cell differentiation and gene expression; there are not many studies concerning the osteoblast cell differentiation on composites (coatings) with a biocide added, such as silver. The effect of the silver on cell differentiation and gene expression is poorly understood. In addition, cell differentiation on nano silver and nano HA coating compared to nano silver and micro HA coating still needs to be further investigated to study the effect of dissolved silver on cell differentiation and mineralisation.

In the previous chapters, the biocompatibility of nano silver and nano HA coating on titanium dental implants has been demonstrated. However, the ability of the silver-coated specimens to release a constant supply of an antibacterial dissolved silver without interfering with the mineralisation process needs to be investigated. This

is to ensure that the coating provides a long-term antibacterial activity without distracting the osseointegration process around the coated dental implant inside the jawbone. The aim of this study was to investigate the ability of primary human osteoblast cells to differentiate and mineralise on silver and HA coatings, layered onto the Ti alloy used for titanium dental implants. The study also aimed to explore the effects of silver released from the coatings on osteoblast cell gene expression. The specific objectives included to assess the cell viability and silver release over 21 days, and then examining the cells under SEM and performing an EDS analysis to confirm mineralisation. Moreover, to study the osmotic status of the cells and silver exposure to the cell monolayer after 21 days, also to study the expression of osteoblast cell differentiation genes to investigate the contribution of silver to gene expression.

6.2 Materials and methods

6.2.1 Cell culture

Human primary osteoblast cells were cultured in DMEM + 10% FBS + 1% antimicrobial and the culture conditions were the same as described in Chapter 3. Cells on passage 4 and 5 were used for this experiment.

6.2.2 Experimental design

This experiment was conducted to investigate the effect of the coatings on cell differentiation, mineralisation and gene expression after 21 days. The experiment was conducted in 24-well microplates, and the study design included two separate runs of the experiment, each with its own triplicate (n = 6). The first triplicated run was

assigned for the gene expression study (n = 3), the second run for the cell homogenisation and subsequent biochemistry (n = 3). All specimens were pre-treated with DMEM + 10%FBS + 1% antimicrobials for 2 days prior to the experiment. For sample sterilisation, the same protocol was followed as described in Chapter 2. In the actual experiment, initially, 30,000 cells were added to each well. This was achieved by adding 50000 cells/ml initially from the stock cultures and then 0.6 ml of media was added to each well to give a final cell density of 3×10^4 cells/well. The microplate was the unit of replication in the study design with all treatments and controls on each plate. The cell culture medium used for the experiments was DMEM + 10% FBS + 1% antimicrobials, as in the previous chapters. However on day 7 of the experiment, the media was also supplemented with 50 mg L^{-1} ascorbic acid, 7 mM β-glycerol phosphate and 10 nM dexamethasone (all purchased from Sigma–Aldrich) to induce cell differentiation and mineralisation (Langenbach and Handschel, 2013). However, the differentiation supplements were not added to the negative control on day 7.

The negative control in this experiment was undifferentiated cells grown on culture dishes. Other treatments included: differentiated cells (reference control), uncoated titanium (Ti), silver plated titanium (Ag), silver plated and HA nanoparticles (Ag+nHA), and silver plated plus HA microparticles (Ag+mHA). The media was sampled at days 1, 4, 7, 10, 13, 16, 19 and 21. The media collected at each time point were used to measure the total concentration of Ag, Ca^{2+}, P, Na^+ and K^+ using ICP-OES (iCAP 7400 RADIAL, Hemel Hempstead, UK) and also to measure LDH and ALP enzyme activities in the media on days 1, 7 and 21 (n = 6). The Alamar blue assay was used to investigate the cell viability in all time points (n = 6).

On day 21, the first triplicate was used for gene expression after mRNA extraction, the later was destructive sampling. While in the second triplicate, the cell

were homogenised using the same procedure as described in chapter 3 section 3.2.3, then the samples were immediately analysed for biochemistry and measured for Ag, Ca^{2+}, P, Na^{+} and K^{+} using ICP-OES (iCAP 7400 RADIAL, Hemel Hempstead, UK). Another run of the experiment was conducted (n = 3) and specified for SEM and EDS analysis of the cells after 21 days growth on the specimens (destructive sampling).

6.2.3 Alamar blue assay

The alamar blue assay was carried out to follow the cell viability on days 1, 4, 7, 10, 13, 16, 19 and 21. The protocol was exactly the same as described in chapter 5, and the volume of cells used was also the same (30,000 cells/well).

6.2.4 Enzyme activity assays

ALP and LDH activities were determined in both the cell homogenates after 21 days, and the cell culture medium on day 1, 7, and 21. For LDH activity, briefly, 100 µl of the sample was added to 2800 µl test reagents and the change in absorbance was taken kinetically at 340 nm wavelength. For ALP, 30 µl of the test sample was added to 250 µl of the assay reagent and the absorbance measured kinetically at 405 nm. The assay protocols are fully described in Chapter 3.

6.2.5 Silver and electrolyte balance

Total Ag, Ca^{2+}, P, Na^{+} and K^{+} were determined by ICP-OES in both the cell homogenates after 21 days (n = 3), and the cell culture medium on days 1, 4, 7, 10, 13, 16, 19 and 21 (n = 6). This served to measure the release of apparent dissolved silver from the discs and also the silver accumulated in/on the cell monolayer. Calcium

and P were measured to check whether the cells had mineralised and produced mineralised nodules. Na^+ and K^+ were measured to determine the osmotic status of the cells. The procedures for sample preparation and acidification are described in Chapter 3.

6.2.6 Studying the cell morphology using SEM and EDS

After 21 days, a triplicate of each group was subjected to dehydration and fixation procedure (chapter 3) to be prepared for SEM and EDS. The point of interest in using SEM and EDS was to examine the cell confluence, contact with each other through extending filopodia, and also the membrane integrity through examining the presence of membrane blebs and rupture. EDS was performed to confirm that any apparent mineral mass observed was mineralised tissue composed of calcium and phosphorus.

6.2.7 RNA extraction

Messenger ribonucleic acid (mRNA) was extracted from the cells after 21 days and the mRNA was then converted to cDNA to study the expression of the particular gene of interest. The procedure for RNA extraction followed a QIAGEN protocol for RNA extraction (RNeasy Mini Kit, cat. nos. 74104 and 74106). The protocol started with adding 10 µl β-mercaptethanol to 1 ml of buffer 'RLT'; to prepare the lysis buffer, then 350 µl RLT lysis buffer were added to each well and then vortexed for 3 minutes. This step was to lyse and homogenise the cells. The cell lysate was transferred to RNase-free Eppendorf tubes and centrifuged for 3 min at maximum speed. After that, 1 volume of 70% alcohol was added to each tube and then 700 µl of the sample (including any precipitate) was transferred to an RNeasy Mini spin column placed in a

2 ml collection tube then centrifuged for 15 seconds ≥ 8000 x *g*. Alcohol was used to force the precipitation of RNA out of solution. After that, buffer 'RW1' was added to the spin column and centrifuged for 15 second at ≥ 8000 x *g*. The RW1 buffer is a washing buffer containing guanidine salt and ethanol, and it is used to remove biomolecules such as carbohydrates, proteins, fatty acids. After adding the 'RW1' buffer, bufffer 'RPE' was added to the spin column and then centrifuged for 15 second at ≥ 8000 x *g*. Buffer RPE is a mild washing buffer which is used to remove traces of salts left in the column due to buffers used previously in the procedure.

Finally, the RNeasy spin column was placed in a new 1.5 ml collection tube and then 30 µl RNase-free water was added directly to the spin column membrane then centrifuged for 1 min at ≥ 8000 x *g* to elute the RNA. The 'Nano drop' instrument (Thermo Scientific NanoDrop, 2000) was used to calculate the RNA content of each sample. For the latter, 1 µl of RNA in an RNase free water was placed on the sensor of the device and then the amount of RNA was directly measured.

6.2.8 Studying the gene expression using quantitative real time polymerase chain reaction (qPCR)

Gene expression was studied to investigate the effect of the coatings on osteoblast functional genes. The house keeping gene in this study was β-actin and target genes were for ALP, osteocalcin, Runt-related transcription factor 2 (RUNX-2) and interleukin (IL-6), primer sequences are shown in (Table 6.1). ALP, osteocalcin and RUNX-2 were selected because they are expressed during osteoblast cell differentiation and mineralisation. IL-6 was selected to check for the presence of inflammation in the cells. The RT-PCR was conducted in 384 well plates (n = 3 samples (extracted RNA) per each treatment) and a duplicate of each sample were used. The concentration of RNA

in each sample was 10 ng μl^{-1} RNA in RNase free water, and the volume of the sample was 30 µl. The volumes of reagents are listed in (Table 6.2) and the total reaction volume was 10 µl. Target genes were normalised to the house keeping gene (β-actin) to calculate the fold change. Data were processed by working out the change in CT value (ΔCT) between target gene and the house keeping gene of each sample in each treatment, and then ΔΔCT was calculated between the tested samples (treatments) and the negative control. Finally, the ΔΔCT values were subjected to (2^-ΔΔCT) to calculate the fold change of the target gene.

Table 6.1. Genetic sequence of the primers used in this study

ALP (Forward)	5-GAC AAT CGG AAT GAG CCC ACG C.3
ALP (Reverse)	5-GTA CTT ATC CCG CGC CTT CA CAC-3
Osteocalcin (Forward)	5-AGC CCA CGC GTC GAG AGT CCA-3
Osteocalcin (Reverse)	5-GCC GTA GAA GCG CCG ATA GG-3
RUNX-2 (Forward)	5-TGC CCG GCC AGC CAG GTC CAG A-3
RUNX-2 (Reverse)	5-ACC CGC CAT GAC AGT ACC CAC AGT-3
IL-6 (Forward)	5-AGT TGC CTT CTT GGG ACT GA-3
IL-6 (Reverse)	5-GAC AAT CGG AAT GAG AGA AC-3
β-Actin (Forward)	5-CCC AAG GCC AAC CGC GAG AAG ATG-3
β-Actin (Reverse)	5-GTC CCG GCC AGC CAG GTC CAG A-3

Table 6.2. Components and volume of the reaction mixture used in qPCR

Component	Volume in reaction
QuantiNova SYBR Green RT-PCR Master Mix 10	5 µl
QN ROX Reference Dye	0.5 µl
QN SYBR Green RT-Mix	0.1 µl
10x primer mix	1 µl (0.5 µl forward primer, 0.5 µl reverse primer
Sample (RNA)	1 µl
RNase-Free Water	2.4 µl

The RT-PCR process was carried out following the QuantiNova SYBR green RT-PCR kit using (Quant Studio 12K Flex Real-Time PCR System, Thermo Fisher SCIENTIFIC) instrument; the RT-PCR process started with reverse transcription for 10 minutes at 50 °C to activate reverse transcription, then PCR initial activation step for 2 min at 95 °C. Later, two-step cycling started; the first step was denaturation for 5 seconds at 95 °C and then a combined annealing/extension step for 10 seconds at 60 °C, and finally a melting curve analysis step.

6.2.9 Statistical analysis

All data are presented as mean ± S.E.M and analysed using Statgraphics version 16. Data were subjected to the normality test to check whether that data are normally distributed. To remove any outlying values, Box and Whisker plots were used. Difference between the treatments, or between the time points of the same treatment,

were evaluated using one-way analysis of variance (ANOVA, then Tukey's test). For data which were not normally distributed, the Kruskal Wallis test was used, and significant differences were located using Box and Whisker plots. Two-way analysis of variance was used to evaluate the combined time and treatment effect. All statistical analysis used a 95% confidence limit, p values < 0.05 were considered statistically significant.

6.3 Results

6.3.1 Silver release to the external media and exposure to the cell monolayer

Concentration of total silver in the external media and the cell homogenate were measured over 21 days using ICP-OES. Table 6.3 shows that there was a significantly lower silver concentration in the media from the negative control, reference control and Ti compared to the other treatments (one way ANOVA, $p < 0.05$). The background values for total silver in the media were around 0.03 mg L^{-1} or less. Moreover, the Ag, Ag+nHA and Ag+mHA showed similar amounts of silver release over time; with the values being around 1 mg L^{-1} at day 1, then increased to around 2 mg L^{-1} at day 4, and then gradually decreased over time to reach to approximately 0.3 mg L^{-1} on day 21. The difference between day 21 and day 1 was significant for Ag, Ag+nHA and Ag+mHA (one way ANOVA, $p < 0.05$, Table 6.3). Two way ANOVA showed that there were both treatment and time effects on Ag release ($p < 0.05$, Table 6.3). Silver exposure to the cell monolayer was confirmed by measuring the total silver in the homogenates. The concentration of silver in the homogenates from the negative control, reference control and Ti were significantly lower than Ag, Ag+nHA and Ag+mHA. Also, the total silver in the Ag treatment was significantly higher than the Ag+nHA or Ag+mHA treatments (one way ANOVA, $p < 0.05$, Table 6.3).

Table 6.3. Concentration of Ag in the external media over 21 days

Treatment	Day 1	Day 4	Day 7	Day 10	Day 13	Day 16	Day 19	Day 21	Homogenate
					mg L^{-1}				
Negative control	0.06 ± 0.01 B	0.08 ± 0.01 B	0.08 ± 0.01 B	0.04 ± 0.01 B	0.09 ± 0.01 B	0.06 ± 0.01 B	0.07 ± 0.01 B	0.07 ± 0.01 B	0.03 ± 0.02 C
Reference control	0.03 ± 0.01 B	0.04 ± 0.01 B	0.08 ± 0.01 B	0.07 ± 0.01 B	0.06 ± 0.01 B	0.03 ± 0.01 B	0.02 ± 0.01 B	0.01 ± 0.01 B	0.01 ± 0.00 C
Ti	0.02 ± 0.01 B	0.02 ± 0.01 B	0.04 ± 0.01 B	0.04 ± 0.01 B	0.03 ± 0.01 B	0.02 ± 0.01 B	0.01 ± 0.00 B	0.01 ± 0.00 B	0.24 ± 0.12 C
Ag	0.86 ± 0.11 Ay	2.34 ± 0.49 Ax	1.69 ± 0.32 Ax	1.33 ± 0.22 Ax	1.02 ± 0.25 Ax	0.68 ± 0.09 Ay	0.64 ± 0.17 Ay	0.37 ± 0.10 Az	44.81 ± 20.5 A
Ag+nHA	1.04 ± 0.30 Ax	2.08 ± 0.54 Ax	1.61 ± 0.85 Ax	1.08 ± 0.30 Ax	0.91 ± 0.25 Ax	0.52 ± 0.11 Ay	0.52 ± 0.18 Ay	0.26 ± 0.05 Ay	13.50 ± 2.21 B
Ag+mHA	0.70 ± 0.16 Axy	1.51 ± 0.31 Ax	1.26 ± 0.24 Ax	1.27 ± 0.09 Ax	1.03 ± 0.06 Ax	0.50 ± 0.11 Ay	0.46 ± 0.07 Ay	0.25 ± 0.05 Ay	13.08 ± 5.97 B

Data are expressed as mean ± S.E.M. (n = 6). Different capital letters within the column indicate a significant difference between material types, while different small letters within the row indicates a statistically significant time-effect within treatment. One way ANOVA or Kruskal-Wallis test ($p < 0.05$) were used for treatment or time-effects.

6.3.2 Cell health, morphology and mineralisation assessment over 21 days

SEM images showed cells on Ti and also Ag+nHA were confluent, attached to each other, having an intact membrane, while cells on Ag and Ag+mHA were less confluent and there was a slight noticeable shrinkage but with an intact cell membrane and also cell to cell attachment (Figure 6.1). Light microscopy images of the negative control and the reference control showed confluent cells, well attached to each other and having an intact cell membranes. The difference was the presence of some orange/red deposits of the cell monolayer in the reference control (Figure 6.1). EDS showed that the cell on the specimens in all treatments were mineralised and produced calcium and phosphorus after 21 days (Figure 6.2).

Cell viability was assessed using the alamar blue assay. Table 6.4, shows that and there was no statistically significant change in cell viability over time in the reference control (Kruskal Wallis test, $p = 0.968$) and Ti (one way ANOVA, $p = 0.141$). Cell viability in the Ag+nHA treatment increased over time, and at day 21 the cell viability was significantly higher than earlier time points (one way ANOVA, $p < 0.05$), (Table 6.4). For the Ag and Ag+mHA treatments, the cell viability showed a trend of steadily decreasing values (not always statistically significant) over time. Two way ANOVA showed that there were both time and treatments effect of cell viability ($p < 0.05$).

The electrolyte composition of the homogenates were measured to access the osmotic health of the cells. The Na^+ concentration in the cell homogenate was significantly lower in the negative and reference control compared to all the other treatments (one way ANOVA, $p < 0.05$) measuring less than 0.5 mmol L^{-1} in the negative and reference control (Figure 6.3). Moreover, the Ag+mHA treatment was significantly lower than the Ti (one way ANOVA, $p < 0.05$) measuring 1 and 2.5 mmol L^{-1} respectively. Moreover,

Ag and Ag+nHA were not significantly different from Ti. The concentration of K^+ in the reference control was not significantly different from the Ti treatment (one way ANOVA, $p = 0.0004$), with both measuring around 0.5 mmol L^{-1} (Figure 6.3). However, K^+ concentration in the homogenate was significantly lower in the Ag+mHA treatment compared to all others (one way ANOVA, $p < 0.05$), measuring around 0.3 mmol L^{-1} (Figure 6.3). Ca^+ concentrations in the cell homogenates was significantly lower in the negative control compared to the others (Kruskal Wallis test, $p = 0.014$), (Figure 6.5). Concentration of P, was also significantly lower in the negative control compared to test samples (Kruskal Wallis test, $p = 0.022$), (Figure 6.3).

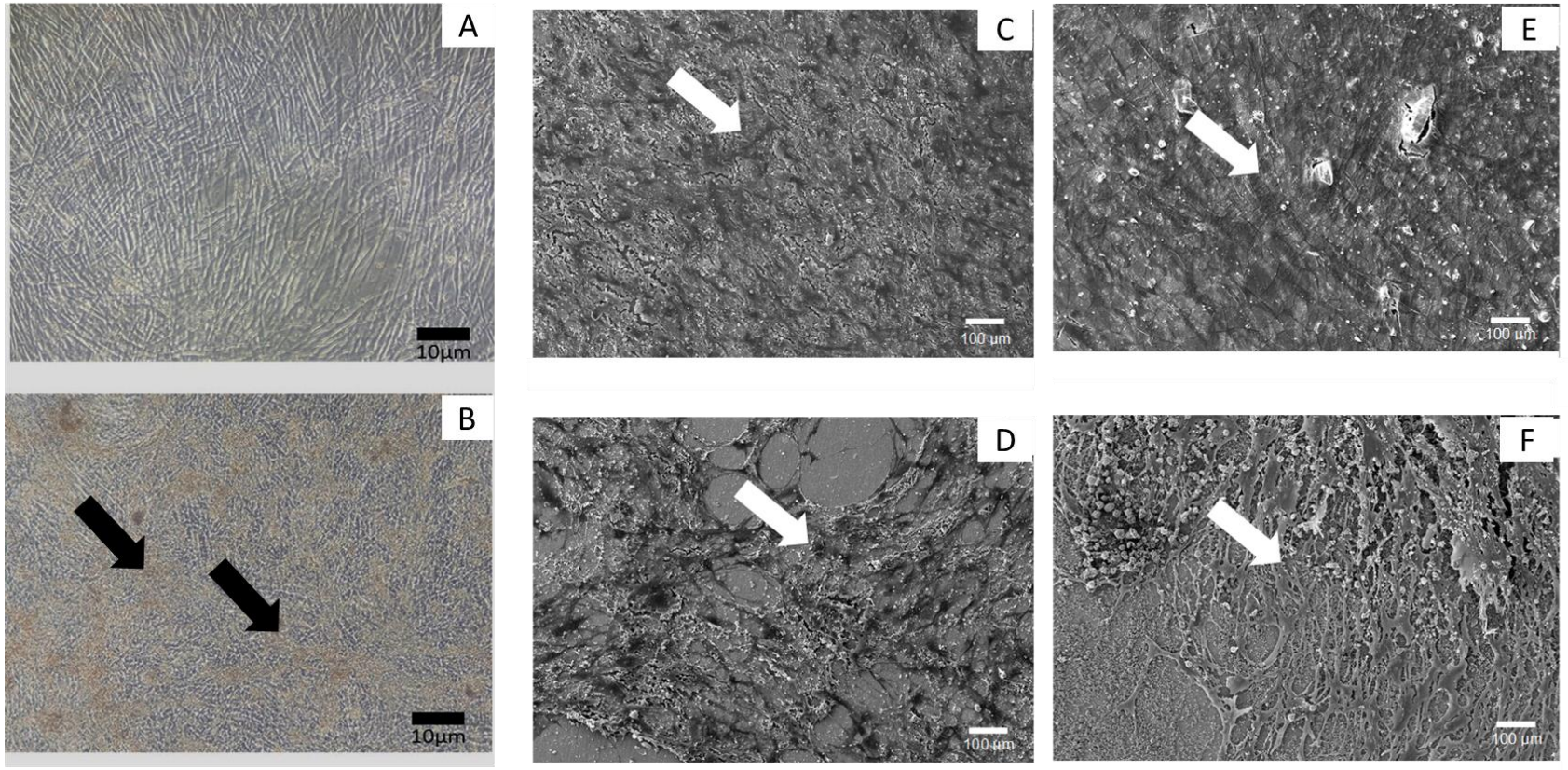

Figure 6.1. (A) and (B) light microscopic image of primary human osteoblast cells after 21 days growth in negative control and reference control respectively, (Scale bar is 10 µm, magnification is x50. Note the arrows pointing to orange/red deposits in image (B) which is argued to be mineral deposits. Other are SEM images of differentiated primary human osteoblast cells on (C) Ti, (D) Ag, (E) Ag+nHA, and (F) Ag+mHA. Note the confluence of the cells and their attachment to each other. Magnifications are x100 and the scale bars are 100 µm.

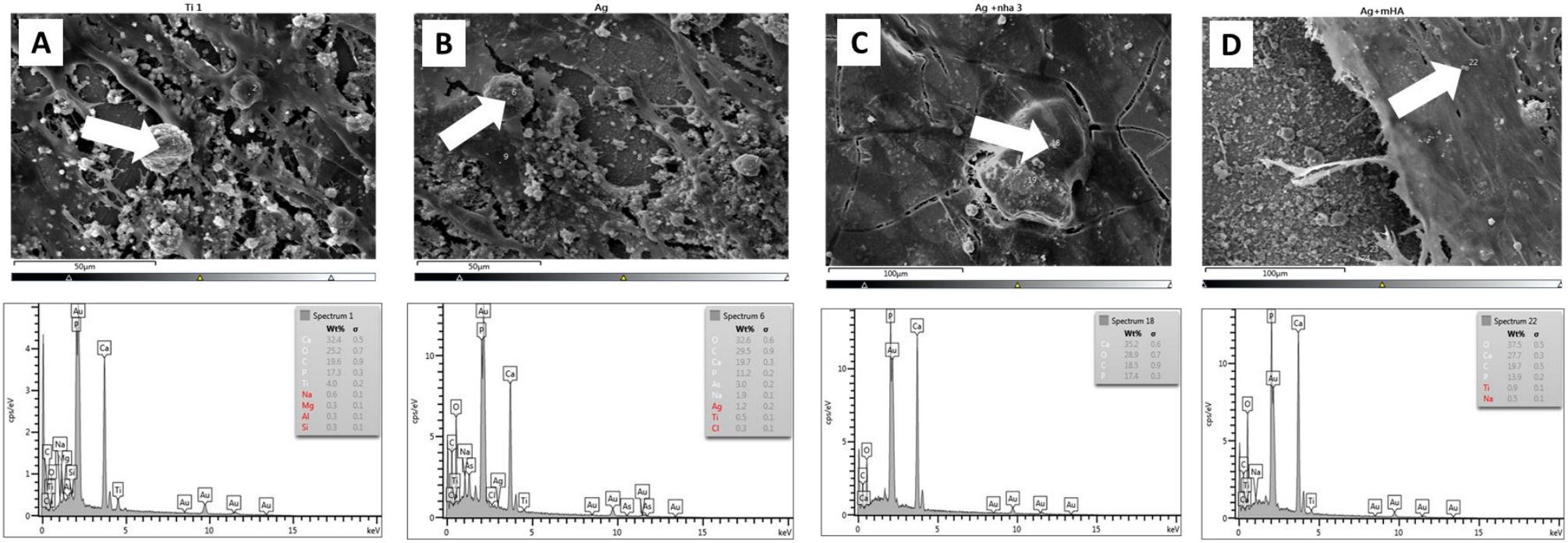

Figure 6.2. EDS spectra showing the composition of calcified masses produced by human primary osteoblast cells cultured on (A): Ti, (B): Ag, (C): Ag+nHA and (D): Ag+mHA. Arrows are pointing to the calcified mass from which the composition is been confirmed by EDS. It can be noticed that the composition of the calcified masses is mainly Ca and P. The presence of a high amount of Au is because the specimens were coated with gold to make the surface conductive. The negative control and reference control were not included because it was not possible to perform EDS spectra for the cells grown on culture dishes.

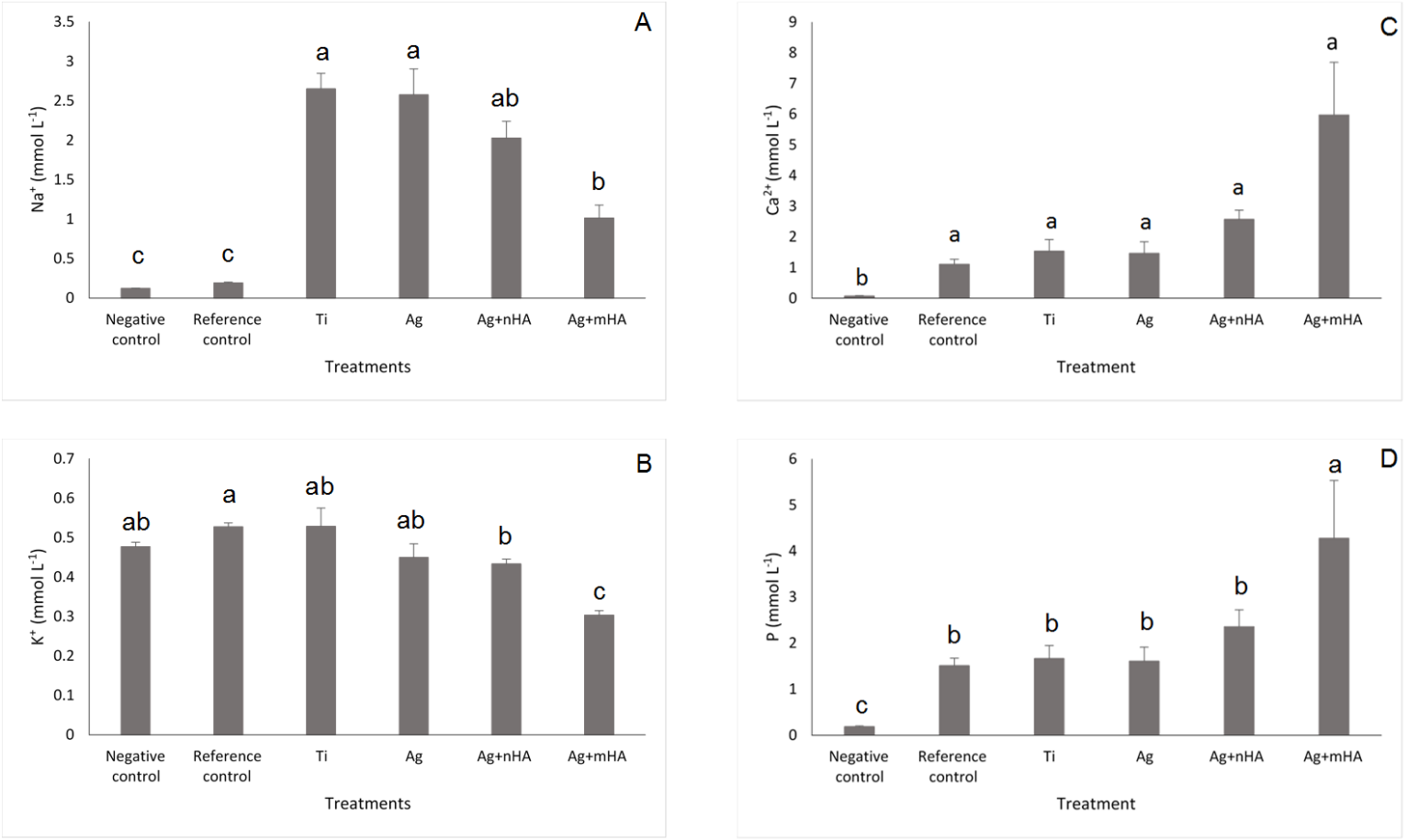

Figure 6.3. Concentration of Na^+ (A), K^+ (B), Ca^{2+} (C) and P (D) in the cell homogenate after 21 days. Data are mean ± S.E.M, (n = 3). Different letters indicate a significant difference between treatments (one way ANOVA or Kruskal Wallis, $p < 0.05$). No label means no significant difference between treatments.

Table 6.4. Percentage cell viability relative to the negative control determined by Alamar blue assay over 21 days

Treatments	Day 1	Day 4	Day 7	Day 10	Day 13	Day 16	Day 19	Day 21
Reference control	104.6 ± 9.6 A a	96.6 ± 3.8 A a	102.1 ± 10.1 A a	90.2 ± 6.1 AB a	87.7 ± 12.1 AB a	79.4 ± 16.1 B a	92.0 ± 12.8 A a	84.1 ± 17.8 AB a
Ti	97.4 ± 7.2 AB a	75.1 ± 4.8 B ab	75.4 ± 7.6 B ab	73.3 ± 11.1 AB ab	73.9 ± 15.1 AB ab	54.6 ± 7.4 B b	69.3 ± 12.0 AB b	60.5 ± 8.1 B b
Ag	75.5 ± 6.9 C a	45.6 ± 0.8 C ab	49.6 ± 8.9 C ab	64.3 ± 10.5 BC ab	63.1 ± 14.5 BC ab	39.2 ± 3.2 B b	61.4 ± 12.6 AB ab	67.7 ± 17.4 B ab
Ag+nHA	83.8 ± 6.7 ABC bcd	56.4 ± 6.1 C d	74.7 ± 9.6 B cd	82.9 ±10.5 AB bcd	87.2 ± 7.1 AB bcd	115.7 ± 5.2 A ab	90.3 ± 7.0 A abc	123.6 ± 4.9 A a
Ag+mHA	80.5 ± 5.0 BC a	48.3 ± 6.6 C ab	44.1 ± 7.4 C b	42.9 ± 7.4 C ab	43.5 ± 5.7 C b	47.8 ± 12.3 B b	51.0 ± 9.1 B b	62.5 ± 13.1 B ab

Data are mean ± S.E.M, (n = 6). Different small letters within the raw indicate a significant difference, while different capital letters within the column indicate a significant difference, one way ANOVA or Kruskal Wallis, ($p < 0.05$).

6.3.3 Alkaline phosphatase and lactate dehydrogenase enzyme activities

ALP activity was also measured in the cell homogenates and the external media. There was detectable ALP activity in the cell homogenate, but without any significant difference between the treatments (Kruskal Wallis, $p > 0.676$). There was also a trace amount of ALP detected in the cell culture media, but values were less than 0.1 nmol min^{-1} ml^{-1} (Figure 6.4 and Table 6.5). LDH enzyme activity was also measured in the external media and the cell homogenate. Figure 6.5 shows that there was a detectable LDH activity in the cell homogenate in all groups. However, there was no significant difference between them (one way ANOVA, $p = 0.428$). In the external media, there was also detectable LDH activity, but no significant difference was located between the groups (Kruskal Wallis, $p > 0.05$). Values for LDH activity in the external media were less than 10 nmol min^{-1} ml^{-1} (Table 6.6).

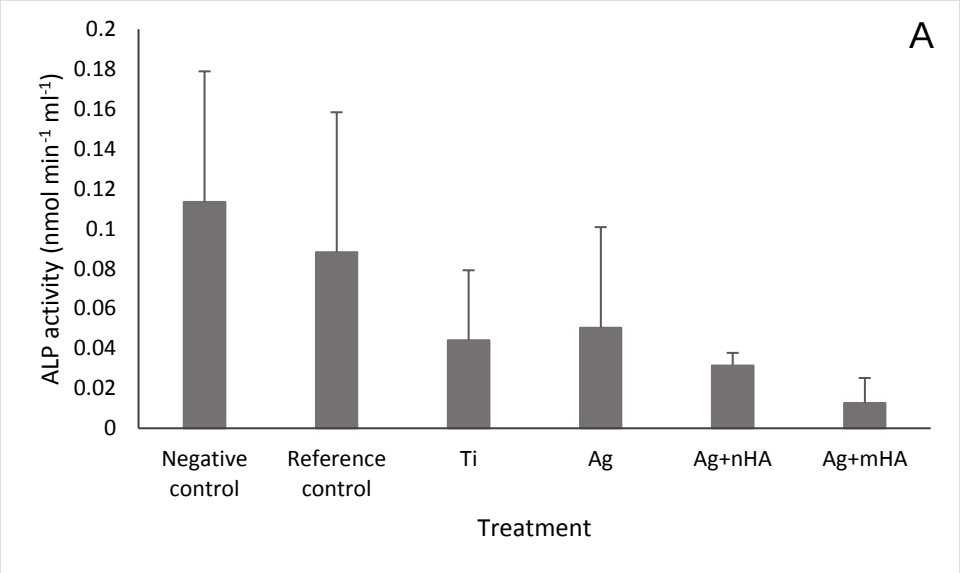

Figure 6.4. ALP enzyme activity in the cell homogenate after 21 days. Data are represented as mean ± S.E.M, (n = 3) there were no significant differences between the groups (Kruskal Wallis test, $p = 0.676$).

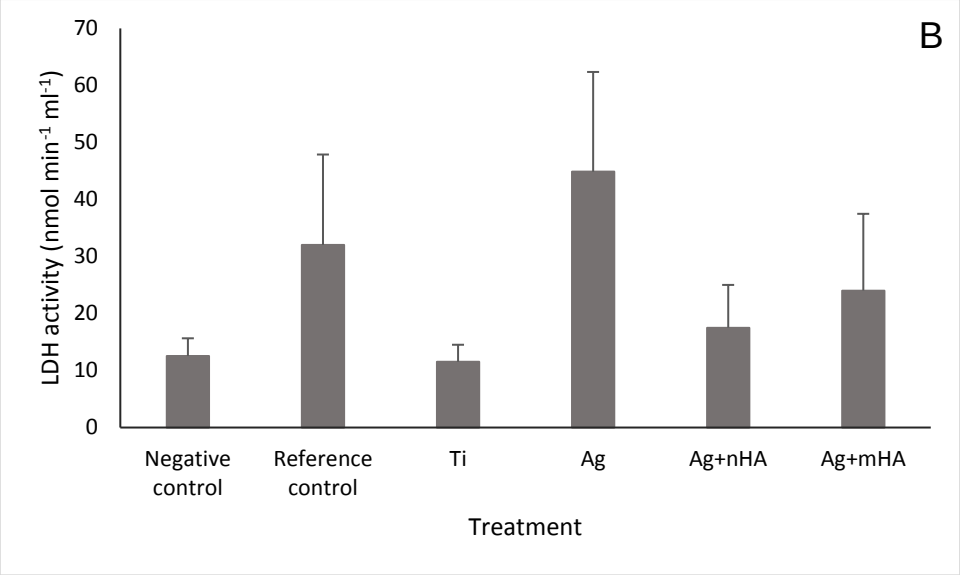

Figure 6.5. LDH in the cell homogenate after 21 days. Data are represented as mean ± S.E.M, (n = 3) there were no significant differences between the groups (one way ANOVA, p = 0.428).

Table 6.5. ALP enzyme activity in the external media over 21 days

Treatment	Day 1	Day 7	Day 21
	ALP activity (nmol min^{-1} ml^{-1})		
Negative control	< 0.004	0.032 ± 0.007	< 0.004
Reference control	0.101 ± 0.009	0.039 ± 0.011	0.045 ± 0.003
Ti	0.103 ± 0.022	0.029 ± 0.007	< 0.004
Ag	0.054 ± 0.021	0.036 ± 0.004	0.025 ± 0.001
Ag+nHA	0.057 ± 0.004	0.026 ± 0.007	0.023 ± 0.001
Ag+mHA	0.068 ± 0.004	0.034 ± 0.004	0.026 ± 0.001

Data are mean ± S.E.M, (n = 6). There were no significant differences between the treatments or between the time point within the same treatment (Kruskal Wallis test, p > 0.05).

Table 6.6. LDH enzyme activity in the external media over 21 days.

Treatments	Day 1	Day 7	Day 21
	LDH activity (nmol min^{-1} ml^{-1})		
Negative control	9.02 ± 8.67	1.42 ± 0.94	0.92 ± 0.56
Reference control	9.07 ± 6.86	2.43 ± 1.16	3.22 ± 2.45
Ti	3.21 ± 1.91	0.74 ± 0.22	1.69 ± 0.75
Ag	9.97 ± 3.44	1.29 ± 0.45	0.95 ± 0.34
Ag+nHA	3.26 ± 1.52	0.74 ± 0.10	1.26 ± 0.64
Ag+mHA	1.93 ± 0.81	0.95 ± 0.22	1.26 ± 0.45

Data are mean ± S.E.M, (n = 6) there are no significant differences between the groups or between the time points of the same group (Kruskal Wallis test, $p > 0.05$).

6.3.4. Concentration of electrolytes in the cell culture media

Concentration of Na^+ in the media was around 60 mmol L^{-1} on day 1 in all treatments, but then the values slightly increased over time (Table 6.7). Moreover, the concentration of K^+ remained constant at around 5.5 mmol L^{-1} in all treatments at all time points, without any statistically significant differences (one way ANOVA, $p < 0.05$, Table 6.8). Two way ANOVA showed that there was no time effect on Na^+ and K^+, just treatment effect ($P < 0.05$). However, the Ca^{2+} concentration in the media was significantly higher in the negative control, reference control, Ti and Ag treatments compared to the Ag+nHA and Ag+mHA treatments (one way ANOVA, $p < 0.05$). Values for Ca^{2+} concentration were between 0.2 to 2 mmol L^{-1} in all treatments. Ca^{2+} concentrations in the Ag+nHA treatment gradually decreased over time and the mean value at day 7 was significantly different from that at day 1 (one way ANOVA, $p < 0.05$, Table 6.9). P concentrations in the media were also significantly higher in the negative

control, reference control, Ti and Ag treatments compared to the Ag+nHA and Ag+mHA treatments (one way ANOVA, $p < 0.05$). The values for all treatments were between 1 to 6 mmol L^{-1}. However, from day 16 and onward, there were no significant differences between the treatments (one way ANOVA, $p > 0.05$, Table 6.10).

Table 6.7. Concentration of Na^+ in the external media over 21 days.

Treatment	Day 1	Day 4	Day 7	Day 10	Day 13	Day 16	Day 19	Day 21
	mmol L^{-1}							
Negative control	180.09 ± 8.66 ^{A}	167.05 ± 9.18 ^{A}	206.70 ± 8.29 ^{A}	140.50 ± 3.89 ^{A}	142.70 ± 5.68 ^{A}	143.96 ± 2.08 ^{A}	139.55 ± 13.88 ^{A}	161.32 ± 9.87 ^{A}
Reference control								
Ti	64.090 ± 1.602 ^{By}	85.678 ± 11.479 ^{Bxy}	101.673 ±5.754 ^{Bx}	100.450 ±11.355 ^{Bxy}	80.319 ± 8.392 ^{Bxy}	79.980 ± 15.626 ^{Bx}	95.922 ± 3.063 ^{Bx}	77.976 ± 9.663 ^{Bx}
Ag	70.034 ± 9.187 ^{By}	88.071 ± 8.898 ^{Bxy}	95.336 ± 6.105 ^{Bx}	102.188 ± 12.459 ^{Bxy}	86.979 ± 8.825 ^{Bxy}	96.697 ± 2.725 ^{Bx}	77.316 ± 15.485 ^{Bx}	82.450 ± 2.973 ^{Bx}
Ag+nHA	59.383 ± 1.041 ^{By}	84.451 ± 8.318 ^{Bxy}	110.325 ± 23.290 ^{Bx}	94.091 ± 12.254 ^{Bxy}	77.543 ± 12.989 ^{Bxy}	89.262 ± 3.513 ^{Bx}	86.558 ± 2.713 ^{Bx}	77.566 ± 2.055 ^{Bx}
Ag+mHA	58.495 ± 1.086 ^{By}	86.779 ± 8.946 ^{Bxy}	83.811 ± 5.897 ^{Bxy}	100.045 ± 11.178 ^{Bxy}	86.426 ± 11.728 ^{Bxy}	89.618 ± 3.420 ^{Bx}	82.215 ± 1.920 ^{Bx}	73.455 ± 5.352 ^{Bxy}
	59.282 ± 1.162 ^{By}	82.798 ± 14.385 ^{Bxy}	91.835 ± 6.075 ^{Bxy}	100.421 ± 11.903 ^{Bx}	94.734 ± 12.239 ^{Bxy}	91.563 ± 2.855 ^{Bxy}	84.615 ± 1.063 ^{Bxy}	76.732 ± 4.076 ^{Bxy}

Data are expressed as mean ± S.E.M, (n = 6). Different capital letters within the column indicate a significant difference, while different small letters within the row locates a significant difference. One way ANOVA or Kruskal Wallis test ($p < 0.05$). Unlabelled means no significant difference.

Table 6.8. Concentration of K^+ in the external media over 21 days.

Treatment	Day 1	Day 4	Day 7	Day 10	Day 13	Day 16	Day 19	Day 21
	mmol L^{-1}							
Negative control	8.72 ± 0.39	8.28 ± 0.52	9.17 ± 0.29	6.17 ± 0.17	5.64 ± 0.37	6.38 ± 0.12	6.26 ± 0.74	7.53 ± 0.39
Reference control	6.071 ± 0.226	5.900 ± 0.453	7.200 ± 0.534	6.732 ± 0.131	4.892 ± 0.484	4.544 ± 0.949	6.904 ± 0.281	5.145 ± 0.711
Ti	6.288 ± 0.458 ^{xy}	6.397 ± 0.236 ^{xy}	6.616 ± 0.435 ^{xy}	7.200 ± 0.288 ^{x}	5.264 ± 0.258 ^{y}	5.864 ± 0.249 ^{xy}	5.115 ± 1.045 ^{xy}	5.499 ± 0.153 ^{xy}
Ag	5.783 ± 0.103	6.029 ± 0.286	7.373 ± 0.928	6.307 ± 0.132	4.546 ± 0.920	5.344 ± 0.207	6.255 ± 0.197	4.957 ± 0.314
Ag+nHA	5.683 ± 0.087 ^{y}	6.367 ± 0.494 ^{xy}	6.071 ± 0.509 ^{xy}	6.392 ± 0.095 ^{x}	5.565 ± 0.065 ^{y}	5.335 ± 0.172 ^{y}	5.641 ± 0.184 ^{xy}	4.798 ± 0.532 ^{y}
Ag+mHA	5.616 ± 0.236 ^{xy}	5.296 ± 0.568 ^{xy}	6.488 ± 0.404 ^{xy}	6.737 ± 0.197 ^{x}	5.881 ± 0.116 ^{y}	5.412 ± 0.253 ^{y}	5.757 ± 0.150 ^{y}	5.048 ± 0.353 ^{y}

Data are expressed as mean ± S.E.M, (n = 6). Different capital letters within the column indicate a significant difference, while different small letters within the row locates a significant difference. One way ANOVA or Kruskal-Wallis test ($p < 0.05$). Unlabelled means no significant difference.

Table 6.9. Concentration of Ca^{2+} in the external media over 21 days.

Treatment	Day 1	Day 4	Day 7	Day 10	Day 13	Day 16	Day 19	Day 21
	mmol L^{-1}							
Negative control	2.12 ± 0.05 A	1.95 ± 0.14 A	2.10 ± 0.28 A	1.93 ± 0.05 A	1.40 ± 0.07 A	2.24 ± 0.06 A	1.93 ± 0.03 A	2.32 ± 0.19 A
Reference control	1.937 ± 0.070 A x	1.836 ± 0.138 A xy	1.892 ± 0.091 A xy	1.455 ± 0.020 A xy	1.175 ± 0.128 A z	1.100 ± 0.214 A z	1.264 ± 0.161 A yz	0.878 ± 0.195 A z
Ti	1.965 ± 0.172 A x	1.917 ± 0.132 A x	1.782 ± 0.065 A x	1.566 ± 0.065 A x	0.667 ± 0.043 A y	0.803 ± 0.141 A y	0.542 ± 0.110 B y	0.825 ± 0.062 A y
Ag	1.728 ± 0.035 A x	1.856 ± 0.096 A x	1.955 ± 0.345 A x	1.412 ± 0.050 A y	0.795 ± 0.173 A yz	0.772 ± 0.128 A z	0.685 ± 0.042 B z	0.837 ± 0.040 A z
Ag+nHA	0.730 ± 0.072 B wx	0.686 ± 0.077 B xy	0.324 ± 0.028 B y	0.353 ±0.017 B yz	0.345 ± 0.038 B yz	0.300 ± 0.043 B yz	0.338 ± 0.068 C z	0.388 ± 0.079 B yz
Ag+mHA	0.970 ± 0.153 xy B	0.737 ± 0.109 B xy	0.532 ± 0.072 B xy	0.537 ± 0.060 B y	0.667 ± 0.050 A x	0.649 ± 0.038 AB xy	0.661 ± 0.014 B x	0.857 ± 0.07 A x

Data are expressed as mean ± S.E.M, (n = 6). Different capital letters within the column indicate a significant difference, while different small letters within the row locates a significant difference. One way ANOVA or Kruskal-Wallis test ($p < 0.05$). Unlabelled means no significant difference.

Table 6.10. Concentration of P in the external media over 21 days.

Treatment	Day 1	Day 4	Day 7	Day 10	Day 13	Day 16	Day 19	Day 21
	mmol L^{-1}							
Negative control	1.53 ± 0.06 A	2.27 ± 0.77 A	6.61 ± 1.40 A	1.53 ± 0.06 A	3.71 ± 1.17 A	2.32 ± 0.71 A	3.43 ± 0.99 A	2.01 ± 0.09 A
Reference control	1.328 ± 0.033 A y	0.969 ± 0.169 A y	4.677 ± 1.577 A xy	4.596 ± 1.021 A x	3.890 ± 0.815 A x	2.176 ± 0.807 A xy	2.288 ± 0.689 A xy	2.457 ± 0.745 A xy
Ti	1.473 ± 0.177 A y	0.846 ± 0.204 A y	4.036 ± 1.421 A xy	4.372 ± 1.279 A xy	5.869 ± 0.808 B x	2.321 ± 0.364 A xy	1.486 ± 0.548 A xy	3.500 ± 0.404 A xy
Ag	1.469 ± 0.103 A z	1.026 ± 0.135 A z	4.217 ± 0.139 A xyz	4.230 ± 0.854 A xyz	5.464 ± 1.231 B x	1.993 ± 0.322 A yz	1.971 ± 0.478 A yz	3.858 ± 0.536 A y
Ag+nHA	0.864 ± 0.068 B yz	0.451 ± 0.058 B z	3.273 ± 0.980 B xy	3.988 ± 0.881 B x	5.055 ± 0.647 B x	2.142 ± 0.353 A xyz	2.406 ± 0.453 A xyz	3.923 ± 0.490 A x
Ag+mHA	0.786 ± 0.172 B y	0.490 ± 0.066 B y	3.672 ± 1.066 B wxy	4.217 ± 0.891 B wx	5.322 ± 0.716 Bw	1.877 ± 0.276 A x	2.520 ± 0.486 A x	2.977 ± 0.668 A wx

Data are expressed as mean ± S.E.M, (n = 6). Different capital letters within the column indicate a significant difference, while different small letters within the row locates a significant difference. One way ANOVA or Kruskal-Wallis test ($p < 0.05$). Unlabelled means no significant difference.

6.3.5 Gene expression study

Quantitative real time PCR was performed at the end of the experiment to study the mRNA of the functional genes in the osteoblasts that related to the cell differentiation and mineralisation processes. The values were fold changes relative to the negative control. The results showed that the expression of β-actin was constant between the treatments, however, Ag and Ag+mHA showed significantly less expression compared to others. The mRNA expression in ALP in the reference control was increased approximately 1 fold relative to the negative control. However, the fold change in other treatments were less than 1 relative to the negative control (Figure 6.6). The expression of mRNA in ALP was significantly higher in the reference control compared to the Ti, Ag and Ag+mHA treatment (one way ANOVA, $p = 0.03$), however, there was no significant change between and reference control and Ag+nHA (Figure 6.6). Regarding osteocalcin, the mRNA expression was measurable in all samples in reference control and Ag+nHA, but it was measurable in only 1 sample in Ti, Ag and Ag+mHA, other samples were undetermined. There was no significant difference between the reference control and Ag+nHA (one way ANOVA, $p > 0.05$), values of osteocalcin mRNA expression were approximately 1-2 fold change relative to the negative control (Figure 6.6). Expression of RUNX-2 gene worked in all treatments, but there was no significant difference between the treatments (one way ANOVA, $p = 0.57$), the values were around 1.5 – 2.5 fold change relative to the negative control. There was no IL-6 expression in any of the treatments as the threshold cycle (CT) values were undetermined.

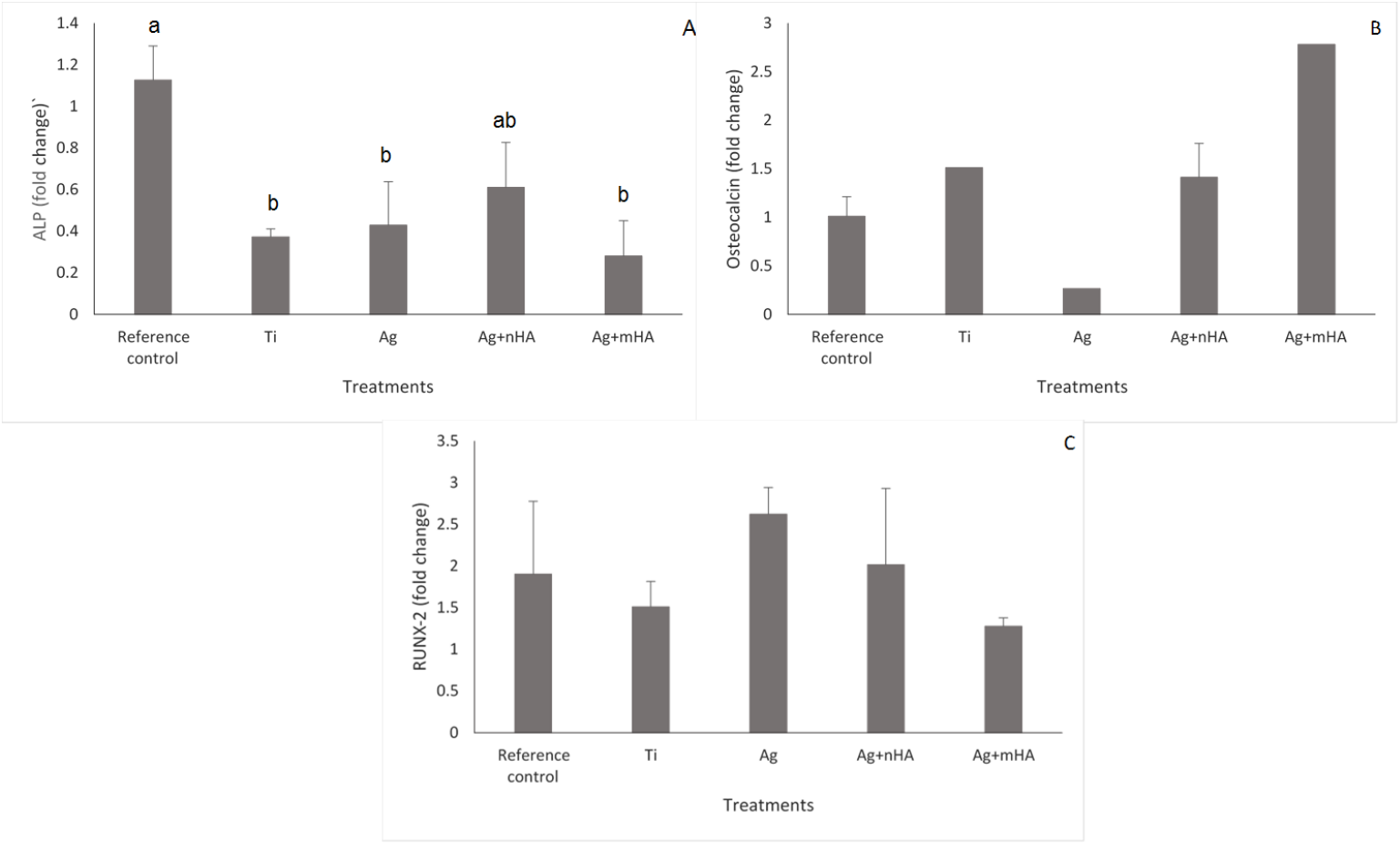

Figure 6.6. Fold changes in the expression of mRNA for ALP (A), osteocalcin (B) and RUNX-2 (C) in cultured human osteoblasts grown on; culture dishes (reference control), Ti, Ag, Ag+nHA and Ag+mHA. Data are mean ± S.E.M, (n = 3). Different letters indicate a significant difference between treatments (one way ANOVA, $p < 0.05$). Unlabelled indicates no statistically significant differences between the treatments was observed.

6.4 Discussion

In this study, differentiation and mineralisation of human primary human osteoblast cells on nano silver and nano HA coating of titanium dental implants were investigated. The results showed that the reference control cells were differentiated and mineralised after 21 days, and there was noticeable calcified masses on the cell monolayer under the microscope (Figure 6.1). Also, Ca^{2+} and P in the reference control was significantly higher than the negative control indicating extracellular matrix mineralisation. Moreover, EDS reports showed that osteoblast cells on Ti, Ag, Ag+nHA and Ag+mHA were calcified and showed increased calcium and phosphorus presence. Molecular investigations on the gene expression showed that there was an mRNA expression of osteoblast cell differentiation genes (ALP, osteocalcin and RUNX-2) in all treatments (Figure 6.6). There was a consistent release of silver from the silver plated titanium discs to the external media measuring around 1 mg L^{-1} at the beginning of the experiment and 0.3 mg L^{-1} on day 21. This confirms that the amount of released silver over 21 days was above the antibacterial dose which is around 0.2 mg L^{-1} (Besinis *et al*., 2017). In addition to the release of silver to the media, the measured silver concentrations in the cell homogenates confirmed silver exposure to the cell monolayer; but without inducing toxicity to the cells as measured by normal cell morphology, electrolyte composition and the presence of normal LDH and ALP enzyme activities.

6.4.1 Long term silver release and cell viability

Released silver was measured in the external media over 21 days. The Alamar blue assay was also conducted to study the cell viability on the same time points over 21

days. Results showed that there was a similar and constant silver release of approximately 1-2 mg L^{-1} from the Ag, Ag+nHA and Ag+mHA treatments at the beginning of the experiment, but later, they decreased to around 0.3 mg L^{-1}. Cell viability in these treatments remained above 60% relative to the negative control. This result reveals that silver has not induced a significant cytotoxicity to the cells. There was a decrease in cell viability after few days of the experiment but then increased until the end of the experiment. This may be explained by the fact that the released silver to the external media had killed some cells at the beginning of the exposure due to the silver shock, but later, the surviving cells had become tolerant to the environment (Table 6.3 and Table 6.4). Moreover, cell viability on the Ag+nHA treatment was increasing over time, but the viability of the cells from the Ag+mHA treatment was decreasing even in the presence of similar amount of released silver. This observation could be explained by the fact that the surface of Ag+nHA is uniform and fully covering the silver layer underneath, so the cells came in contact with the nano HA surface, while, the HA particles on the surface of Ag+mHA are sparse and the cells were attaching to the silver layer rather than the micro HA. Moreover, nano HA surface induces cell growth and proliferation and attachment with each other (Shi *et al*., 2013; Huan *et al*., 2016; Cheng *et al*., 2018).

Regarding cell morphology, osteoblast cells grown on the Ti and Ag+nHA treatments were confluent and attached to each other without having obvious membrane damage. However, the cells on the Ag and Ag+mHA treatments exhibited an obvious shrinkage, but there was also cell attachment with each other and no noticeable cell membrane rupture. In addition, the expression of β-actin also confirmed the cell shrinkage, as it was found that the mRNA expression of β-actin was significantly lower in Ag and Ag+mHA compared to others. The expression of actin

proteins is involved in the cell volume control (Chowdhury *et al*., 1992; Kapus *et al*., 1999). Cell shrinkage can be caused by osmotic shrinkage with likely water loss; and it is known that Ag interferes with Na^+/K^+ pump leading to the outward diffusion gradient of the Na^+ (Hussain *et al*., 1994). However, due to the Na^+ adsorption from the media to the disc surface, the actual Na^+ content of the cells was masked. The cell shrinkage due to silver is further confirmed by Pauksch *et al*. (2014) who showed that the presence of silver with primary osteoblast cells was associated with 60% cell viability with a noticeable cellular shrinkage when the cells were examined under SEM. The LDH activity in the external media was low in all treatments, this indicates that although there was some cell shrinkage, there was not a significant amount of LDH release from the cells due to the cell membrane rupture. In addition, there was not a high LDH activity in the cell homogenate indicating that the cells were not depending on anaerobic respiration for ATP production, so the respiratory status of the cells was not altered by the presence of silver.

In the cell homogenate, exposure of silver to the cell monolayer was confirmed in all the treatments where silver was intended to be present: Ag, Ag+nHA and Ag+mHA. The concentration of Na^{2+} in the cell homogenate of negative and reference control was significantly lower compared to all other treatments, this is explained by the fact that Na^+ and proteins from the cell culture medium are adsorbed to the surface of the discs (see Chapter 3). Ca^{2+} and P concentration in the cell homogenate showed significantly higher values in the Ag+mHA treatment compared to all other treatments. However, this value might have been masked by the presence of HA on the specimen surface that can subsequently be mixed with the cell lysate. In addition, the presence of adsorbed Ca^{2+} and P from the external media to the HA surface of the disc can mask the actual Ca^{2+} and P values of the cell homogenate (Harding *et al*., 2005).

6.4.2 Cell differentiation and mineralisation

The osteoblast cell mineralisation in the reference control (differentiated cells) compared to the negative control (undifferentiated cells) was assessed by observing the mineral deposits under the microscope, and also measuring the Ca^{2+} and P content in the cell homogenate after 21 days. The reference control was mineralised and differentiated. Figure 6.1 shows the mineralised human primary osteoblast cells on the surface of the culture dish. Cells in the reference control showed orange/red deposits while cells in the negative control did not, the deposits might be calcified masses produced by the differentiated cells. This argument was also confirmed by the ICP-OES finding as it showed that Ca^{2+} and P in the cell homogenate of the reference control was significantly higher than the negative control. In addition, in all treatments, cell differentiation and mineralisation were achieved, these were confirmed by the SEM and EDS spectra that clearly show that the cells in all treatments produced calcium and phosphorus deposits (Figure 6.1 and 6.2). This result is supported by Tian *et al*. (2016) that used SEM and EDS to qualitatively investigate the production of calcium and phosphorus deposits by osteoblast cells cultured on titanium surface for 21 days. In addition, SEM findings of the current study showed that there were cellular extensions to the calcified matrix (Figure 6.1). Similar observation was noticed by Jones *et al*. (2007) after studying the mineralisation of human primary osteoblast cells on a phosphate-free porous bioactive glass scaffold. It was found that the cells were extending filopodia to the calcified masses. This was also observed by Linder *et al*. (1983) during electron microscopic analysis of the bone-implant interface. Linder and co-workers installed dental implants in rabbits for 12 weeks and then the animals were

sacrificed and implants removed for electron microscopical analysis of the bone-implant interface.

Silver release to the external media and silver exposure to the cell homogenate did not induce a significant interference with the differentiation/mineralisation process of any of the treatment groups. Since it was found that cells in all treatments were produced calcium and phosphorus deposits (Figure 6.2). This finding corroborates with another study that tested the effect of silver with primary human osteoblast cell differentiation grown in DMEM media supplemented with 10% fetal calf serum. It was found that 10 μg g^{-1} of silver nano particles did not induce a significant change in ALP activity after 34 days compared to the control (Paukch *et al*., 2014). Moreover, Tilmaceau *et al*. (2015) also tested mesenchymal stem cell differentiation on silver-containing phosphonate monolayers on titanium, the results showed that the differentiation and mineralisation were not affected by the presence of silver since ALP enzyme activity and mRNA expression were not significantly different from uncoated titanium. However, the presence of silver was only confirmed by surface characterisation of the coated discs. The silver release to the external media was not measured. Consequently, it is difficult to compare the amount of silver release with the current study.

In this study, osteoblast functional gene expression study showed that the mRNA encoding ALP, osteocalcin and RUNX-2 was expressed in all treatments. There were no differences in the mRNA expression for osteocalcin and RUNX-2 relative to β-actin housekeeping gene between the treatments, for ALP, there was no significant difference between the reference control and the Ag+nHA. A similar finding was observed by Masaki *et al*. (2005) that ALP and osteocalcin mRNA expression were not significantly different between the treatments although the cell viability was

significantly different between them. Moreover, Masaki and co-workers found that changes in ALP and osteocalcin mRNA expression were around one fold relative to controls; similar values were obtained in the current study (Figure 6.6). The mRNA expression for ALP was higher in the Ag+nHA treatment compared to that in cells grown on Ti (Figure 6.6). This result is supported by another study; Tian *et al*. (2016) found that ALP mRNA expression in osteoblast cells grown on silver nanoparticle-doped HA coating on titanium was higher compared to uncoated titanium. ALP hydrolyses pyrophosphates to produce phosphates for matrix mineralisation (Orimo, 2014). This result supports the fact that nano HA surface can induce osteoblast mineralisation as HA resembles the mineral constituents of living bone. Thus, nano HA coated titanium dental implants can potentially enhance the ossteointegration process inside the jawbone.

6.4.3 Conclusions

In this experiment, the *in vitro* culture time was enough to allow the cells to differentiate and mineralise. This study demonstrated the ability of primary human osteoblast cells to grow, differentiate and mineralise on the silver and HA coatings in the presence of an antibacterial dissolved silver. In addition, prolonged antibacterial activity was also insured through the continuous release of silver over 21 days. However, the interpretation of the gene expression work is hampered by the ubiquitous effects of silver on the cellular machinery. It is therefore recommended to use more than one housekeeping gene for performing gene expression studies with silver. Moreover, measuring Ca^{2+} and P in the cell homogenate can be a better alternative than just relying on ALP enzyme activity to assess the differentiation and mineralisation.

Nonetheless, the results did confirm the biocompatibility of Ag+nHA coatings, and so this composite especially has utility to be used as a novel dental implant material in dental clinics to minimise the incidence of dental implant failure due to infection. However, *in vivo* studies are needed to further confirm the dental implant integration with the surrounding bone. After that, the coating can be suggested for clinical trials.

Chapter 7

General Discussion

Peri-implant infections are one of the major causes of implant failure. Peri-implantitis often requires revision surgery and can be compounded with long-term post-operative treatment; which can have a negative impact on the physical and psychological wellbeing of patients. To prevent this undesirable clinical outcome, the implant can be made antibacterial by applying a bactericidal agent on the implant surface. Silver is a metal well-known for its antibacterial properties (Chapter 1), and it can prevent bacterial growth when applied as a coating to titanium alloy (Zhao *et al*., 2009). However, all the active coatings which are able to release particles or silver ions to the surrounding environment can also present a toxicity hazard to the healthy human cells in the vicinity to the implant site (Besinis *et al*., 2015), especially those involved in wound healing or providing stability for the implant. Therefore, silver coatings on dental implants must be tested for biocompatibility with a relevant cell type, such as primary osteoblast cells, prior to the clinical use.

The hypothesis of this study was that coating the dental implant surface with nano silver and nano HA would provide antibacterial activity whilst maintaining the biocompatibility of the implant surface with human osteoblast cells. The results of this study confirmed the hypothesis, since the coatings demonstrated biocompatibility with human primary osteoblast cells over 7 days; as demonstrated by the biocompatibility experiment (Chapter 5). The ability of osteoblast cells to survive for longer periods and achieve mineralisation was confirmed on the specimens after 21 days as shown in the differentiation experiment (Chapter 6).

7.1 Coating application and stability

The first objective of this study was to successfully coat the medical grade titanium specimens with silver and HA. It was found that the coatings were successfully applied on the substrate and the particles were at the nano-scale. The quality of the coatings and the chemical composition was confirmed by SEM and EDS images of the coatings (see chapter 2). The electroplating process successfully resulted in the formation of uniform layer of silver nanoparticles on titanium, and the sintering technique was also a successful method for HA application (Figure 2.2).

Nano coatings on dental implants are vulnerable to physical and chemical damage during implant placement and while exposed to blood during/after surgery. Cell culture medium substances can cause nanoparticle dissolution, so there can be a direct effect of cell culture substances on the implant coating stability (Loza *et al*., 2014). In the current study, the results of coating stability tests in cell culture medium showed that the coatings remained intact, even after 21 days (Figure 6.1). In addition, there was a constant silver release to the external media over 21 days (Table 6.1), which was higher than the antibacterial concentration needed to prevent microbial growth (Besinis *et al*., 2017). This shows the ability of the coating to stay intact with a cell culture media that is broadly similar to the chemical composition of blood; and release a long-term consistent antibacterial silver. Mechanical adhesion of the coatings on the discs was also studied through conducting the pull-off test (Table. 2.4). The bonding strength between the coating and the substrate was acceptable and similar to previous reports (Mohseni *et al*., 2014; Asri *et al*., 2016). This confirms the utility of the coatings and ability to stay attached to the substrate while implant insertion.

7.2 Biocompatibility of the coatings

In the first biocompatibility experiment of the current study, the silver release was constant over 7 days (around 1 mg L^{-1}). The experiment used low number of cells so that their proliferation could be observed, but the low amount of cells created some experimental challenges that made the cell viability data difficult to interpret. These logistical challenges included not enough sample to measure all the enzyme activities one would like and the absence of additional cell viability assays. However, the findings showed that the cells were unable to survive on Ag and Ag+mHA, but only a few cells survived on Ag+nHA (Chapter 3).

Moreover, it was unclear whether the toxicity was from the dissolved silver released into the media, or if it was direct contact toxicity with the coating surface. Thus, another experiment was conducted to study the toxicity of dissolved silver from the specimens (Chapter 4). The results of that study showed that the released silver, which was around 1 mg L^{-1}, was compatible with the human osteoblast cells used in the experiment. Another experiment was conducted to investigate the contact toxicity and also the effect of surface geometry on cell health (Chapter 5). In this experiment, more cells were used to have sufficient sampling to reliably measure enzyme activity and to be able to better interpret the data. Furthermore, two control were added to the experimental design to assess the effect of surface geometry which included Ti plus nHA and Ti plus mHA, (Chapter 5). The experiment demonstrated that, of the silver-containing materials, the Ag+nHA was the most biocompatible with human primary osteoblast cells. Having established biocompatibity, a differentiation experiment was conducted to study the cell mineralisation on the coatings (Chapter 6).

The amount of released silver in all biocompatibility experiments was 1-2 mg L^{-1}, this confirms the reproducibility of silver release and constant supply in different

experiments. In the differentiation experiment, silver release from the discs decreased over time to reach to 0.2 mg L^{-1} on day 21, but it was still above the effective antibacterial concentration. Besinis *et al*. (2017) found that 0.2 mg L^{-1} silver release from nano silver and nano HA coated titanium dental implants was enough to kill *Streptococcus sanguinis* after 24 hours growth on the coating. Regarding the cell health, it was found in all experiments that osteoblast cells were healthier on Ag+nHA compared to Ag and Ag+mHA in the presence of similar amounts of silver release. The cell health was assessed using the alamar blue assay, LDH assay and SEM images to investigate the cell morphology.

LDH activity was used in all cell experiments to assess the cell health. It was difficult to detect the LDH activity in the media due to very low amount of LDH, which indicates that the cell membrane was intact, and did not release LDH enzyme to the media. Alternatively, the LDH activity was always measurable in the cell homogenate. The LDH activity in the cell homogenate was not significantly different between the treatments in all experiments; this indicates that the cells were not in need of using anaerobic respiration for ATP production. An additional viability assay that used in this study was alamar blue. This assay was more sensitive to assess the cell viability compared to LDH activity as the latter can lead to high standard deviations between the samples. Thus, alamar blue might be better to interpret the cell viability.

The ALP activity assay was also used to assess the osteoblast cell health and function. Very low activity was detected in the media and the homogenate after 7 days (0.006 nmol min^{-1} ml^{-1}) in the homogenate, while the activity was around 0.03 nmol min^{-1} ml^{-1} after 21 days in the homogenate. This indicates that the ALP activity was relatively low at the beginning of the experiment and later increases during the differentiation. Moreover, it supports the argument that ALP activity increases during

osteoblast cell differentiation (Yamaguchi *et al*., 2000). However, to assess the mineralisation status of the cells, it is recommended to actually measure the Ca^{2+} and P content of the cell homogenate rather than just relying on ALP activity.

The protein assay was used in the first experiment (chapter 3), and aimed to measure the protein content of the cell homogenate at the end of experiment. However, the protein adsorption test (Chapter 3) showed that there was protein adsorption from the external media to the surface of the specimens resulting in biasing the actual protein content of the cells. As a result of this, neither the enzyme activities, nor the concentration of silver and electrolytes in the cell homogenate were normalised with the protein content of the cell homogenate. It is a common rule in biochemistry to normalise enzyme activities in the cell homogenate to the protein content of the cells. However, for any experiment with growing cells on solid surfaces (e.g., titanium) or nano-coated surfaces, values are better to be expressed per volume of homogenate rather than per amount of protein; this is to prevent including the adsorbed proteins and biasing the data. Protein adsorption can pose difficulties for *in vitro* experiments because of the problems discussed above, however, protein adsorption is clinically essential, as the adsorption of proteins on the dental implant surface do provide a base for osteoblast cells adhesion during ossoeintegration (de Jonge *et al*., 2008).

Cell differentiation and mineralisation experiment showed that the cells were able to produce calcium and phosphorus nodules after 21 days *in vitro*. The cells were growing and the gene expression study showed that the fold changes of the target genes in the treatments relative to the negative control was approximately 1-2. However, 1-2 fold change in gene expression may not be a true response, it might be the issue of variability and the fact that every gene shows switching on and off all the time, and so a 1-2 fold change might be within the normal homeostatic range of the

genes. Nevertheless, this result was also observed by Masaki *et al*. (2005) who found that the fold changes of ALP and osteocalcin mRNA expression in osteoblasts cultured on titanium implants were approximately 1 relative to the control. Moreover, Schneider *et al*. (2003) argued that the expression of RUNX-2 in osteoblasts cultured on titanium implants was approximately 2 folds relative to the control. Since other studies have obtained similar values, so 1-2 fold change might be enough to regulate protein expression. However, to confirm this argument, it might be necessary to conduct the protein expression study (using western blot test) aiming to detect and confirm the presence of osteoblast specific extracellular matrix proteins (i.e. Collagen I, Osteocalcin, Ostepontin and Bone Sialoproteins), (Kirkham and Cartmell, 2007).

7.3 Clinical perspectives

For any biomaterial to be used in clinics, several *in vitro* and *in vivo* experiments are needed to demonstrate the safety and efficacy of the material. Current regulatory procedures for clinically approving new medicines or biomaterials also apply to nanomaterials. For any new biomaterial to be used, there are some criteria on which the approval of any new biomaterial is based: the efficacy of the new biomaterial should be higher compared to the existing ones, offer benefits to the patient, utility and compatibility with neighbouring vital structures (safety), (Juillerat-Jeanneret *et al*., 2013). In dentistry, Annex I of the Medical Devices Directive 93/42/EC identifies some legal requirements on the use of dental materials that include dentures and dental implants, regardless of having engineered nanomaterials. So there are no regulations which are specific for nanomaterials used in dental implants. The use of nanomaterials (especially silver and HA) in dentistry is arising, for example, silver nanoparticles can be used as an alternative to chlorhexidine disinfectant as Besinis *et al*. (2014) showed a better antibacterial activity of silver nanoparticles compared to the dental disinfectant

chlorhexidine. The prospects of silver nanoparticles are good: they may be widely used as an antibacterial agent in dentistry in the future.

7.4 Limitations and future recommendations

Protein adsorption on the surface of the discs were biasing the actual protein content of the cell homogenate. This created a challenge in normalising the enzyme activity and electrolyte concentration of the cell homogenate per mg cell protein. Overall LDH and ALP activity in the cell homogenate and external were low, this was because of the limited cell number due to the specimen size. It would be better to use bigger samples to conduct experiments in 12 or even 6 well micro plates, hence, larger amount of cells could be used leading to significantly higher enzyme activity in the cell homogenate.

In addition, LDH and ALP activities were not enough to precisely assess the cell viability, using alamar blue in parallel with LDH and ALP activities resulted in having clearer understanding of the cell health. Thus, it is recommended to use more than one viability assays to assess the cell viability especially with nanomaterials. Furthermore, the presence of high amounts of Na^+ and K^+ in the external media masked the cellular Na^+ and K^+ detection in the homogenates. Therefore, it was difficult to compare the electrolyte concentration of the cell homogenate with the electrolyte concentration in the external media. Moreover, as the coatings were composed of silver and HA, so there was possibility of mixing Ag, Ca^{2+} and P in the coatings with the cell homogenate; with homogenisation resulting in biasing the actual Ag Ca^{2+} and P content in the cell homogenate. In the gene expression study, the β-actin housekeeping gene was not consistent between the treatments as the mRNA

expression was significantly lower in Ag and Ag+mHA treatments compared to the others. This was due to the difference in cell viability and cell volume which directly attributed to the alteration in β-actin mRNA expression. It can be recommended to use more than one housekeeping genes so that to find the most consistent one that can be used with target genes to calculate ΔCT values. Nevertheless, in the presence of silver, it can always be challenging to have a constant mRNA expression of the housekeeping gene, this is because silver is interfering with cell health, cell volume, cell proteins, reactive oxygen species production, etc. Thus, finding a housekeeping gene that can remain constant even in the presence of those conditions is difficult. Another limitation of this study was the lack of protein expression data which can clarify whether or not the expressed genes has resulted in the formation of specific proteins.

7.5 Future works

Further to the conducted experiments in this project. There are few more scientific questions to be answered. It is crucial to optimise the coating methods, instead of manually adding HA by pipetting. HA is better to be sputter coated on silver plated titanium discs, and then the sintering process can be carried out. This is particularly useful while coating cylindrical implants, as it is very difficult to precisely coat a cylindrical surface with a pipette. Regarding the cell biology, it is important to investigate whether or not primary osteoblast cells can survive in the presence of bacteria (infectious environment), as implants can face the same environment clinically. This can be conducted by growing the cells on the specimens for 24 hours, and then replacing the media with a fresh one containing living bacteria, after that, the specimens can be placed under SEM to investigate the cell morphology. Furthermore, it is important to study whether the proteomic profile of mature osteoblasts at 21 days of growth indicative of normal cells, or if the cells have adapted for development on

the nano surfaces compared to controls. In addition, investigating if the cells have produced extra cellular matrix proteins that are usually expressed during mineralisation. It would also be interesting to coat cylindrical titanium specimens with silver and HA using exactly the same coating method as used in this study, then, conducting the differentiation experiment using 3D culture technique and investigate the mineralisation of osteoblast cells on the coated titanium discs in three dimensions prior *in-vivo* studies. This is to evaluate the bone formation around the implant and working out the surface area covered by bone compared to control. Finally, to conduct *in vivo* studies to further confirm the utility of the coating. This can be carried out by coating cylindrical titanium specimens with silver and HA using exactly the same coating method as used in this study, then, install the implants in rabbit bone. After 3 months, conducting pull-off test to evaluate the osseointegration of the coated titanium implants compared to uncoated implants.

7.6 Conclusions

In this project, the Ag+nHA coating showed an acceptable bonding strength to the substrate (see chapter 2). Moreover, since this coating was developed to provide an antibacterial activity to the implant surface, so a continuous supply of an antibacterial silver to the surrounding environment is necessary. The coating demonstrated that there was a long-term (21 days) silver supply that was above the antibacterial dose. Furthermore, the coating showed an acceptable compatibility with the human primary osteoblast cells in terms of cell growth and mineralisation over 21 days. This confirms the utility of the coating in terms of preserving an antibacterial activity and maintaining biocompatibility with the surrounding tissues.

Appendix

This section contains some data which could provide extra information about the presented data in the experimental chapters.

Appendix 1

Table: 1 pH values of the media over 24 hours in dialysis experiment (chapter 2).

A: in Milli-Q water (control)

Treatments	Time points (hour)								
	0	0.5	1	2	3	4	6	8	24
Blank	5.7 ± 0.1	5.8 ± 0.1	5.4 ± 0.1	5.9 ± 0.1	4.9 ± 0.1	5.2 ± 0.1	6.3 ± 0.1	5.4 ± 0.1	6.9 ± 0.1
Ag	5.8 ± 0.2	5.6 ± 0.2	4.9 ± 0.1	5.3 ± 0.1	4.8 ± 0.1	5.3 ± 0.2	5.7 ± 0.1	5.1 ± 0.1	6.5 ± 0.1
Ag+nHA	6.1 ± 0.1	5.8 ± 0.1	5.3 ± 0.1	6.0 ± 0.1	5.1 ± 0.1	4.9 ± 0.1	5.5 ± 0.1	5.7 ± 0.2	6.7 ± 0.3
Ag+mHA	5.4 ± 0.2	5.8 ± 0.2	5.9 ± 0.1	6.1 ± 0.2	4.9 ± 0.1	4.9 ± 0.1	5.3 ± 0.1	5.8 ± 0.1	6.7 ± 0.1

B: in DMEM

Treatments	Time points (hour)								
	0	0.5	1	2	3	4	6	8	24
Blank	7.3 ± 0.1	7.4 ± 0.1	7.5 ± 0.1	7.5 ± 0.1	7.6 ± 0.1	7.6 ± 0.1	7.3 ± 0.1	7.3 ± 0.1	7.9 ± 0.1
Ag	7.4 ± 0.1	7.5 ± 0.1	7.6 ± 0.1	7.5 ± 0.1	7.6 ± 0.1	7.6 ± 0.1	7.7 ± 0.1	7.7 ± 0.1	7.9 ± 0.1
Ag+nHA	7.4 ± 0.1	6.8 ± 0.1	7.5 ± 0.1	7.4 ± 0.1	7.5 ± 0.1	7.6 ± 0.1	7.6 ± 0.1	7.6 ± 0.1	7.8 ± 0.1
Ag+mHA	7.4 ± 0.1	7.4 ± 0.1	7.5 ± 0.1	7.4 ± 0.1	7.6 ± 0.1	7.6 ± 0.1	7.6 ± 0.1	7.6 ± 0.1	7.8 ± 0.1

Data are presented as mean ± S.E.M (n = 3), no significant difference were located between the treatments (one way ANOVA, $p > 0.05$).

Appendix 2

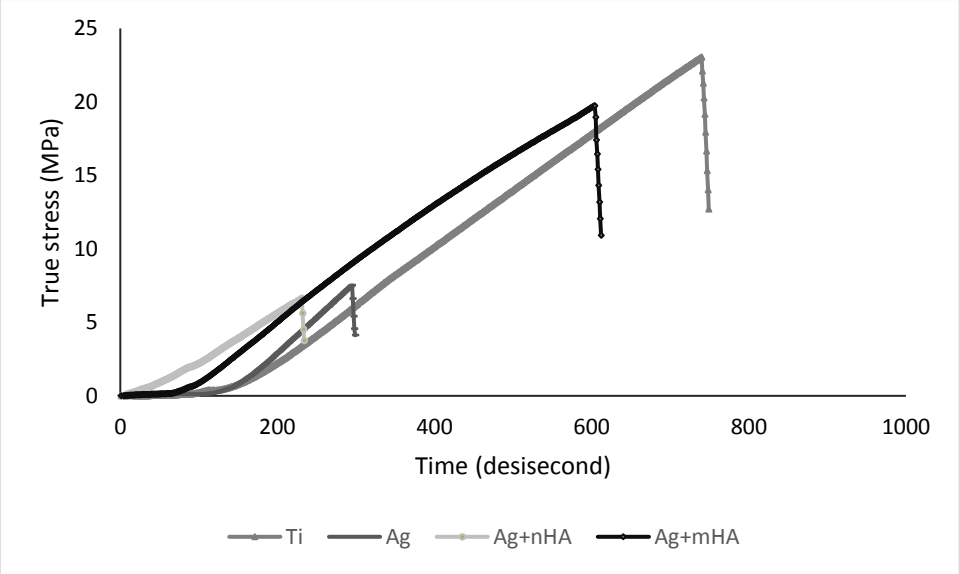

Figure 1. Stress/strain curves from the Pull-off test (chapter 2). The curves are representative examples and taken from a specimen in each treatment. Note the point where each curve declines, this is where the failure occurs.

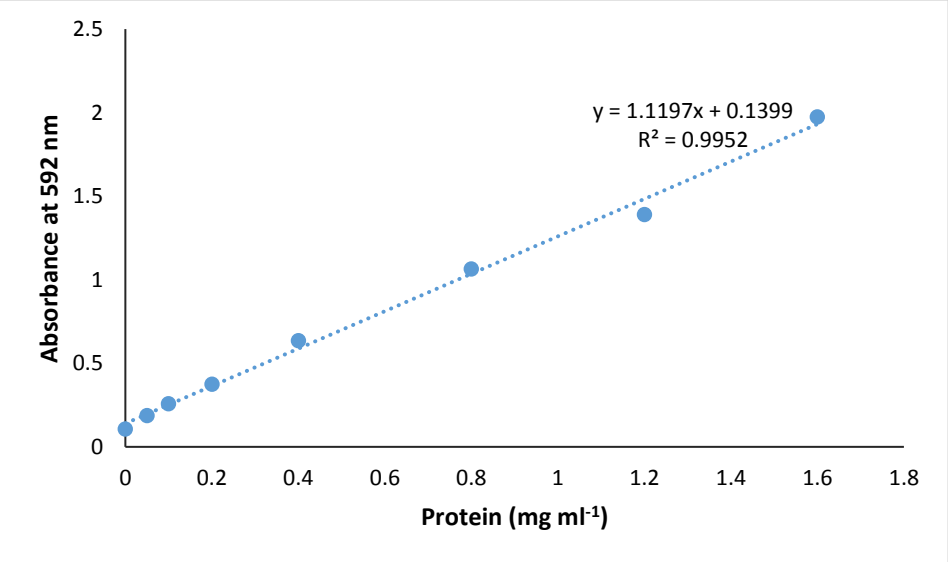

Figure 2. BCA Protein assay standard curve from bovine serum albumin (BSA).

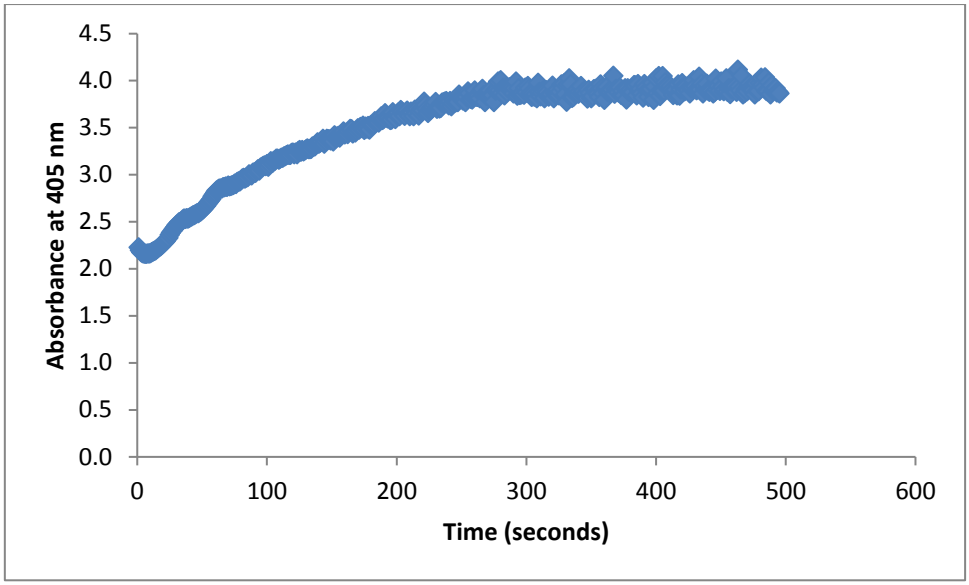

Figure 3. An example of ALP activity curve, note the change (increase) in absorbance due to pNPP conversion to pNP by ALP enzyme. The curve flats when the ALP enzyme action ends.

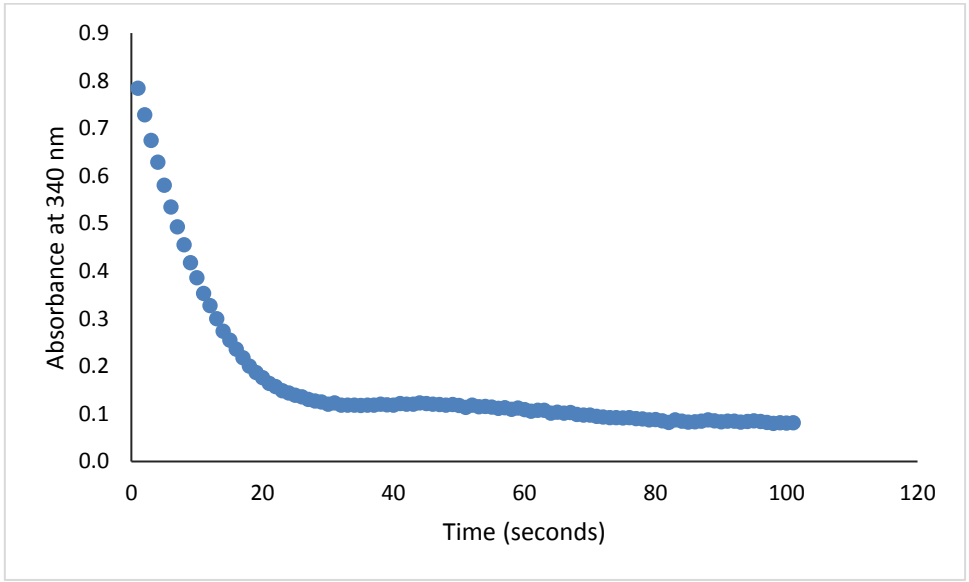

Figure 4. An example of LDH activity curve, note the change (decrease) in absorbance due to pyruvate conversion to lactate, and NADH conversion to NAD by ALP enzyme. The curve flats when the LDH enzyme action ends.

Appendix 3: poster presentation at BSODR conference (September 2015, Cardiff)

PLYMOUTH UNIVERSITY PENINSULA
SCHOOLS OF MEDICINE & DENTISTRY

Poster: 66

plymouth.ac.uk/peninsula
ranj.salaie@plymouth.ac.uk

Biocompatibility Of Surface-modified Titanium Dental Implants With Silver and Hydroxyapatite Nanoparticles

Ranj N.Salaie[1,2] , Alexandros Besinis[1,2], Huirong Le [2], Christopher Tredwin[2], Richard D.Handy[1]
[1]School of Biological Sciences, University of Plymouth, UK, [2]Plymouth University Peninsula Dental School, University of Plymouth, UK

Introduction

- The surface of dental implants is subject to bacterial colonisation and infection that may cause implant failure (Zhao et al., 2009).
- Coating the implant surface with an antibacterial agent can be effective. Besinis et al. (2014) found that metal nanoparticles (e.g., silver) can have potential antibacterial activity against oral pathogens.
- Nevertheless, silver nanoparticles can exert toxic effects on human cells. So biocompatibility of a silver coating on titanium implants to human primary osteoblast cells should be evaluated before moving towards clinical application.
- To mask the toxic effect of silver nanoparticles, the silver layer can be coated with nanoparticles of hydroxyapatite. The latter resembles the inorganic constituent of the natural bone (Tomsia et al., 2011).

Aim and objectives

The aim of this study is to investigate the biocompatibility of silver and hydroxyapatite nanoparticles coating on medical grade titanium dental implants. Objectives were to successfully coat the surface of the implant with silver and hydroxyapatite nanoparticles and microparticles, investigate the stability of the coatings and examine their biocompatibility.

Methods & Materials

- Ti6Al4V discs were polished and coated with,
  - Silver nanoparticles (Ag NPs)
  - Silver and hydroxyapatite nanoparticles (Ag+nHA)
  - Silver and hydroxyapatite microparticles (Ag+mHA)
- Silver and HA coatings were applied using the electroplating and sintering techniques respectively.
- The surface morphology and quality of the coatings on the titanium implants was examined by scanning electron microscopy (SEM) and energy dispersive spectroscopy (EDS).
- The stability of the silver-hydroxyapatite coatings was tested in different cell culture media (physiological saline, DMEM, human osteoblast growth medium; HOB). Silver concentration was measured using inductively coupled plasma mass spectrometry (ICP-MS).
- The biocompatibility of coatings was tested with primary human osteoblasts in 24-well microplates (n = 9 discs/treatment; 12,000 cells/well). The cell viability was assessed by measuring the protein content of the cells over 7 days.

Results

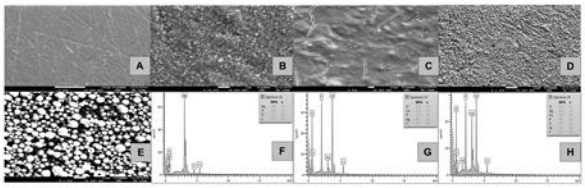

Figure 1: SEM images of coated titanium discs: A (x 250) and B (x 10.0 K) silver plated titanium, C (x 500) and D (x 1.0 K) Ag+nHA, E (x 1.0 K) Ag+mHA. EDS spectra of coated samples: (F) silver plated titanium, (G) Ag+nHA, (H) Ag+mHA. The images show that the samples have been successfully coated. Size difference between nanoparticles and microparticles of hydroxyapatite can also be easily noticed.

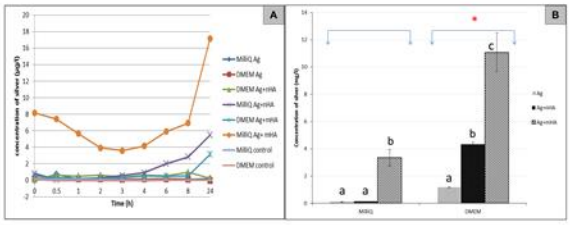

Figure 2: A: Total concentration (µg/l) of silver ion release from discs to the external media in the beakers (n = 3). External media was either cell culture medium (DMEM) or ultrapure water (MilliQ). Abbreviations refer to the type of sample in a specific media. **B:** Concentration of silver (mg/l) in 4 ml solution in dialysis bags after 24 hours. Error bars represent S.E.M (n = 3). Asterisk means statistically significant difference between the treatment (DMEM) and control (MilliQ) groups. Different letters between bars mean statistically significant difference within each media. (one way ANOVA, $p < 0.05$).

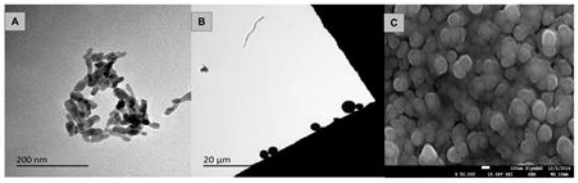

Figure 3: A and B: TEM images of hydroxyapatite nanoparticles and microparticles showing their primary particle size which is 23.90 ± 1.4 nm and 4.72 ± 0.38 µm respectively. C: SEM image of silver nanoparticles showing the primary particle size which is 111.58 ± 14.99 nm.

Table 1: Total amount of silver release (mg/l) from Ag+nHA discs to the media after 72 hours of incubation. Data is expressed as mean ± S.E.M (n = 3). Different capital letters within each column indicate statistically significant difference, while different small letters within each row indicate statistically significant difference (one way ANOVA, $p < 0.05$).

Groups	Day 1	Day 2	Day 3
DMEM + 10% FBS + 1% antimicrobial. No disc (blank 1)	0.00 ± 0.00 A a	0.00 ± 0.00 A a	0.00 ± 0.00 A a
Physiological saline + 10% FBS + 1% antimicrobial. No disc (blank 2)	0.00 ± 0.00 A a	0.00 ± 0.00 A a	0.00 ± 0.00 A a
HOB + 1% antimicrobial. No disc (Blank 3)	0.00 ± 0.00 A a	0.00 ± 0.00 A a	0.00 ± 0.00 A a
DMEM + 10% FBS + 1% antimicrobial (Control)	18.83 ± 2.38 B a	2.61 ± 0.52 B b	1.75 ± 0.11 B b
DMEM + 1% antimicrobial (without FBS) (G3)	0.07 ± 0.00 D a	0.19 ± 0.04 D a	0.17 ± 0.04 E a
(75% DMEM + 25% physiological saline) + 10% FBS + 1% antimicrobial (G4)	10.82 ± 0.60 C a	2.59 ± 0.29 B b	1.80 ± 0.07 B b
(50% DMEM + 50% physiological saline) + 10% FBS + 1% antimicrobial (G5)	10.85 ± 1.10 C a	2.67 ± 0.38 B b	1.92 ± 0.17 B b
Physiological saline + 10% FBS + 1% antimicrobial (G6)	4.77 ± 0.96 E ab	7.04 ± 0.46 C a	2.67 ± 0.45 C b
HOB + 1% antimicrobial (G7)	4.70 ± 0.54 E a	1.68 ± 0.08 B b	0.96 ± 0.01 D b

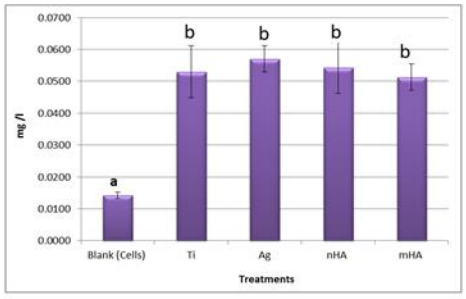

Figure 4: Protein content of the cell homogenate after 7 days exposure. Error bars represent S.E.M (n = 6). Different letters within bars indicate statistically significant difference from each other (one way ANOVA, $p < 0.05$).

Conclusions

- Titanium discs were successfully coated with silver and hydroxyapatite nanoparticles and microparticles. Coatings were stable in cell culture media although silver dissolution was higher compared to MilliQ water .
- Primary results showed that all coated titanium discs were biocompatible and allowed for better osteoblast cell growth as compared to the control over 7 days. However, further studies are needed to confirm whether or not these coatings can allow for osteoblast cell differentiation and mineralisation.

References

- Besinis, A., De Peralta, T. & Handy, R. D. (2014) 'The antibacterial effects of silver, titanium dioxide and silica dioxide nanoparticles compared to the dental disinfectant chlorhexidine on Streptococcus mutans using a suite of bioassays'. Nanotoxicology, 8 (1). pp 1-16.
- Tomsia, A. P., Launey, M. E., Lee, J. S., Mankani, M. H., Wegst, U. G. & Saiz, E. (2011) 'Nanotechnology approaches for better dental implants'. The International journal of oral & maxillofacial implants, 26 (Suppl). pp 25.
- Zhao, L., Chu, P. K., Zhang, Y. & Wu, Z. (2009) 'Antibacterial coatings on titanium implants'. J Biomed Mater Res B Appl Biomater, 91 (1). pp 470-480

Acknowledgments:
Special thanks to Ministry of Higher Education of Kurdistan for the support

Appendix 4. Best presentation award from Postgraduate Society Conference of Plymouth University

References

Abraham, C.M. 2014. Suppl 1: A brief Historical Perspective on dental Implants, their surface coatings and treatments . *The Open Dentistry Journal,* 8, 50-55.

Ahamed, M., Alsalhi, M. S. and Siddiqui, M. 2010. Silver nanoparticle applications and human health. *Clinica Chimica Acta,* 411 (23-24), 1841-1848.

Albers, C. E., Hofstetter, W., Siebenrock, K. A., Landmann, R. and Klenke, F. M. 2013. In vitro cytotoxicity of silver nanoparticles on osteoblasts and osteoclasts at antibacterial concentrations. *Nanotoxicology,* 7 (1), 30-36.

Albrektsson, T. and Wennerberg, A. 2004. Oral implant surfaces: Part 1--review focusing on topographic and chemical properties of different surfaces and in vivo responses to them. *International Journal of Prosthodontics,* 17 (5), 536-543.

Albrektsson, T., Brånemark, P.-I., Hansson, H.-A. and Lindström, J. 1981. Osseointegrated titanium implants: requirements for ensuring a long-lasting, Direct Bone-To-Implant Anchorage In Man. *Acta Orthopaedica,* 52 (2), 155-170.

Alt, V., Bitschnau, A., Österling, J., Sewing, A., Meyer, C., Kraus, R., Meissner, S.A., Wenisch, S., Domann, E. and Schnettler, R., 2006. The effects of combined gentamicin–hydroxyapatite coating for cementless joint prostheses on the reduction of infection rates in a rabbit infection prophylaxis model. *Biomaterials,* 27 (26), 4627-4634.

Al-Radha, A.S.D., Dymock, D., Younes, C. and O'Sullivan, D., 2012. Surface properties of titanium and zirconia dental implant materials and their effect on bacterial adhesion. *Journal of Dentistry,* 40(2), 146-153.

Arora, S., Jain, J., Rajwade, J. and Paknikar, K. 2009. Interactions of silver nanoparticles with primary mouse fibroblasts and liver cells. *Toxicology and Applied Pharmacology,* 236(3), 310-318.

Asharani, P., Low Kah Mun, G., Hande, M. P. and Valiyaveettil, S. 2008. Cytotoxicity and genotoxicity of silver nanoparticles in human cells. *ACS Nano,* 3(2), 279-290.

Asri, R.I.M., Harun, W.S.W., Hassan, M.A., Ghani, S.A.C. and Buyong, Z., 2016. A review of hydroxyapatite-based coating techniques: Sol–gel and electrochemical depositions on biocompatible metals. *Journal of the mechanical behavior of biomedical materials,* 57, 95-108.

Bacchelli, B., Giavaresi, G., Franchi, M., Martini, D., De Pasquale, V., Trirè, A., Fini, M., Giardino, R. and Ruggeri, A., 2009. Influence of a zirconia sandblasting treated surface on peri-implant bone healing: an experimental study in sheep. *Acta Biomaterialia,* 5 (6), 2246-2257.

Bachle, M. and Kohal, R. J. 2004. A systematic review of the influence of different titanium surfaces on proliferation, differentiation and protein synthesis of osteoblast-like MG63 cells. *Clinical Oral Implants Research,* 15 (6), 683-92.

Bagno, A. and Di Bello, C. 2004. Surface treatments and roughness properties of Ti-based biomaterials. Journal of Materials Science: *Materials in Medicine,* 15 (9), 935-949.

Besinis, A., De Peralta, T. and Handy, R. D. 2014a. The antibacterial effects of silver, titanium dioxide and silica dioxide nanoparticles compared to the dental disinfectant chlorhexidine on *Streptococcus mutans* using a suite of bioassays. *Nanotoxicology,* 8 (1), 1-16.

Besinis, A., De Peralta, T, Handy R. D. 2014b. Inhibition of biofilm formation and antibacterial properties of a silver nano-coating on human dentine. *Nanotoxicology*, 8 (7), 745–754

Besinis, A., De Peralta, T., Tredwin, C.J. and Handy, R.D., 2015. Review of nanomaterials in dentistry: interactions with the oral microenvironment, clinical applications, hazards, and benefits. *ACS nano,* 9 (3), 2255-2289.

Besinis, A., Hadi, S. D., Le, H., Tredwin, C. and Handy, R. 2017. Antibacterial activity and biofilm inhibition by surface modified titanium alloy medical implants following application of silver, titanium dioxide and hydroxyapatite nanocoatings. *Nanotoxicology,* 11 (3), 327-338.

Beyth, N., Yudovin-Farber, I., Bahir, R., Domb, A. J. and Weiss, E. I. 2006. Antibacterial activity of dental composites containing quaternary ammonium

polyethylenimine nanoparticles against Streptococcus mutans. *Biomaterials,* 27 (21), 3995-4002.

Borsari, V., Giavaresi, G., Fini, M., Torricelli, P., Salito, A., Chiesa, R., Chiusoli, L., Volpert, A., Rimondini, L. and Giardino, R. 2005. Physical characterization of different ‐ roughness titanium surfaces, with and without hydroxyapatite coating, and their effect on human osteoblast ‐ like cells. *Journal of Biomedical Materials Research Part B: Applied Biomaterials,* 75 (2), 359-368.

Braceras, I., De Maeztu, M., Alava, J. and Gay-Escoda, C. 2009. In vivo low-density bone apposition on different implant surface materials. *International Journal of Oral and Maxillofacial Surgery,* 38 (3), 274-278.

Branemark, R., Branemark, P., Rydevik, B. and Myers, R. R. 2001. Osseointegration in skeletal reconstruction and rehabilitation: a review. *Journal of Rehabilitation Research and Development,* 38 (2), 175-182.

Budynas, R.G. and Nisbett, J.K., 2008. *Shigley's mechanical engineering design* (Vol. 8). New York: McGraw-Hill.

Buser, D., Janner, S.F., Wittneben, J.G., Brägger, U., Ramseier, C.A. and Salvi, G.E., 2012. 10 ‐ year survival and success rates of 511 titanium implants with a sandblasted and acid ‐ etched surface: A retrospective study in 303 partially edentulous patients. *Clinical Implant Dentistry and Related Research,* 14 (6), 839-851.

Campbell, A. A., Song, L., Li, X. S., Nelson, B. J., Bottoni, C., Brooks, D. E. and Dejong, E. S. 2000. Development, characterization, and anti ‐ microbial efficacy of hydroxyapatite ‐ chlorhexidine coatings produced by surface ‐ induced mineralization. *Journal of Biomedical Materials Research,* 53 (4), 400-407.

Campbell, H. A., Handy, R. D. and Nimmo, M. 1999. Copper uptake kinetics across the gills of rainbow trout (Oncorhynchus mykiss) measured using an improved isolated perfused head technique. *Aquatic Toxicology,* 46 (3-4), 177-190.

Carlson, C., Hussain, S. M., Schrand, A. M., K. Braydich-Stolle, L., Hess, K. L., Jones, R. L. and Schlager, J. J. 2008. Unique cellular interaction of silver nanoparticles:

size-dependent generation of reactive oxygen species. *The Journal of Physical Chemistry B,* 112 (43), 13608-13619.

Chee, W. and Jivraj, S. 2007. Failures in implant dentistry. *British Dental Journal,* 202, 123-129.

Cheng, H., Chabok, R., Guan, X., Chawla, A., Li, Y., Khademhosseini, A. and Jang, H.L., 2018. Synergistic interplay between the two major bone minerals, hydroxyapatite and whitlockite nanoparticles, for osteogenic differentiation of mesenchymal stem cells. *Acta Biomaterialia*, 69, 342-351.

Cho, S.A. and Park, K.T., 2003. The removal torque of titanium screw inserted in rabbit tibia treated by dual acid etching. *Biomaterials,* 24 (20), 3611-3617.

Chowdhury, S., Smith, K.W. and Gustin, M.C., 1992. Osmotic stress and the yeast cytoskeleton: phenotype-specific suppression of an actin mutation. *The Journal of Cell Biology*, *118* (3), 561-571.

Chung, K. H., Hsiao, L. Y., Lin, Y. S. and Duh, J. G. 2008. Morphology and electrochemical behavior of Ag-Cu nanoparticle-doped amalgams. *Acta Biomateria*, 4 (3), 717-24.

Coelho, P. G., Granjeiro, J. M., Romanos, G. E., Suzuki, M., Silva, N. R., Cardaropoli, G., Thompson, V. P. and Lemons, J. E. 2009. Basic research methods and current trends of dental implant surfaces. *Journal of Biomedical Materials Research Part B: Applied Biomaterials*, 88 (2), 579-96.

Coelho, P.G., Jimbo, R., Tovar, N. and Bonfante, E.A., 2015. Osseointegration: hierarchical designing encompassing the macrometer, micrometer, and nanometer length scales. *Dental Materials,* 31 (1),.37-52.

Costerton, J., Stewart, P. S. and Greenberg, E. 1999. Bacterial biofilms: a common cause of persistent infections. *Science,* 284 (5418), 1318-1322.

Davis, J.R. ed., 2001. *Surface engineering for corrosion and wear resistance*. ASM international.

De Jonge, L. T., Leeuwenburgh, S. C., Wolke, J. G. and Jansen, J. A. 2008. Organic–inorganic surface modifications for titanium implant surfaces. *Pharmaceutical Research,* 25 (10), 2357-2369.

Dos Santos, M. V., Elias, C. N. and Cavalcanti Lima, J. H. 2011. The effects of superficial roughness and design on the primary stability of dental implants. *Clinical Implant Dentistry and Related Research,* 13 (3), 215-223.

Ducy, P., Zhang, R., Geoffroy, V., Ridall, A.L. and Karsenty, G., 1997. Osf2/Cbfa1: a transcriptional activator of osteoblast differentiation. *cell*, *89* (5), 747-754.

Ducy, P. and Karsenty, G., 1995. Two distinct osteoblast-specific cis-acting elements control expression of a mouse osteocalcin gene. *Molecular and Cellular Biology*, *15* (4), 1858-1869.

Elias, C. N. 2011. Factors affecting the success of dental implants. In: Turkyilmaz, I., (Ed.), *Implant Dentistry - A Rapidly Evolving Practice*, pp 319-364.

Ehrenfest, D.M.D., Coelho, P.G., Kang, B.S., Sul, Y.T. and Albrektsson, T., 2010. Classification of osseointegrated implant surfaces: materials, chemistry and topography. *Trends in Biotechnology,* 28 (4),198-206.

Esposito, M., Ardebili, Y. and Worthington, H.V., 2014. Interventions for replacing missing teeth: different types of dental implants. *The Cochrane Library.*

Engel, E., Michiardi, A., Navarro, M., Lacroix, D. and Planell, J. A. 2008. Nanotechnology in regenerative medicine: the materials side. *Trends in Biotechnology,* 26 (1), 39-47.

Ewald, A., Glückermann, S. K., Thull, R. and Gbureck, U. 2006. Antimicrobial titanium/silver PVD coatings on titanium. *Biomedical Engineering Online, 5, 22.*

Fischer, K. and Stenberg, T., 2012. Prospective 10 ‐ year cohort study based on a randomized controlled trial (RCT) on implant ‐ supported full ‐ arch maxillary prostheses. Part 1: sandblasted and acid ‐ etched implants and mucosal tissue. *Clinical implant dentistry and related research,* 14 (6), 808-815.

Foldbjerg, R., Olesen, P., Hougaard, M., Dang, D. A., Hoffmann, H. J. and Autrup, H. 2009. PVP-coated silver nanoparticles and silver ions induce reactive oxygen species, apoptosis and necrosis in THP-1 monocytes. *Toxicology letters*, 190 (2), 156-162.

Frandsen, C. J., Brammer, K. S., Noh, K., Johnston, G. and Jin, S. 2014. Tantalum coating on TiO_2 nanotubes induces superior rate of matrix mineralization and osteofunctionality in human osteoblasts. *Materials Science and Engineering: C,* 37 (1), 332-341.

Giavaresi, G., Fini, M., Cigada, A., Chiesa, R., Rondelli, G., Rimondini, L., Torricelli, P., Aldini, N. N. and Giardino, R. 2003. Mechanical and histomorphometric evaluations of titanium implants with different surface treatments inserted in sheep cortical bone. *Biomaterials,* 24 (9), 1583-1594.

Gibbons, R. J. and Houte, J. V. 1973. On the formation of dental plaques. *Journal of Periodontology,* 44 (6), 347-360.

Gitrowski, C., Al-Jubory, A.R. and Handy, R.D., 2014. Uptake of different crystal structures of TiO_2 nanoparticles by Caco-2 intestinal cells. *Toxicology letters*, *226*(3), 264-276.

Gliga, A. R., Skoglund, S., Wallinder, I. O., Fadeel, B. and Karlsson, H. L. 2014. Size-dependent cytotoxicity of silver nanoparticles in human lung cells: the role of cellular uptake, agglomeration and Ag release. *Particle and Fibre Toxicology,* 11, 11.

Gombos, Z.J. and Summerscales, J., 2016. In-mould gel-coating for polymer composites. *Composites Part A: Applied Science and Manufacturing*, 91, 203-210.

Gondikas, A. P., Morris, A., Reinsch, B. C., Marinakos, S. M., Lowry, G. V. and Hsu-Kim, H. 2012. Cysteine-induced modifications of zero-valent silver nanomaterials: implications for particle surface chemistry, aggregation, dissolution, and silver speciation. *Environmental Science & Technology,* 46 (13), 7037-7045.

Greulich, C., Braun, D., Peetsch, A., Diendorf, J., Siebers, B., Epple, M. and Köller, M. 2012. The toxic effect of silver ions and silver nanoparticles towards bacteria and human cells occurs in the same concentration range. *RSC Advances,* 2, 6981-6987.

Gunputh, U.F., 2018. Antibacterial Properties of TiO2 Nanotubes coated with nano-ZnO and nano-Ag (Doctoral dissertation, University of Plymouth).

Guo, C.Y., Matinlinna, J.P. and Tang, A.T.H., 2012. Effects of surface charges on dental implants: past, present, and future. *International journal of biomaterials, 2012.*

Hadi, S., Ashfaq, N., Bey, A. and Khan, S. 2011. Biological factors responsible for failure of osseointegration in oral implants. *Biology and Medicine,* 3 (2), 164-170*.*

Hadi, S.D., 2014. The Antibacterial Properties and Biocompatibility of Silver and Hydroxyapatite Nanoparticles Coating on Dental Implants. (ResM dissertation, University of Plymouth).

Hajipour, M. J., Fromm, K. M., Akbar Ashkarran, A., Jimenez De Aberasturi, D., Larramendi, I. R. D., Rojo, T., Serpooshan, V., Parak, W. J. and Mahmoudi, M. 2012. Antibacterial properties of nanoparticles. *Trends in Biotechnology,* 30 (10), 499-511.

Han, X., Gelein, R., Corson, N., Wade-Mercer, P., Jiang, J., Biswas, P., Finkelstein, J. N., Elder, A. and Oberdörster, G. 2011. Validation of an LDH assay for assessing nanoparticle toxicity. *Toxicology,* 287 (1), 99-104*.*

Ha, H. and Payer, J., 2011. The effect of silver chloride formation on the kinetics of silver dissolution in chloride solution. *Electrochimica acta,* 56 (7), 2781-2791.

Handy, R. D., Eddy, F. B., Romain G. 1989. In vitro evidence for the ionoregulatory role of rainbow trout mucus in acid, acid/aluminium and zinc toxicity. *Journal of Fish Biology,* 35 (5), 737–747

Handy, R. D. and Shaw, B. J. 2007. Toxic effects of nanoparticles and nanomaterials: Implications for public health, risk assessment and the public perception of nanotechnology. *Health, Risk & Society,* 9 (2), 125-144.

Hansen, U. and Thünemann, A.F., 2015. Characterization of silver nanoparticles in cell culture medium containing fetal bovine serum. *Langmuir*, *31* (24), 6842-6852.

Harding, I., Rashid, N. and Hing, K. 2005. Surface charge and the effect of excess calcium ions on the hydroxyapatite surface. *Biomaterials,* 26 (34), 6818-6826.

Hadrup, N. and Lam, H.R., 2014. Oral toxicity of silver ions, silver nanoparticles and colloidal silver–a review. *Regulatory Toxicology and Pharmacology,* 68 (1), 1-7.

Harris, L., Mead, L., Müller‐Oberländer, E. and Richards, R. 2006. Bacteria and cell cytocompatibility studies on coated medical grade titanium surfaces. *Journal of Biomedical Materials Research Part A,* 78 (1), 50-58.

Hasegawa, M., Kudo, T.A., Kanetaka, H., Miyazaki, T., Hashimoto, M. and Kawashita, M., 2016. Fibronectin adsorption on osteoconductive hydroxyapatite and non-osteoconductive α-alumina. *Biomedical Materials,* 11 (4), 045006*.*

Hellstrand, E., Lynch, I., Andersson, A., Drakenberg, T., Dahlbäck, B., Dawson, K. A., Linse, S. and Cedervall, T. 2009. Complete high‐density lipoproteins in nanoparticle corona. *Febs Journal,* 276 (12), 3372-3381.

Hessle, L., Johnson, K.A., Anderson, H.C., Narisawa, S., Sali, A., Goding, J.W., Terkeltaub, R. and Millán, J.L., 2002. Tissue-nonspecific alkaline phosphatase and plasma cell membrane glycoprotein-1 are central antagonistic regulators of bone mineralization. *Proceedings of the National Academy of Sciences, 99 (14), 9445-9449.*

Huang, Q., Elkhooly, T.A., Liu, X., Zhang, R., Yang, X., Shen, Z. and Feng, Q., 2016. Effects of hierarchical micro/nano-topographies on the morphology, proliferation and differentiation of osteoblast-like cells. *Colloids and Surfaces B: Biointerfaces*, *145*, 37-45.

Hung, K.Y., Lo, S.C., Shih, C.S., Yang, Y.C., Feng, H.P. and Lin, Y.C., 2013. Titanium surface modified by hydroxyapatite coating for dental implants. *surface and coatings technology,* 231, 337-345.

Hussain, S., Meneghini, E., Moosmayer, M., Lacotte, D. and Anner, B. 1994. Potent and reversible interaction of silver with pure Na, K-ATPase and Na, K-ATPase-liposomes. *Biochimica et Biophysica Acta (BBA)-Biomembranes,* 1190 (2), 402-408.

Hussain, S.M., Javorina, A.K., Schrand, A.M., Duhart, H.M., Ali, S.F. and Schlager, J.J., 2006. The interaction of manganese nanoparticles with PC-12 cells induces dopamine depletion. *Toxicological sciences*, 92 (2), 456-463.

Iwaya, Y., Machigashira, M., Kanbara, K., Miyamoto, M., Noguchi, K., Izumi, Y. and Ban, S., 2008. Surface properties and biocompatibility of acid-etched titanium. *Dental Materials Journal,* 27 (3), 415-421.

Jemat, A., Ghazali, M.J., Razali, M. and Otsuka, Y., 2015. Surface modifications and their effects on titanium dental implants. *BioMed research international,* 2015.

Jones, J.R., Tsigkou, O., Coates, E.E., Stevens, M.M., Polak, J.M. and Hench, L.L., 2007. Extracellular matrix formation and mineralization on a phosphate-free porous bioactive glass scaffold using primary human osteoblast (HOB) cells. *Biomaterials*, *28* (9),1653-1663.

Juan, L., Zhimin, Z., Anchun, M., Lei, L. and Jingchao, Z. 2010. Deposition of silver nanoparticles on titanium surface for antibacterial effect. *International Journal of Nanomedicine,* 5, 261-267.

Junker, R., Dimakis, A., Thoneick, M. and Jansen, J.A., 2009. Effects of implant surface coatings and composition on bone integration: a systematic review. *Clinical oral implants research,* 20 (s4), 185-206.

Kapus, A., Szászi, K., Sun, J., Rizoli, S. and Rotstein, O.D., 1999. Cell shrinkage regulates Src kinases and induces tyrosine phosphorylation of cortactin, independent of the osmotic regulation of Na^+/H^+ exchangers. *Journal of Biological Chemistry*, *274* (12), 8093-8102.

Kilpadi, K. L., Chang, P. L. and Bellis, S. L. 2001. Hydroxylapatite binds more serum proteins, purified integrins, and osteoblast precursor cells than titanium or steel. *Journal of Biomedical Materials Research,* 57 (2), 258-267.

Kim, H., Choi, S.H., Ryu, J.J., Koh, S.Y., Park, J.H. and Lee, I.S., 2008. The biocompatibility of SLA-treated titanium implants. *Biomedical Materials, 3 (2), 025011.*

Kim, T. H., Kim, M., Park, H. S., Shin, U. S., Gong, M. S. and Kim, H. W. 2012. Size-dependent cellular toxicity of silver nanoparticles. *Journal of Biomedical Material Research A*, 100 (4), 1033-1043.

Kirkham, G.R. and Cartmell, S.H., 2007. Genes and proteins involved in the regulation of osteogenesis. *Ashammakhi N, Reis R, Chiellini E, editores. Topics in Tissue Engineering*, *3*.

Kittler, S., Greulich, C., Diendorf, J., Koller, M. and Epple, M. 2010. Toxicity of silver nanoparticles increases during storage because of slow dissolution under release of silver ions. *Chemistry of Materials,* 22 (16), 4548-4554.

Kroll, A., Pillukat, M.H., Hahn, D. and Schnekenburger, J., 2012. Interference of engineered nanoparticles with in vitro toxicity assays. *Archives of toxicology*, *86* (7),1123-1136.

Kuroda, D., Niinomi, M., Morinaga, M., Kato, Y. and Yashiro, T. 1998. Design and mechanical properties of new β type titanium alloys for implant materials. *Materials Science and Engineering*: A, 243 (1-2), 244-249.

Kwok, C., Wong, P., Cheng, F. and Man, H. 2009. Characterization and corrosion behavior of hydroxyapatite coatings on Ti6Al4V fabricated by electrophoretic deposition. *Applied Surface Science,* 255 (13-14), 6736-6744.

Langenbach, F. and Handschel, J., 2013. Effects of dexamethasone, ascorbic acid and β-glycerophosphate on the osteogenic differentiation of stem cells in vitro. *Stem Cell Research and Therapy*, *4* (5), 117.

Lavenus, S., Louarn, G. and Layrolle, P. 2010. Nanotechnology and dental implants. *International Journal of Biomaterials,* 2010.

Lee, J.K., Choi, D.S., Jang, I. and Choi, W.Y., 2015. Improved osseointegration of dental titanium implants by TiO_2 nanotube arrays with recombinant human bone morphogenetic protein-2: a pilot in vivo study. *International journal of nanomedicine,* 10, 1145-1154

Le Guehennec, L., Soueidan, A., Layrolle, P. and Amouriq, Y. 2007. Surface treatments of titanium dental implants for rapid osseointegration. *Dental Materials,* 23 (7), 844-854.

Li, D., Li, D. W., Li, Y., Fossey, J. S. and Long, Y. T. 2010. Cyclic electroplating and stripping of silver on Au@ SiO 2 core/shell nanoparticles for sensitive and recyclable substrate of surface-enhanced Raman scattering. *Journal of Materials Chemistry,* 20, 3688-3693.

Li, L., Pan, H., Tao, J., Xu, X., Mao, C., Gu, X. and Tang, R. 2008. Repair of enamel by using hydroxyapatite nanoparticles as the building blocks. *Journal of Materials Chemistry,* 18, 4079-4084.

Liau, S., Read, D., Pugh, W., Furr, J. and Russell, A. 1997. Interaction of silver nitrate with readily identifiable groups: relationship to the antibacterial action of silver ions. *Letters in Applied Microbiology*, 25 (4), 279-283.

Linder, L., Albrektsson, T., Branemark, P.I., Hansson, H.A., Ivarsson, B., Jonsson, U. and Lundström, I., 1983. Electron microscopic analysis of the bone-titanium interface. *Acta Orthopaedica Scandinavica*, *54* (1), 45-52.

Lindhe, J. and Meyle, J. 2008. Peri‐implant diseases: Consensus Report of the Sixth European Workshop on Periodontology. *Journal of Clinical Periodontology,* 35 (8), 282-285.

Lioubavina-Hack, N., Lang, N. P. and Karring, T. 2006. Significance of primary stability for osseointegration of dental implants. *Clincal Oral Implants Research,* 17 (3), 244-50.

Liu, D.-M., Yang, Q. and Troczynski, T. 2002. Sol–gel hydroxyapatite coatings on stainless steel substrates. *Biomaterials,* 23 (3), 691-698.

Liu, X., Chu, P. and Ding, C. 2004. Surface modification of titanium, titanium alloys, and related materials for biomedical applications. *Materials Science and Engineering: R: Reports*, 47 (3-4), 49-121.

Loza, K., Diendorf, J., Sengstock, C., Ruiz-Gonzalez, L., Gonzalez-Calbet, J., Vallet-Regi, M., Köller, M. and Epple, M. 2014. The dissolution and biological effects of silver nanoparticles in biological media. *Journal of Materials Chemistry B, 2, 1634-1643.*

Mahé, M., Heintz, J.M., Rödel, J. and Reynders, P., 2008. Cracking of titania nanocrystalline coatings. *Journal of the European Ceramic Society, 28 (10), 2003-2010.*

Maluf, P.S.Z., Ching, A.W., Angeletti, P., Bretos, J.L.G. and Ferreira, L.M., 2015. Insertion torque of dental implants after microvascular fibular grafting. *British Journal of Oral and Maxillofacial Surgery*, 53 (7), 647-649.

Marambio-Jones, C. and Hoek, E. M. 2010. A review of the antibacterial effects of silver nanomaterials and potential implications for human health and the environment. *Journal of Nanoparticle Research,* 12 (5), 1531-1551.

Marinucci, L., Balloni, S., Becchetti, E., Belcastro, S., Guerra, M., Calvitti, M., Lull, C., Calvi, E.M. and Locci, P., 2006. Effect of titanium surface roughness on human osteoblast proliferation and gene expression in vitro. *International Journal of Oral & Maxillofacial Implants*, 21 (5), 719-725.

Masaki, C., Schneider, G.B., Zaharias, R., Seabold, D. and Stanford, C., 2005. Effects of implant surface microtopography on osteoblast gene expression. *Clinical Oral Implants Research,* 16 (6), 650-656.

Mccracken, M. 1999. Dental implant materials: commercially pure titanium and titanium alloys. *Journal of Prosthodontics*, 8 (1), 40-43.

Mei, S., Wang, H., Wang, W., Tong, L., Pan, H., Ruan, C., Ma, Q., Liu, M., Yang, H., Zhang, L. and Cheng, Y., 2014. Antibacterial effects and biocompatibility of titanium surfaces with graded silver incorporation in titania nanotubes. *Biomaterials*, 35(14), 4255-4265.

Melo, M.A., Guedes, S.F., Xu, H.H. and Rodrigues, L.K., 2013. Nanotechnology-based restorative materials for dental caries management. *Trends in biotechnology,* 31(8),.459-467*.*

Mendonca, G., Mendonca, D. B., Aragao, F. J. and Cooper, L. F. 2008. Advancing dental implant surface technology--from micron- to nanotopography. *Biomaterials,* 29 (28), 3822-35.

Meran, Z., 2013. The use of silver nanoparticles as an antifungal coating on silicone facial prosthesis. pearl.plymouth.ac.uk.

Meran, Z., Besinis, A., De Peralta, T. and Handy, R.D., 2018. Antifungal properties and biocompatibility of silver nanoparticle coatings on silicone maxillofacial prostheses in vitro. *Journal of Biomedical Materials Research Part B: Applied Biomaterials,* 106 (3), 1038-1051.

Misch, C. E. 2007. Contemporary Implant Dentistry, *Elsevier Health Sciences*.

Mohseni, E., Zalnezhad, E. and Bushroa, A.R., 2014. Comparative investigation on the adhesion of hydroxyapatite coating on Ti–6Al–4V implant: A review paper. *International Journal of Adhesion and Adhesives*, *48*, 238-257.

Morones, J. R., Elechiguerra, J. L., Camacho, A., Holt, K., Kouri, J. B., Ramírez, J. T. and Yacaman, M. J. 2005. The bactericidal effect of silver nanoparticles*. Nanotechnology,* 16 (10), 2346-2353*.*

Natali, A.N., Carniel, E.L. and Pavan, P.G., 2009. Investigation of viscoelastoplastic response of bone tissue in oral implants press fit process. *Journal of Biomedical Materials Research Part B: Applied Biomaterials*, 91 (2), 868-875.

Navalakhe, R. M. and Nandedkar, T. D. 2007. Application of nanotechnology in biomedicine*. Indian Journal of Experimental Biology,* 45 (2), 160-165*.*

Norowski, P. A. and Bumgardner, J. D. 2009. Biomaterial and antibiotic strategies for peri‐implantitis: A review. *Journal of Biomedical Materials Research Part B: Applied Biomaterials*, 88 (2), 530-543.

O'brien, J., Wilson, I., Orton, T. and Pognan, F., 2000. Investigation of the Alamar Blue (resazurin) fluorescent dye for the assessment of mammalian cell cytotoxicity. *The FEBS Journal*, 267 (17), 5421-5426.

Oh, S. J., Kim, H., Liu, Y., Han, H. K., Kwon, K., Chang, K. H., Park, K., Kim, Y., Shim, K. and An, S. S. A. 2014. Incompatibility of silver nanoparticles with lactate dehydrogenase leakage assay for cellular viability test is attributed to protein binding and reactive oxygen species generation. *Toxicology Letters*, 225 (3), 422-432.

Olivares-Navarrete, R., Hyzy, S.L., Hutton, D.L., Erdman, C.P., Wieland, M., Boyan, B.D. and Schwartz, Z., 2010. Direct and indirect effects of microstructured titanium substrates on the induction of mesenchymal stem cell differentiation towards the osteoblast lineage. *Biomaterials*, *31* (10), 2728-2735.

Ong, K.J., MacCormack, T.J., Clark, R.J., Ede, J.D., Ortega, V.A., Felix, L.C., Dang, M.K., Ma, G., Fenniri, H., Veinot, J.G. and Goss, G.G., 2014. Widespread nanoparticle-assay interference: *implications for nanotoxicity testing*. *PLoS One*, *9* (3), 90650.

Orimo, H., 2010. The mechanism of mineralization and the role of alkaline phosphatase in health and disease. *Journal of Nippon Medical School*, 77 (1), 4-12.

Özcan, M. and Hämmerle, C. 2012. Titanium as a reconstruction and implant material in dentistry: advantages and Pitfalls. *Materials,* 5 (9), 1528-1545.

Pal, T., Sau, T. K. and Jana, N. R. 1997. Reversible formation and dissolution of silver nanoparticles in aqueous surfactant media*. Langmuir,* 13 (6), 1481-1485.

Pal, S., Tak, Y.K. and Song, J.M., 2007. Does the antibacterial activity of silver nanoparticles depend on the shape of the nanoparticle? A study of the gram-negative bacterium Escherichia coli. *Applied and environmental microbiology,* 73 (6),1712-1720*.*

Parekh, R. B., Shetty, O. and Tabassum, R. 2012. Surface Modifications for Endosseous Dental Implants. *International Journal of Oral Implantology & Clinical Research*, 3 (3), 116-121.

Pauksch, L., Hartmann, S., Rohnke, M., Szalay, G., Alt, V., Schnettler, R. and Lips, K. S. 2014. Biocompatibility of silver nanoparticles and silver ions in primary human mesenchymal stem cells and osteoblasts. *Acta Biomaterialia*, 10 (1), 439-449.

Piattelli, A., Trisi, P. and Emanuelli, M. 1993. Bone Reactions to Hydroxyapatite-Coated Dental Implants in Humans: Histologic Study Using SEM, Light Microscopy, and Laser Scanning Microscopy. *International Journal of Oral & Maxillofacial Implants*, 8 (1), 69-74.

Prosser, B., Taylor, D., Dix, B. A. and Cleeland, R. 1987. Method of evaluating effects of antibiotics on bacterial biofilm. *Antimicrobial Agents and Chemotherapy*, 31 (10), 1502-1506.

Quirynen, M., De Soete, M. and Van Steenberghe, D. 2002. Infectious risks for oral implants: a review of the literature. Clinical Oral Implants Research, 13 (1), 1-19.

Radin, S., Campbell, J. T., Ducheyne, P. and Cuckler, J. M. 1997. Calcium phosphate ceramic coatings as carriers of vancomycin*. Biomaterials,* 18 (11), 777-782*.*

Rawadi, G., Vayssiere, B., Dunn, F., Baron, R. and Roman-Roman, S., 2003. BMP-2 controls alkaline phosphatase expression and osteoblast mineralization by a Wnt autocrine loop. *Journal of Bone and Mineral Research*, *18* (10), 1842-1853.

Reidy, B., Haase, A., Luch, A., Dawson, K. A. and Lynch, I. 2013. Mechanisms of silver nanoparticle release, transformation and toxicity: a critical review of current knowledge and recommendations for future studies and applications. *Materials,* 6 (6), 2295-2350*.*

Renvert, S., Roos‐Jansåker, A. M. and Claffey, N. 2008. Non‐surgical treatment of peri‐implant mucositis and peri‐implantitis: a literature review. *Journal of Clinical Periodontology,* 35 (8), 305-315*.*

Romanos, G. E., Toh, C. G., Siar, C. H., Swaminathan, D. and Ong, A. H. 2002. Histologic and histomorphometric evaluation of peri-implant bone subjected to

immediate loading: an experimental study with Macaca fascicularis. *International Journal of Oral & Maxillofacial Implants,* 17 (1), 44-51.

Romanos, G.E. and Johansson, C.B., 2005. Immediate loading with complete implant-supported restorations in an edentulous heavy smoker: histologic and histomorphometric analyses*. International Journal of Oral & Maxillofacial Implants*, 20(2), 282-290.

Rupp, F., Liang, L., Geis-Gerstorfer, J., Scheideler, L. and Hüttig, F., 2018. Surface characteristics of dental implants: A review. *Dental Materials,* 34(1), 40-57.

Sakka, S. and Coulthard, P. 2011. Implant failure: etiology and complications. *Med Oral Patol Oral Cir Bucal,* 16 (1), 42-44*.*

Samberg, M. E., Oldenburg, S. J. and Monteiro-Riviere, N. A. 2010. Evaluation of silver nanoparticle toxicity in skin in vivo and keratinocytes in vitro. *Environmental Health Perspectives (Online)*, 118 (3), 407-413.

Selck, H., Handy, R.D., Fernandes, T.F., Klaine, S.J. and Petersen, E.J., 2016. Nanomaterials in the aquatic environment: A European Union–United States perspective on the status of ecotoxicity testing, research priorities, and challenges ahead. *Environmental Toxicology and Chemistry*, 35 (5), 1055-1067*.*

Shaw, B.J., Ramsden, C.S., Turner, A. and Handy, R.D., 2013. A simplified method for determining titanium from TiO2 nanoparticles in fish tissue with a concomitant multi-element analysis. *Chemosphere*, 92(9),.1136-1144.

Shi, J., Dong, L.L., He, F., Zhao, S. and Yang, G.L., 2013. Osteoblast responses to thin nanohydroxyapatite coated on roughened titanium surfaces deposited by an electrochemical process. *Oral Surgery, Oral Medicine, Oral Pathology and Oral Radiology*, *116* (5), 311-316.

Shi, J., Karlsson, H.L., Johansson, K., Gogvadze, V., Xiao, L., Li, J., Burks, T., Garcia-Bennett, A., Uheida, A., Muhammed, M. and Mathur, S., 2012. Microsomal glutathione transferase 1 protects against toxicity induced by silica nanoparticles but not by zinc oxide nanoparticles. *ACS nano*, *6* (3),1925-1938.

Shi, Z., Huang, X., Cai, Y., Tang, R. and Yang, D. 2009. Size effect of hydroxyapatite nanoparticles on proliferation and apoptosis of osteoblast-like cells. *Acta Biomaterialia,* 5 (1), 338-345.

Schneider, G.B., Perinpanayagam, H., Clegg, M., Zaharias, R., Seabold, D., Keller, J. and Stanford, C., 2003. Implant surface roughness affects osteoblast gene expression. *Journal of Dental Research*, *82* (5), 372-376.

Schroeder, A., Van der zypen, E., Stich, h. and Sutter, F. 1981. The reactions of bone, connective tissue, and epithelium to endosteal implants with titanium-sprayed surfaces. *Journal of Maxillofacial Surgery,* 9, 15-25.

Shrivastava, S., Bera, T., Roy, A., Singh, G., Ramachandrarao, P. and Dash, D. 2007. Characterization of enhanced antibacterial effects of novel silver nanoparticles. *Nanotechnology,* 18 (22), 225103.

Singh, R. P. and Ramarao, P. 2012. Cellular uptake, intracellular trafficking and cytotoxicity of silver nanoparticles. *Toxicology Letters, 213 (2), 249-259*.

Smeets, R., Stadlinger, B., Schwarz, F., Beck-Broichsitter, B., Jung, O., Precht, C., Kloss, F., Gröbe, A., Heiland, M. and Ebker, T., 2016. Impact of dental implant surface modifications on osseointegration. *BioMed Research International, 2016.*

Spadaro, J., Berger, T., Barranco, S., Chapin, S. and Becker, R. 1974. Antibacterial effects of silver electrodes with weak direct current. *Antimicrobial Agents and Chemotherapy, 6, 637-642.*

Subramani, K., Jung, R. E., Molenberg, A. and Hämmerle, C. H. 2009. Biofilm on dental implants: a review of the literature. *International Journal of Oral & Maxillofacial Implants, 24, 616-626.*

Sykaras, N., Iacopino, A. M., Marker, V. A., Triplett, R. G. and Woody, R. D. 2000. Implant materials, designs, and surface topographies: their effect on osseointegration. A literature review. *International Journal of Oral & Maxillofacial Implants, 15, 675-690.*

Tian, B., Chen, W., Yu, D., Lei, Y., Ke, Q., Guo, Y. and Zhu, Z., 2016. Fabrication of silver nanoparticle-doped hydroxyapatite coatings with oriented block arrays for enhancing bactericidal effect and osteoinductivity. *Journal of the mechanical behavior of biomedical materials*, 61, 345-359.

Tîlmaciu, C.M., Mathieu, M., Lavigne, J.P., Toupet, K., Guerrero, G., Ponche, A., Amalric, J., Noël, D. and Mutin, P.H., 2015. In vitro and in vivo characterization of antibacterial activity and biocompatibility: a study on silver-containing phosphonate monolayers on titanium. *Acta Biomaterialia*, *15*, 266-277.

Tomsia, A. P., Launey, M. E., Lee, J. S., Mankani, M. H., Wegst, U. G. and Saiz, E. 2011. Nanotechnology approaches for better dental implants. *The International Journal of Oral & Maxillofacial Implants, 26, 25-49.*

Tomsia, A.P., Lee, J.S., Wegst, U.G. and Saiz, E., 2012. Nanotechnology for dental implants. *Oral & Craniofacial Tissue Engineering,* 2 (1), 23-34.

Tsui, Y.C., Doyle, C. and Clyne, T.W., 1998. Plasma sprayed hydroxyapatite coatings on titanium substrates Part 1: Mechanical properties and residual stress levels. *Biomaterials*, *19* (22), 2015-2029.

Vander Heiden, M.G., Cantley, L.C. and Thompson, C.B., 2009. Understanding the Warburg effect: the metabolic requirements of cell proliferation. *science*, *324* (5930), 1029-1033.

Van Noort, R. 1987. Titanium: the implant material of today. *Journal of Materials Science, 22, 3801-3811.*

Vrček, I.V., Žuntar, I., Petlevski, R., Pavičić, I., Dutour Sikirić, M., Ćurlin, M. and Goessler, W., 2016. Comparison of in vitro toxicity of silver ions and silver nanoparticles on human hepatoma cells. *Environmental toxicology, 31 (6), 679-692.*

Verran, J., Sandoval, G., Allen, N.S., Edge, M. and Stratton, J., 2007. Variables affecting the antibacterial properties of nano and pigmentary titania particles in suspension. *Dyes and Pigments, 73 (3), .298-304.*

Wan, Y., Raman, S., He, F. and Huang, Y. 2007. Surface modification of medical metals by ion implantation of silver and copper. *Vacuum, 81, 1114-1118*.

Wang, H., Li, Y., Zuo, Y., Li, J., Ma, S. and Cheng, L., 2007. Biocompatibility and osteogenesis of biomimetic nano-hydroxyapatite/polyamide composite scaffolds for bone tissue engineering. *Biomaterials*, *28* (22*), 3338-3348*.

Weng, W. and Baptista, J. L. 1999. Preparation and Characterization of Hydroxyapatite Coatings on Ti6Al4V Alloy by a Sol‐Gel Method*. Journal of the American Ceramic Society, 82, 27-32.*

Wennerberg, A. 1998. The importance of surface roughness for implant incorporation. *International Journal of Machine Tools and Manufacture, 38, 657-662.*

Williams, D. F. 2008. On the mechanisms of biocompatibility. *Biomaterials, 29, 2941-2953.*

Woodard, J. R., Hilldore, A. J., Lan, S. K., Park, C., Morgan, A. W., Eurell, J. A. C., Clark, S. G., Wheeler, M. B., Jamison, R. D. and Johnson, A. J. W. 2007. The mechanical properties and osteoconductivity of hydroxyapatite bone scaffolds with multi-scale porosity. *Biomaterials,* 28, 45-54.

Yokoyama, K. I., Ichikawa, T., Murakami, H., Miyamoto, Y. and Asaoka, K. 2002. Fracture mechanisms of retrieved titanium screw thread in dental implant. *Biomaterials,* 23, 2459-2465.

Yang, W., Han, W., He, W., Li, J., Wang, J., Feng, H. and Qian, Y., 2016. Surface topography of hydroxyapatite promotes osteogenic differentiation of human bone marrow mesenchymal stem cells*. Materials Science and Engineering: C, 60, 45-53.*

Yang, X., Gondikas, A.P., Marinakos, S.M., Auffan, M., Liu, J., Hsu-Kim, H. and Meyer, J.N., 2011. Mechanism of silver nanoparticle toxicity is dependent on dissolved silver and surface coating in Caenorhabditis elegans. *Environmental science & technology*, *46* (2), 1119-1127.

Yamaguchi, A., Komori, T. and Suda, T., 2000. Regulation of osteoblast differentiation mediated by bone morphogenetic proteins, hedgehogs, and Cbfa1. *Endocrine reviews*, *21* (4*), 393-411*.

Zhao, L., Chu, P. K., Zhang, Y. and Wu, Z. 2009. Antibacterial coatings on titanium implants., *Journal of Biomedical Materials Research Part B: Applied Biomaterials,* 91, 470-480.

Zinger, O., Anselme, K., Denzer, A., Habersetzer, P., Wieland, M., Jeanfils, J., Hardouin, P. and Landolt, D., 2004. Time-dependent morphology and adhesion of osteoblastic cells on titanium model surfaces featuring scale-resolved topography. *Biomaterials,* 25 (14), 2695-2711.

Zmeili, S.O.T.S.M., Shubair, M.N.G.M.S. and Salhab, A.S., 1998. Toxicity of a new antismoking mouthwash 881010 in rats and rabbits. *Journal of Toxicology and Environmental Health Part A,* 53 (1), 47-60.

Zook, J. M., Long, S. E., Cleveland, D., Geronimo, C. L. A. and Maccuspie, R. I. 2011. Measuring silver nanoparticle dissolution in complex biological and environmental matrices using UV–visible absorbance. *Analytical and Bioanalytical Chemistry,* 401, 1993-2002.